

UC Riverside

UC Riverside Electronic Theses and Dissertations

Title

Using Stable Isotopes of Nitrogen and Oxygen as Environmental Indicators of Nitrogen Deposition in the Sonoran Desert

Permalink

<https://escholarship.org/uc/item/4sr0x3cz>

Author

Bell, Michael David

Publication Date

2012

Peer reviewed|Thesis/dissertation

UNIVERSITY OF CALIFORNIA
RIVERSIDE

Using Stable Isotopes of Nitrogen and Oxygen as Environmental Indicators of Nitrogen
Deposition in the Sonoran Desert

A Dissertation submitted in partial satisfaction
of the requirements for the degree of

Doctor of Philosophy

in

Plant Biology

by

Michael D. Bell

December 2012

Dissertation Committee:

Dr. Edith B. Allen, Chairperson

Dr. James O. Sickman

Dr. G. Darrel Jenerette

Copyright by
Michael D. Bell
2012

The Dissertation of Michael D. Bell is approved:

Committee Chairperson

University of California, Riverside

ACKNOWLEDGEMENTS

“Study nature. Obey the laws of it. You can't go wrong. It pays compound interest for life and not one penny invested”

-John Samuelson

This dissertation has been a journey unlike any that I have ever taken. It has pushed me to the limits of my abilities at which I have achieved immense personal growth. I could not have made the strides in knowledge that I have without a superb support group of friends, family, and colleagues.

First, and most importantly I would like to thank my advisor and mentor Dr. Edith B. Allen. To put it bluntly, Edie is the best. A guiding hand through my time at UCR, she gave me freedom to develop my ideas and pursue the research questions that I found most interesting, while always being there when I got stuck to answer my questions or lead me to someone who could. I also worked closely with Jim Sickman to dig deep into the world of stable isotopes. He guided me patiently through the procedures of operating multiple new instruments and developing protocols to answer my research questions. Darrel Jenerette was always there to help me develop the next question to ask of my project with a new set of results. Our conversations were always stimulating and help me wrap my head around what my data was showing. Together, my committee had a tangible passion for science and research that was infectious.

I would also like to thank my three pre-graduate school supervisors who provided the kindling, lit the fire, and fanned the flames of my now burning passion for botanical knowledge. Dr. Susan Mazer at UC Santa Barbara gave me my first research opportunity and taught me how to labor away in the lab on monotonous tasks, Paige Wolken at Craters of the Moon National Monument shared her passion for plants and made me realize that playing outside for a living was as good as it sounded, and Dr. Tasha La Doux at Joshua Tree National Park grabbed me by the loupe and led me on the path to full Plank Geekdom. I would not be here today without their early leadership.

All of the atmospheric monitoring contained within would not have been possible without the input of Andrzej Bytnerowicz, Mark Fenn, and Pam Padgett. My wet chemistry and lab skills got a huge boost through the oversight of Diane Alexander at the USFS Fire Lab and Dee Lucero at UCR.

As with many Allen Lab members before me, the field components of my research would have been much less substantial without the unwavering spirit of Chris True. Rain or Shine, windy or calm, he was wired on coffee and ready to go. Other lab members Leela Rao, Chip Steers, Sara Jo Dickens, Heather Schneider, Kris Weathers, Bridget Hilbig, Justin Valliere, and Amanda Swanson provided field, lab, and mental health assistance. My Idaho 'lab mate' Ben Wissinger spent countless hours in the car driving around the desert with me setting up sites and sharing stories. I would also acknowledge the relentless undergraduate workforce that has helped count, weigh, and

measure the samples that I collected. I would finally like to thank the graduate community at UCR, in which I have formed lasting friendships and endless memories.

ABSTRACT OF THE DISSERTATION

Using Stable Isotopes of Nitrogen and Oxygen as Environmental Indicators of Nitrogen
Deposition in the Sonoran Desert

by

Michael D. Bell

Doctor of Philosophy, Graduate Program in Plant Biology
University of California, Riverside, December 2012
Dr. Edith B. Allen, Chairperson

Undisturbed wildland ecosystems are impacted by anthropogenic nitrogen (N) emissions being deposited significant distances from their sources. The main sources of atmospheric N inputs in the United States include industrial and automotive exhaust and emissions from agricultural wastes and fertilizers. Emission sources can be differentiated by analyzing the $\delta^{18}\text{O}$ and $\delta^{15}\text{N}$ of emitted compounds. Through a combination of field and laboratory studies, this dissertation aims to identify the various emission sources impacting the western Sonoran Desert and to determine how they are altering plant available nitrogen in the region. The first objective of this research was to measure if fractionation of HNO_3 $\delta^{18}\text{O}$ and $\delta^{15}\text{N}$ occurs to filters of commonly used ambient HNO_3 collectors. These collectors were then placed along a N deposition gradient to measure the isoscapes of HNO_3 $\delta^{15}\text{N}$ and $\delta^{18}\text{O}$ and extrapolate how each emission source contributes to regional anthropogenic N. Lastly, soil and plant tissue

were collected at each site to evaluate whether atmospheric patterns were conserved through the ecosystem.

Results suggest that ambient HNO_3 does not fractionate isotopically when binding to the passive sampler filters when exposed in a continuous stirred tank reactor. The HNO_3 $\delta^{18}\text{O}$ and $\delta^{15}\text{N}$ were within 0.5‰ of the source HNO_3 when exposed to controlled high ($20 \mu\text{g}/\text{m}^3$) and low ($10 \mu\text{g}/\text{m}^3$) concentrations for four weeks. When exposed under field conditions, the samplers verified that anthropogenic nitrogen impacting the Coachella Valley came from two sources based on the changes to HNO_3 $\delta^{18}\text{O}$ and $\delta^{15}\text{N}$ across the area; vehicle emissions from the Los Angeles air basin and agricultural emissions from around the Salton Sea. There was also a distinct separation in values for sites within Joshua Tree National Park suggesting that the Little San Bernardino Mountains act as effective barrier from air pollution moving in the park. Finally, surface soil NO_3^- was the most effective indicator of anthropogenic additions; with NO_3^- concentrations and $\delta^{18}\text{O}$ linearly tracking atmospheric HNO_3 concentrations. The leaf tissue $\delta^{15}\text{N}$ of the regionally dominant shrub, *Larrea tridentata*, also decreased at sites with increasing anthropogenic inputs. Both the atmospheric samplers and soil surface N analyses will provide land managers with effective tools to quickly identify regions of high anthropogenic inputs in a desert environment.

Table of Contents

Introduction	1
References	6

Chapter 1: Correcting for background nitrate contamination from crystalline KCl during stable isotopic analysis of oxygen and nitrogen by denitrification

Abstract	10
Introduction	11
Methods	14
Results and Discussion	16
Conclusion	21
References	22
Tables and Figures	23

Chapter 2: Consistency of isotopologues of atmospheric nitric acid in passively collected samples

Abstract	29
Introduction	31
Methods	35
Results	39
Discussion	43

Conclusion.....	48
References	50
Figures.....	54

Chapter 3: Evaluation of nitrogen and oxygen isotopes as indicators of nitrate contamination sources across a nitrogen deposition gradient in the Sonoran Desert

Abstract.....	61
Introduction	62
Methods.....	67
Results.....	71
Discussion.....	75
Conclusion.....	81
References	83
Figures.....	88

Chapter 4: Isotopes of nitrogen and oxygen in soil and plant material as indicators of anthropogenic nitrogen additions to the Sonoran Desert

Abstract.....	99
Introduction	100
Methods.....	105

Results.....	109
Discussion.....	113
Conclusion.....	119
References	121
Figures.....	128
Conclusion	135
References	139

List of Figures

Figure 1.1: KCl concentration vs blank sample m/v 44 peak.....	25
Figure 1.2: KCl concentration vs USGS 32/34/35 $\delta^{15}\text{N}$ and $\delta^{18}\text{O}$	26
Figure 1.3: KCl concentration vs USGS 32/34/35 m/v 44 peak	27
Figure 2.1: Site location of field sampling sites	54
Figure 2.2: CSTR Exposure length vs N-NO_3^- on Nylasorb filter.....	55
Figure 2.3: Mean HNO_3 $\delta^{15}\text{N}$ and $\delta^{18}\text{O}$ vs CSTR exposure length.....	56
Figure 2.4: Mean HNO_3 collect at each field site.....	57
Figure 2.5: Comparison of mean HNO_3 $\delta^{15}\text{N}$ and $\delta^{18}\text{O}$ at each field site	58
Figure 2.6: HNO_3 $\delta^{15}\text{N}$ vs HNO_3 $\delta^{18}\text{O}$	59
Figure 2.7: $1/\text{HNO}_3$ Exposure vs HNO_3 $\delta^{15}\text{N}$ and $\delta^{18}\text{O}$	60
Figure 3.1: Site locations of atmospheric samplers.....	88
Figure 3.2: Interpolated summer 2010 HNO_3 concentration, $\delta^{18}\text{O}$, and $\delta^{15}\text{N}$	89
Figure 3.3: Summer 2010 HNO_3 concentration vs $\delta^{18}\text{O}$ and $\delta^{15}\text{N}$	90
Figure 3.4: Interpolated summer 2011 HNO_3 concentration, $\delta^{18}\text{O}$, and $\delta^{15}\text{N}$	91
Figure 3.5: Mean HNO_3 concentration: summer 2010 vs summer 2011	92
Figure 3.6: Summer 2011 HNO_3 concentration vs. $\delta^{18}\text{O}$, and $\delta^{15}\text{N}$	93
Figure 3.7: Interpolated winter 2011 HNO_3 concentration, $\delta^{18}\text{O}$, and $\delta^{15}\text{N}$	94
Figure 3.8: HYSPLIT back trajectories for winter 2011	95
Figure 3.9: Winter 2011 HNO_3 concentration vs. $\delta^{18}\text{O}$ and $\delta^{15}\text{N}$	96
Figure 3.10: HYSPLIT back trajectories for summer 2010	97

Figure 3.11: HYSPLIT back trajectories for summer 2011	98
Figure 4.1: Location of field sites.....	128
Figure 4.2: Summer ambient HNO ₃ concentration vs soil NO ₃ ⁻ and soil NO ₃ ⁻ δ ¹⁸ O	129
Figure 4.3: Summer 2010 soil NO ₃ ⁻ δ ¹⁸ O vs Summer 2011 soil NO ₃ ⁻ δ ¹⁸ O	130
Figure 4.4: Interpolated regional soil δ ¹⁵ N	131
Figure 4.5: <i>Larrea tridentata</i> leaf δ ¹⁵ N response to soil NO ₃ ⁻ δ ¹⁸ O	132
Figure 4.6: <i>Schismus spp.</i> leaf δ ¹⁵ N and %N response to soil NO ₃ ⁻ δ ¹⁸ O	133
Figure 4.7: <i>Chaenactis fremontii</i> leaf δ ¹⁵ N response to soil NO ₃ ⁻ δ ¹⁸ O	134

List of Tables

Table 1.1: Expected and measured USGS 32/34/35 $\delta^{15}\text{N}$ and $\delta^{18}\text{O}$ 24

Table 1.2: Measured and corrected $\delta^{15}\text{N}$ and $\delta^{18}\text{O}$ for reference standards 28

Introduction

Global anthropogenic nitrogen emissions from industrial and agricultural processes have surpassed the amount of nitrogen (N) created through natural processes (Galloway et al. 2004). Emission sources are centralized around urban areas and near agricultural communities (Fenn et al. 2003b). In the western United States, the proximity of these sources to expansive wildland areas puts many undisturbed ecosystems at risk of shift in vegetation diversity and community structure (Fenn et al. 2003a, Johnson et al. 2003, Fenn et al. 2010, Ochoa-Hueso et al. 2011, Pardo et al. 2011). Emissions from the Los Angeles air basin expose local forests to some of the highest levels of deposition in the United States ($50 \text{ kg N ha}^{-1} \text{ yr}^{-1}$) (Bytnerowicz and Fenn 1996).

The National Atmospheric Deposition Program (NADP) and Environmental Protection Agency Clean Air Status and Trends Network (CASTNET) have national networks designed to measure wet and dry N deposition across the continental United States. Both networks' sites are concentrated in the eastern half of the US and have large data gaps in the western United States due to the presence of these expansive remote areas (NADP 2012). The US Forest Service has developed a simple and inexpensive passive atmospheric sampling system that allows for large scale monitoring of atmospheric nitric acid (HNO_3) in specific areas of interest (Bytnerowicz et al. 2005).

These samplers have been used to determine that NADP and CASNET maps have underestimated levels of deposition in the western US, omitting measures of dry deposition and placing samplers far from anthropogenic sources (Allen et al. 2009, Cisneros et al. 2010, Fenn et al. 2010). Additionally, advancements in stable isotopic analysis of atmospheric N compounds are increasing our ability to differentiate sources affecting these areas (Elliott et al. 2009, Templer and Weathers 2011).

Recent research in the United States has shown the utility of using stable isotopes of N and oxygen (O) within HNO_3 to determine the origins of air pollution (Elliott et al. 2007). NO_x molecules released from anthropogenic sources differ in the ratio of $^{18}\text{O}/^{16}\text{O}$ relative to those from biological sources. Measuring the change in isotopic signature of multiple elements across space will give a clearer image of how molecules are moving through the atmosphere. Combustion creates NO_x $\delta^{18}\text{O}$ between 60-90‰ (Elliott et al. 2007, Elliott et al. 2009) while soil emissions NO_3^- $\delta^{18}\text{O}$ have been measured between 20-30‰ (Michalski et al. 2004, Rock and Ellen 2007).

Atmospheric N levels in the Los Angeles air basin peak during the summer season (Solomon et al. 1992), which coincides with the dry season in this Mediterranean climate. This results in the majority of N in wildlands added as dry deposition (Bytnerowicz and Fenn 1996). Dry atmospheric N particles can readily deposit on any surface and therefore contribute to soil N inputs (Eilers et al. 1992). In semi-arid and arid habitats, deposited N can accumulate in the upper 2cm of the soil profile during the

dry season (Padgett et al. 1999), before entering the rhizosphere soil in a pulse with the initial precipitation event of the season (James et al. 2006).

As vegetation growth is often limited by N, anthropogenic inputs of N to the soil profile are expected to change nutrient dynamics (Vitousek 1994). The majority of N assimilated by plants is in the form of NO_3^- and NH_4^+ , while amino acids make up lower proportions (Schimel and Bennett 2004, Harrison et al. 2007). ^{15}N uptake tends to mimic the pool in which it originates (Evans et al. 1996), although the correlation between soil $\delta^{15}\text{N}$ and vegetation $\delta^{15}\text{N}$ is often muddled by various pools of N available for uptake (Högberg 1997, Evans 2001). Högberg Discrimination of isotopologues during uptake can vary within species and can be dependent on the type and pathway in which it is assimilated (Evans 2001). The accumulation of anthropogenic nitrogen may allow plants to serve as effective bioindicators of an N gradient, if the same species occurs throughout the gradient.

This dissertation continues the exploration of stable isotopes of N and O as indicators of anthropogenic nitrogen through the measurement of atmospheric, soil, and plant isotopic signatures inputs in a desert environment. The first chapter of this dissertation asks: *Does background NO_3^- in KCl contribute to the final isotopic signature of sample NO_3^- and if this value is consistent in different brands of KCl reagents.* Reagent grade KCl reports levels of NO_3^- to be <0.005% by weight. Previous research using KCl extractions of soil and ion exchange resins did not report contamination occurring in their samples (Rock and Ellen 2007, Rock et al. 2011, Templer and Weathers 2011).

These samples came from agricultural soils and bulk deposition samplers which contained much higher amounts of NO_3^- in samples than those in desert soils. During preliminary isotopic analysis, standards created in low NO_3^- concentrations were skewed, especially at high $\delta^{15}\text{N}$.

The second chapter asks the question: *Do standard passive atmospheric HNO_3 samplers accurately measure isotopes of N and O in both field and controlled conditions.* Previous field measurements were made with similar samplers in the northwestern United States and recorded HNO_3 $\delta^{18}\text{O}$ values that were up to 6‰ different than actively collected samples (Elliott et al. 2009). To address this question, samplers were erected in high and low HNO_3 concentrations in controlled greenhouse chambers and in ambient field conditions. HNO_3 $\delta^{15}\text{N}$ and $\delta^{18}\text{O}$ were measured on a series of filters exposed for 1 to 4 weeks to measure the consistency of the ambient HNO_3 $\delta^{15}\text{N}$ and $\delta^{18}\text{O}$ through time. This study was designed to determine the effectiveness of long term passive sampler exposures for measuring HNO_3 $\delta^{15}\text{N}$ and $\delta^{18}\text{O}$.

The third chapter asks: *Are atmospheric HNO_3 $\delta^{15}\text{N}$ and $\delta^{18}\text{O}$ consistent over a nitrogen deposition gradient between years and seasons?* High levels of pollution from the Los Angeles air basin move downwind to the east into the Sonoran Desert depositing N at rates as high as ($12 \text{ kg h}^{-1} \text{ yr}^{-1}$) into a nitrogen deficient ecosystem (Allen et al. 2009). Individual sources of nitrogen emissions have a consistent $\delta^{15}\text{N}$ and $\delta^{18}\text{O}$ values (Kendall et al. 2007), which allowed me to differentiate the sources of nitrogen

impacting the desert region. Samplers were erected during both the winter and summer to capture seasonal changes to pollution sources.

The final chapter of this dissertation asks: *Can soil and plant material be used as environmental indicators of anthropogenic nitrogen inputs?* Soil and plant samples were collected in the summer and winter to measure changes in isotopic composition across the deposition gradient. If plant and soil isotopes respond positively to deposition, then those samples can be used as a proxy for atmospheric sampling and will provide a tool to quickly analyze the anthropogenic contribution to a region.

References:

- Allen, E. B., L. E. Rao, R. J. Steers, A. Bytnerowicz, and M. E. Fenn. 2009. Impacts of atmospheric nitrogen deposition on vegetation and soils in Joshua Tree National Park. Pages 78-100 in R. H. Webb, L. F. Fenstermaker, J. S. Heaton, D. L. Hughson, E. V. McDonald, and D. M. Miller, editors. *The Mojave Desert: Ecosystem Processes and Sustainability*. University of Nevada Press, Las Vegas.
- Bytnerowicz, A. and M. E. Fenn. 1996. Nitrogen deposition in California forests: A review. *Environmental Pollution* 92:127-146.
- Bytnerowicz, A., M. J. Sanz, M. J. Arbaugh, P. E. Padgett, D. P. Jones, and A. Davila. 2005. Passive sampler for monitoring ambient nitric acid (HNO₃) and nitrous acid (HNO₂) concentrations. *Atmospheric Environment* 39:2655-2660.
- Cisneros, R., A. Bytnerowicz, D. Schweizer, S. Zhong, S. Traina, and D. H. Bennett. 2010. Ozone, nitric acid, and ammonia air pollution is unhealthy for people and ecosystems in southern Sierra Nevada, California. *Environmental Pollution* 158:3261-3271.
- Eilers, G., R. Brumme, and E. Matzner. 1992. Aboveground N-uptake from wet deposition by Norway spruce (*Picea-abies karst*). *Forest Ecology and Management* 51:239-249.
- Elliott, E. M., C. Kendall, E. B. Boyer, D. A. Burns, G. Lear, H. E. Golden, K. Harlin, A. Bytnerowicz, T. J. Butler, and R. Glatz. 2009. Dual nitrate isotopes in actively and passively collected dry deposition: Utility for partitioning NO_x sources, understanding reaction pathways, and comparison with isotopes in wet nitrate deposition. *Journal of Geophysical Research: Biogeosciences*.
- Elliott, E. M., C. Kendall, S. D. Wankel, D. A. Burns, E. W. Boyer, K. Harlin, D. J. Bain, and T. J. Butler. 2007. Nitrogen isotopes as indicators of NO_x source contributions to atmospheric nitrate deposition across the Midwestern and northeastern United States. *Environmental Science & Technology* 41:7661-7667.
- Evans, R. D. 2001. Physiological mechanisms influencing plant nitrogen isotope composition. *Trends in Plant Science* 6:121-126.

- Evans, R. D., A. J. Bloom, S. S. Sukrapanna, and J. R. Ehleringer. 1996. Nitrogen isotope composition of tomato (*Lycopersicon esculentum* Mill. cv. T-5) grown under ammonium or nitrate nutrition. *Plant, Cell & Environment* 19:1317-1323.
- Fenn, M. E., E. B. Allen, S. B. Weiss, S. Jovan, L. H. Geiser, G. S. Tonnesen, R. F. Johnson, L. E. Rao, B. S. Gimeno, F. Yuan, T. Meixner, and A. Bytnerowicz. 2010. Nitrogen critical loads and management alternatives for N-impacted ecosystems in California. *Journal of Environmental Management* 91:2404-2423.
- Fenn, M. E., J. S. Baron, E. B. Allen, H. M. Rueth, K. R. Nydick, L. Geiser, W. D. Bowman, J. O. Sickman, T. Meixner, D. W. Johnson, and P. Neitlich. 2003a. Ecological effects of nitrogen deposition in the western United States. *Bioscience* 53:404-420.
- Fenn, M. E., R. Haeuber, G. S. Tonnesen, J. S. Baron, S. Grossman-Clarke, D. Hope, D. A. Jaffe, S. Copeland, L. Geiser, H. M. Rueth, and J. O. Sickman. 2003b. Nitrogen emissions, deposition, and monitoring in the western United States. *Bioscience* 53:391-403.
- Galloway, J. N., F. J. Dentener, D. G. Capone, E. W. Boyer, R. W. Howarth, S. P. Seitzinger, G. P. Asner, C. C. Cleveland, P. A. Green, E. A. Holland, D. M. Karl, A. F. Michaels, J. H. Porter, A. R. Townsend, and C. J. Vorosmarty. 2004. Nitrogen cycles: past, present, and future. *Biogeochemistry* 70:153-226.
- Harrison, K. A., B. Roland, and R. D. Bardgett. 2007. Preferences for Different Nitrogen Forms by Coexisting Plant Species and Soil Microbes. *Ecology* 88:989-999.
- Hogberg, P. 1997. Tansley review No 95 - N-15 natural abundance in soil-plant systems. *New Phytologist* 137:179-203.
- James, J. J., Z. T. Aanderud, and J. H. Richards. 2006. Seasonal timing of N pulses influences N capture in a saltbush scrub community. *Journal of Arid Environments* 67:688-700.
- Johnson, N. C., D. L. Rowland, L. Corkidi, L. M. Egerton-Warburton, and E. B. Allen. 2003. Nitrogen enrichment alters mycorrhizal allocation at five mesic to semiarid grasslands. *Ecology* 84:1895-1908.

- Kendall, C., E. M. Elliott, and S. D. Wankel. 2007. Tracing Anthropogenic Inputs of Nitrogen. *in* R. Michener and K. Lajtha, editors. *Stable Isotopes in Ecology and Environmental Science*. Wiley-Blackwell, Malden, MA.
- Michalski, G., T. Meixner, M. Fenn, L. Hernandez, A. Sirulnik, E. Allen, and M. Thiemens. 2004. Tracing atmospheric nitrate deposition in a complex semiarid ecosystem using $\Delta(17)O$. *Environmental Science & Technology* 38:2175-2181.
- NADP. 2012. National Atmospheric Deposition Program 2011 Annual Summary. Illinois State Water Survey.
- Ochoa-Hueso, R., E. B. Allen, C. Branquinho, C. Cruz, T. Dias, M. E. Fenn, E. Manrique, M. E. Pérez-Corona, L. J. Sheppard, and W. D. Stock. 2011. Nitrogen deposition effects on Mediterranean-type ecosystems: An ecological assessment. *Environmental Pollution* 159:2265-2279.
- Padgett, P. E., E. B. Allen, A. Bytnerowicz, and R. A. Minich. 1999. Changes in soil inorganic nitrogen as related to atmospheric nitrogenous pollutants in southern California. *Atmospheric Environment* 33:769-781.
- Pardo, L. H., M. E. Fenn, C. L. Goodale, L. H. Geiser, C. T. Driscoll, E. B. Allen, J. S. Baron, R. Bobbink, W. D. Bowman, C. M. Clark, B. Emmett, F. S. Gilliam, T. L. Greaver, S. J. Hall, E. A. Lilleskov, L. Liu, J. A. Lynch, K. J. Nadelhoffer, S. S. Perakis, M. J. Robin-Abbott, J. L. Stoddard, K. C. Weathers, and R. L. Dennis. 2011. Effects of nitrogen deposition and empirical nitrogen critical loads for ecoregions of the United States. *Ecological Applications* 21:3049-3082.
- Rock, L. and B. H. Ellen. 2007. Nitrogen-15 and oxygen-18 natural abundance of potassium chloride extractable soil nitrate using the denitrifier method. *Soil Science Society of America Journal* 71:355-361.
- Rock, L., B. H. Ellert, and B. Mayer. 2011. Tracing sources of soil nitrate using the dual isotopic composition of nitrate in 2 M KCl-extracts. *Soil Biology and Biochemistry* 43:2397-2405.
- Schimel, J. P. and J. Bennett. 2004. Nitrogen mineralization: Challenges of a changing paradigm. *Ecology* 85:591-602.

- Solomon, P. A., L. G. Salmon, T. Fall, and G. R. Cass. 1992. Spatial and temporal distribution of atmospheric nitric acid and particulate nitrate concentrations in the Los Angeles area. *Environmental Science & Technology* 26:1594-1601.
- Templer, P. H. and K. C. Weathers. 2011. Use of mixed ion exchange resin and the denitrifier method to determine isotopic values of nitrate in atmospheric deposition and canopy throughfall. *Atmospheric Environment* 45:2017-2020.
- Vitousek, P. M. 1994. Beyond Global Warming: Ecology and Global Change. *Ecology* 75:1861-1876.

Chapter 1: Correcting for background nitrate contamination from crystalline KCl during stable isotopic analysis of oxygen and nitrogen by denitrification

Abstract

Potassium chloride (KCl) is a common reagent for extraction of mineral NO_3^- and NH_4^+ from a soil sample. Previous research has shown that the denitrifying bacteria *Pseudomonas chlororaphis ssp. aureofaciens* (*P. aureofaciens*) can be used to measure $\delta^{15}\text{N}$ and $\delta^{18}\text{O}$ of extracted nitrate using standard procedures. We discovered that when adding a 1M KCl sample to *P. aureofaciens* broth, there was an increase in N_2O production that significantly altered measured isotopic composition of samples. This experiment aimed to determine if the N_2O production was due to contamination in the KCl or if it was due to a biological response by the bacteria. Three different sources of crystalline KCl were dissolved in DDI water to create solutions of increasing molarity (0.1M to 2M) which were added to *P. aureofaciens* broth and measured for N_2O production. International standards USGS-32, USGS-34, and USGS-35 were then dissolved in the same range of KCl concentrations to measure isotopic response. Reference samples were then created to measure the impact of KCl on the range of $\delta^{15}\text{N}$ values.

The amount of N_2O produced by the KCl blanks increased linearly with increasing molarity, but at different rates for each source. Nitrate concentration was measured to be .000052% to 0.00075% by weight of crystalline KCl. Each variety of KCl had unique and consistent $\delta^{15}\text{N}$ and $\delta^{18}\text{O}$ signatures that stabilized with increasing molarity. The $\delta^{15}\text{N}$ and $\delta^{18}\text{O}$ of each international standard changed consistently towards measured KCl values, but when corrected for using a two source mixing model, did not remove all isotopic drift. There is an increase in the rate of fractionation towards less enriched isotopologues of NO_3^- as the sample becomes more enriched. The results of our experiment suggest that there is a small amount of NO_3^- present in crystalline KCl which skews isotopic measurements. The isotopic discrepancies can be corrected for using standards dissolved in KCl and diluting all samples and standards to the same concentration of KCl, and then correcting for fractionation. All samples must be added to the broth at a constant volume, maintaining a constant mixing and fractionation response to KCl. Due to the fractionation that occurs with enriched ^{15}N , standards USGS-32 and IAEA- NO_3 should be used to calibrate for $\delta^{15}\text{N}$ of the samples.

Introduction

Analysis of stable isotopes of oxygen (O) and nitrogen (N) of nitrate through bacterial denitrification has advanced our understanding of anthropogenic nitrate loading to the ecosystem (Kendall 1998, Burns and Kendall 2002, Amundson et al. 2003, Scrimgeour and Robinson 2004). Anthropogenically produced nitrate has distinct

isotopic signatures of both $\delta^{15}\text{N}$ and $\delta^{18}\text{O}$ dependent on its source. Creating dual source mixing models based on these values and background nitrate levels can help determine the amount of nitrogen being added to a local system (Burns and Kendall 2002, Elliott et al. 2007, Rock et al. 2011). Recent studies have analyzed potassium chloride (KCl) solutions (1-2M) containing extracted nitrate samples using the denitrifying bacteria *Pseudomonas chlororaphis ssp. aureofaciens* (*P. aureofaciens*) without measuring any isotopic irregularities in their samples (Rock and Ellert 2007, Rock et al. 2011, Templer and Weathers 2011). When we introduced a 1M KCl solution to the bacterial broth, we measured an increase in N_2O production compared with the DDI samples and a concurrent change in isotopic values of standards.

Potassium chloride is a chemical commonly used as an extraction reagent to measure available NO_3^- and NH_4^+ in a soil sample, and is also used to extract ions from exchange resins (Binkley and Matson 1983, Fenn et al. 2002). *P. aureofaciens* was initially used in salt water samples to measure anthropogenic nitrate additions (Sigman et al. 2001, Casciotti et al. 2002), suggesting that it should be adapted to saline conditions, such as samples extracted with KCl. The label of standard reagent grade KCl indicates purity between 99-100.5% KCl. According to the American Chemical Society Reagent Grade specifications, chlorate and nitrate maybe be present in levels of <.003% by weight (ACS 2005). At the maximum level, a 1M solution of KCl would have a NO_3^- concentration of $6.7 \mu\text{g ml}^{-1}$ which would produce a NO_3^- spike that would overpower

the sample nitrate during analysis. If this is the source of the nitrate, it must exist in a much lower quantity.

When blank samples of a 1M KCl soil extract were initially added to the bacteria broth, the amount of N₂O produced increased from the equivalent of 1% of average sample N₂O production to 11% of N₂O production (Figure 1.1, X symbols). When international standards USGS-32, USGS-34, and USGS-35 were dissolved in 1M KCl solutions, there was a significant effect on measured $\delta^{15}\text{N}$ and $\delta^{18}\text{O}$ values, with a response towards more negative $\delta^{15}\text{N}$ and $\delta^{18}\text{O}$ values (Figure 1.2).

This experiment examined the response of *P. aureofaciens* to KCl to determine if the interaction measured is the result of the mixing of trace amounts of nitrate in the KCl solution or if the ionic matrix is producing a biological response from the bacteria by increasing fractionation during denitrification. This was measured by introducing two additional chemical grades of KCl and measuring the response of N₂O production in blank samples followed by measuring the change in $\delta^{15}\text{N}$ and $\delta^{18}\text{O}$ values of international standards USGS-32, USGS-34, and USGS-35 when dissolved in the same KCl concentration gradient. We hypothesized that increasing the molarity of KCl will result in an increased amount of N₂O produced due to NO₃⁻ in the reagent. We also hypothesized that the isotopic response of the standards will change in accordance with a two source mixing model.

Methods

Sample preparation:

To determine the $\delta^{15}\text{N}$ and $\delta^{18}\text{O}$ values of NO_3^- , a bacterial method was used to convert NO_3^- into N_2O . (Sigman et al. 2001, Casciotti et al. 2002). The bacteria *P. aureofaciens* (ATCC# 13985) lacks nitrous oxide reductase activity and therefore produces nitrous oxide gas as a final product of denitrification which allows the isotopic ratio of N and O to be determined. The bacteria was grown in a modified soy broth solution for 7-10 days, concentrated and sealed in a 20ml headspace vial and sparged with He gas for 2 hours. Samples were then added to the vials which were inverted overnight to allow for complete conversion of nitrate while minimizing N_2O loss. The following morning 0.1 ml 10N NaOH was added to each vial to raise the pH of solution, lysing the bacteria to stop denitrification and immobilizing CO_2 gas as dissolved inorganic carbon. Samples were loaded on a PAL GC and sparged with He gas forcing N_2O gas in the headspace to be cryogenically focused in a liquid nitrogen trap. After separating gases in a GC column, the m/z ratios 44, 45, 46 were measured using a Thermo Delta V isotope ratio mass spectrometer to derive $\delta^{18}\text{O}$ and $\delta^{15}\text{N}$ values for each sample.

Altering sample salinity:

To determine if the increase in N_2O was directly correlated with the KCl addition, two varieties of crystalline KCl [Fisher Chemical, Crystalline/EP/BP/USP/FCC (Fisher-

Reagent) and Acros Organics, Extra Pure (Acros)] were dissolved in DDI water to form concentrations between 0.25 and 2 M KCl. These samples were run concurrently with DDI water samples to account for background NO_3^- . 3 ml samples of each solution were added to a vial of *P. aureofaciens* broth and measured using the above methods.

Response of standards to KCl

USGS 32, USGS-34, and USGS-35 were then dissolved in the same concentrations of the Fisher Chemical KCl as used above, and a 1M concentration of the Acros Organics KCl. Standards were also dissolved in DDI water to set baseline measurements. All samples were diluted to a concentration of $1 \mu\text{g ml}^{-1}$ and were added to the vials in 3ml aliquots providing approximately 50nmols of NO_3^- to the bacteria for conversion. Using the same volume for each sample allowed for any response due to the KCl to be consistent across each set of samples.

International standards USGS-32, USGS-34, and USGS-35 were used as samples of known isotopic composition to correct for instrumental error in isotopic measurements. USGS-32 and USGS-34 were used as endmembers to create a first order calibration curve for N and USGS-34 and USGS-35 were used to create a first order equation to calibrate for O.

Testing calibration

In order to test the efficacy of the calibration, five reference standards between 10 and 125 ‰ were created by mixing USGS-32 and USGS-34 in measured quantities. These standards were chosen because they represent the two endmembers of our isotope calibration curve, and they do not contain any ^{17}O isotopes which can affect the reported $\delta^{15}\text{N}$ value due to it not being fractionated during denitrification. The reference samples were created in DDI water as well as a 1M KCl solution. All samples were diluted to a concentration of $1\ \mu\text{g ml}^{-1}$ and were added to the vials in 3ml aliquots.

Results and Discussion

As the concentration of both KCl varieties increased in the blank samples, the amount of N_2O produced from each sample increased linearly (Figure 1.1). Both the Fisher-Reagent and Acros varieties of KCl had significantly lower N_2O production relative to the original Fisher KCl (ANCOVA Effects: $df=2$, $F=15.78$, $p < 0.0001$). The linear increase of N_2O production with increasing KCl additions suggests that there is NO_3^- in the crystalline KCl. The two new varieties of KCl are also increasing at different rates (ANCOVA Effects: $df=1$, $F=15.78$, $p < 0.05$), meaning that each variety has a unique, but consistent concentration of NO_3^- contamination. Calculating the amount of NO_3^- present in the KCl based on the size of the m/z 44 peak indicates that a 3ml 1M KCl sample contains $0.167\ \mu\text{g NO}_3^-$ or $.000075\ \%$ NO_3^- by weight for the Fisher-Reagent and $0.117\ \mu\text{g NO}_3^-$ or $.000052\ \%$ NO_3^- by weight for the Acros Organics. This is much lower than the

labeled value, but still represents between 3.75 and 5.27% of the total nitrate in a standard diluted sample. This amount of KCl is at the low end of the detectable range on most continuous flow and discrete analyzers.

The measurements of the new varieties of KCl were more consistent than the original KCl values, due to an increase in accuracy of lab analysis and the increase in the purity of the KCl reagents. The $\delta^{15}\text{N}$ and $\delta^{18}\text{O}$ of both the Fisher-Reagent and Acros KCl stabilized with increasing molarity; each increased towards unique values. The change of each isotope value was consistent with a two source mixing model where one source is at a constant concentration (DDI water) and the second is increasing in mass (KCl). Using a logarithmic regression on the slopes provides $\delta^{15}\text{N}$ and $\delta^{18}\text{O}$ values of -7.78 and -2.23 for the Fisher-Reagent KCl and 3.81 and 8.67 for the Acros Organic KCl. The fact that the values were consistent across all samples indicates that the addition of NO_3^- from KCl can be corrected for during analysis, but because the two forms of KCl had independent $\delta^{15}\text{N}$ and $\delta^{18}\text{O}$ signatures, the impact of KCl additions on sample isotopic values will vary with the type of KCl used.

When USGS standards were prepared in Fisher-Reagent KCl solutions, the measured $\delta^{15}\text{N}$ and $\delta^{18}\text{O}$ values were as consistently accurate as DI samples, each having a standard error of 0.2‰ $\delta^{15}\text{N}$ and $\delta^{18}\text{O}$, but were not as precise as samples prepared in DDI water. The measured $\delta^{15}\text{N}$ and $\delta^{18}\text{O}$ of known standards changed with increasing molarity of KCl, responding linearly relative to the size amount of KCl in solution (Figure 1.4). The change in $\delta^{15}\text{N}$ of all standard samples was less enriched than

expected values, which would be expected due to the $\delta^{15}\text{N}$ of Fisher-Reagent KCl being measured at -7.78‰. The relative change in $\delta^{15}\text{N}$ values of 1M Acros USGS-32 and USGS-34 was consistent with a smaller drop in USGS-32 and a slight increase in measured USGS-34. The change in $\delta^{18}\text{O}$ of the samples changed in opposite directions on the outer range for standard values, consistent with what would be expected due to $\delta^{18}\text{O}$ values of both KCl additions.

The presence of a second source of NO_3^- did not account for all of the isotopic drift in measured values. Correcting the delta values of the samples using a two source mixing model (Eq. 1, $X=^{15}\text{N}$ or ^{18}O) shifted the values toward the expected values, but there remained a discrepancy between measured and expected values (Table 1).

$$\delta X_{\text{CORR}} = [(m/z 44_{\text{H}_2\text{O-SAMPLE}} - m/z 44_{\text{KCL BLANK}}) * \delta X_{\text{H}_2\text{O}} + (m/z 44_{\text{KCL BLANK}}) * \delta X_{\text{KCL BLANK}}] / (m/z 44_{\text{SAMPLE}}) \quad \text{Eq. 1}$$

The drift in N values increased with the enrichment of the sample and was most evident in USGS-32. In the 1M KCl samples, the corrected $\delta^{15}\text{N}_{\text{USGS32}}$ was 10.3 – 12.4‰ less enriched than expected, suggesting that there is a secondary interaction between the KCl solution and *P. aureofaciens* that is inducing fractionation during the denitrification process. Correcting the O isotope values tightened the relationship to expected values; differences from expected values were more enriched at negative $\delta^{18}\text{O}$ values and became less enriched as $\delta^{18}\text{O}$ increased.

The standards in a 1M KCl matrix generally produced more N₂O during denitrification compared to standards in DDI water alone, but this was not consistent with the expected amount of N₂O produced by the same KCl concentration alone (Figure 1.3). The difference between the expected N₂O production (sample N₂O + KCl N₂O) and measured N₂O production may be the result of incomplete conversion of sample NO₃⁻ to N₂O due to the KCl matrix. This argument is strengthened by the fact that when the soy broth solution used to grow the bacteria was altered to a 1M KCl concentration, there was no bacterial growth, suggesting that the KCl environment may be toxic to *P. aureofaciens*.

Since N is balanced during denitrification ($2\text{NO}_3^- \rightarrow 2\text{NO}_2^- \rightarrow 2\text{NO} \rightarrow \text{N}_2\text{O}$), the N molecules are most likely to suffer from fractionation due to incomplete conversion to N₂O. Because less enriched NO₃⁻ is processed faster during the denitrification reaction, it would be expected to produce a final product with a less enriched isotopic signature if the entire sample was not denitrified. Only 1 in 6 O atoms are conserved during denitrification by *P. aureofaciens*, suggesting any fractionation of isotopologues of O in NO₃⁻ may be buffered by O from the sample solution.

The relationship among a range of isotopologues of NO₃⁻ is better understood by evaluating the atom percent (^HAP) of the source and measured NO₃⁻ pools. The ^HAP is the percentage of a molecule that is made up of the heavier isotope of the atom (Eq.2, for N-R_{STANDARD}= 0.0036765; O-R_{STANDARD}= 0.0020052). The amount of fractionation (Δ)

that occurs with the change in matrix concentration is the difference between the atom percentage of a sample in H₂O and a sample in KCl (Eq. 3).

$${}^H\text{AP} = 100 * (\delta^{15}\text{N} + 1000) / [(\delta^{15}\text{N} + 1000 + (1000/R_{\text{Standard}}))] \quad \text{Eq. 2}$$

$$\Delta = {}^H\text{AP}_{\text{H}_2\text{O}} - {}^H\text{AP}_{\text{KCl-CORR}} \quad \text{Eq. 3}$$

As the δ of both N and O of the sample increase independently, there is a linear increase in Δ (N: $r^2 = 0.999938$, $p < 0.0001$; O: $r^2 = 0.999464$, $p < 0.0001$). This indicates that as NO_3^- samples become more isotopically enriched, there is an increase in fractionation against the heavier isotope during denitrification. Since the relationship is linear for both elements and across all values, a first order linear regression of δX_{CORR} (Eq. 1; N: USGS-32, USGS-34; O: USGS-34, USGS-35) was developed against their expected values. Inputting the reference samples into the resulting equations results in a precision below the standard error associated with the instrument.

Since fractionation is minimal at lower values, an alternate method would be to use a reference standard with a $\delta^{15}\text{N}$ between 5 and 10‰, e.g. IAEA-5 (4.7‰). This standard will provide accuracy within 0.4 ‰ for samples within the natural abundance range of (-5 to 25‰; (Kendall 1998)) (Table 2). If enriched isotopic tracers are going to be used in conjunction with KCl extracts, it will be imperative to determine the effects of KCl on higher $\delta^{15}\text{N}$ values.

Conclusions

Based on the results, it appears that standard reagent grade KCl has a minute amount of NO_3^- in the crystals that mix with sample KCl. There is also an interaction between *P. aureofaciens* and the KCl matrix that creates fractionation against heavier isotopes of both O and N. The bacteria produce accurate isotopic measurements that can be calibrated to known standards using a two source mixing model based on blank KCl samples and standards created in DDI water. This method provides an effective technique of calibrating for the interaction between a KCl solution and *P. aureofaciens*. When analyzing samples in a KCl matrix, it is imperative that the samples are all diluted to the same concentration so that the same amount of KCl is added to each vial. This way, each sample will be equally contaminated by the KCl NO_3^- and the amount of fractionation that occurs will be consistent. The same source of KCl that was used to extract the samples needs to be used to make the dilutions as NO_3^- in each source of KCl has a unique isotopic signature. The accuracy of the measurements allows the $\delta^{15}\text{N}$ and $\delta^{18}\text{O}$ values to be measured to 0.2‰, equivalent to the error associated with the instrument. This technique will allow accurate measurement of $\delta^{15}\text{N}$ and $\delta^{18}\text{O}$ in KCl extracts of soils or ion exchange resins with low concentrations of NO_3^- .

References

- ACS. 2005. Reagent Chemicals: Specifications and Procedures *in* A. C. Society, editor. Oxford University Press.
- Amundson, R., A. T. Austin, E. A. G. Schuur, K. Yoo, V. Matzek, C. Kendall, A. Uebersax, D. Brenner, and W. T. Baisden. 2003. Global patterns of the isotopic composition of soil and plant nitrogen. *Global Biogeochemical Cycles* 17:11.
- Binkley, D. and P. Matson. 1983. Ion Exchange Resin Bag Method For Assessing Forest Soil Nitrogen Availability. *Soil Sci. Soc. Am. J.* 47:1050-1052.
- Burns, D. A. and C. Kendall. 2002. Analysis of $\delta^{15}\text{N}$ and $\delta^{18}\text{O}$ to differentiate NO_3^- sources in runoff at two watersheds in the Catskill Mountains of New York. *Water Resour. Res.* 38:1051.
- Casciotti, K. L., D. M. Sigman, M. G. Hastings, J. K. Böhlke, and A. Hilkert. 2002. Measurement of the Oxygen Isotopic Composition of Nitrate in Seawater and Freshwater Using the Denitrifier Method. *Analytical Chemistry* 74:4905-4912.
- Elliott, E. M., C. Kendall, S. D. Wankel, D. A. Burns, E. W. Boyer, K. Harlin, D. J. Bain, and T. J. Butler. 2007. Nitrogen isotopes as indicators of NO_x source contributions to atmospheric nitrate deposition across the Midwestern and northeastern United States. *Environmental Science & Technology* 41:7661-7667.
- Fenn, M. E., M. A. Poth, and M. J. Arbaugh. 2002. A Throughfall Collection Method Using Mixed Bed Ion Exchange Resin Columns. *TheScientificWorldJOURNAL* 2:122-130.
- Kendall, C. 1998. Tracing Nitrogen Sources and Cycling in Catchments. Pages 519-576 *in* C. Kendall and J. J. McDonnell, editors. *Isotope Tracers in Catchment Hydrology*. Elsevier Science B.V, Amsterdam.
- Rock, L. and B. H. Ellert. 2007. Nitrogen-15 and Oxygen-18 Natural Abundance of Potassium Chloride Extractable Soil Nitrate Using the Denitrifier Method. *Soil Sci. Soc. Am. J.* 71:355-361.
- Rock, L., B. H. Ellert, and B. Mayer. 2011. Tracing sources of soil nitrate using the dual isotopic composition of nitrate in 2 M KCl-extracts. *Soil Biology and Biochemistry* 43:2397-2405.

- Scrimgeour, C. M. and D. Robinson. 2004. Stable isotope analyses and applications. Page 576 *in* K. A. Smith and M. S. Cresser, editors. Soil and environmental analysis modern instrumental techniques. M. Dekker, New York.
- Sigman, D. M., K. L. Casciotti, M. Andreani, C. Barford, M. Galanter, and J. K. Bohlke. 2001. A bacterial method for the nitrogen isotopic analysis of nitrate in seawater and freshwater. *Analytical Chemistry* 73:4145-4153.
- Templer, P. H. and K. C. Weathers. 2011. Use of mixed ion exchange resin and the denitrifier method to determine isotopic values of nitrate in atmospheric deposition and canopy throughfall. *Atmospheric Environment* 45:2017-2020.

Tables and Figures

Standard	$\delta^{15}\text{N}$				$\delta^{18}\text{O}$			
	Expected	DDI Water	Corrected Fisher-Reagent	Corrected Acros	Expected	DDI Water	Corrected Fisher-Reagent	Corrected Acros
USGS-32	180.00	178.39	164.94	169.72	25.70	22.20	24.00	24.85
USGS-34	-1.80	-1.28	-1.74	-1.55	-27.90	-26.69	-25.71	-25.43
USGS-35	3.80	4.22	2.91	3.69	57.50	53.02	53.69	54.57

Table 1.1: Given $\delta^{15}\text{N}$ and $\delta^{18}\text{O}$ values of internationally accepted standards from IAEA (2009) and recorded values of standards in DDI and KCL matrices.

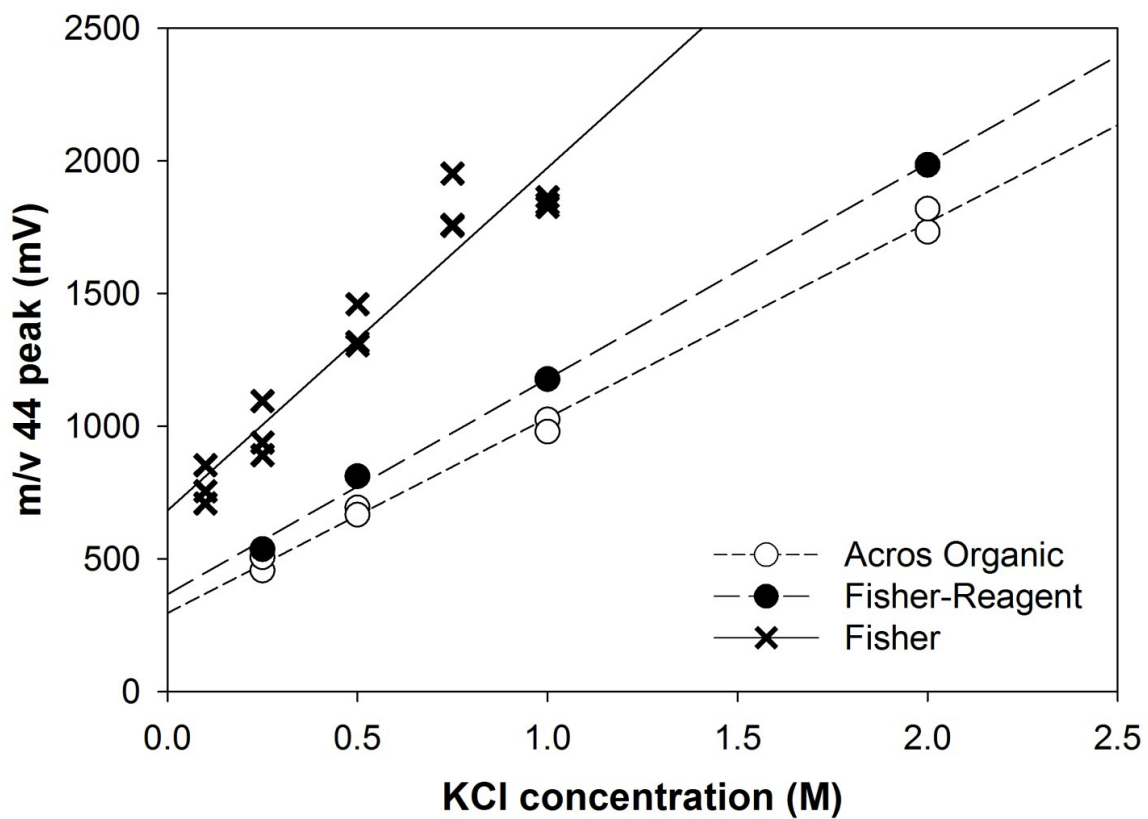


Figure 1.1. The size of the measured m/z 44 peak increases with increasing concentration of KCl dissolved in DDI water using three different varieties of KCl. Each KCl variety has a unique slope and therefore a unique amount of NO_3^- contamination.

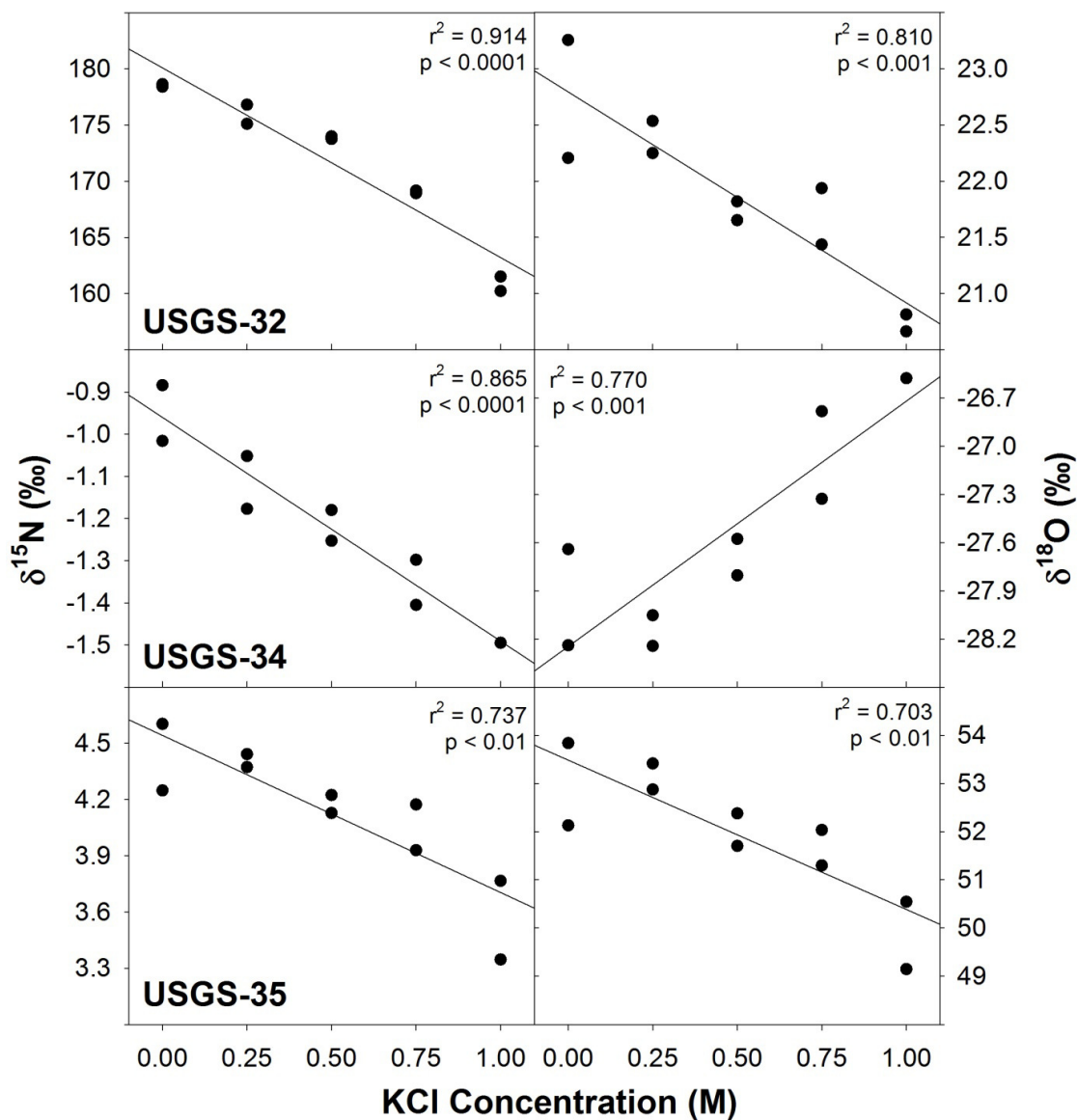


Figure 1.2. As the concentration of the sample matrix increases in concentration of KCl, the measured precision of $\delta^{15}\text{N}$ and $\delta^{18}\text{O}$ of USGS-32, USGS-34, and USGS-35 decreases. All of the $\delta^{15}\text{N}$ values decrease suggesting a secondary source of NO_3^- with a $\delta^{15}\text{N} < -1.8$. Based on the direction of the change in $\delta^{18}\text{O}$ of the standards, the secondary source is between -26 and 21‰.

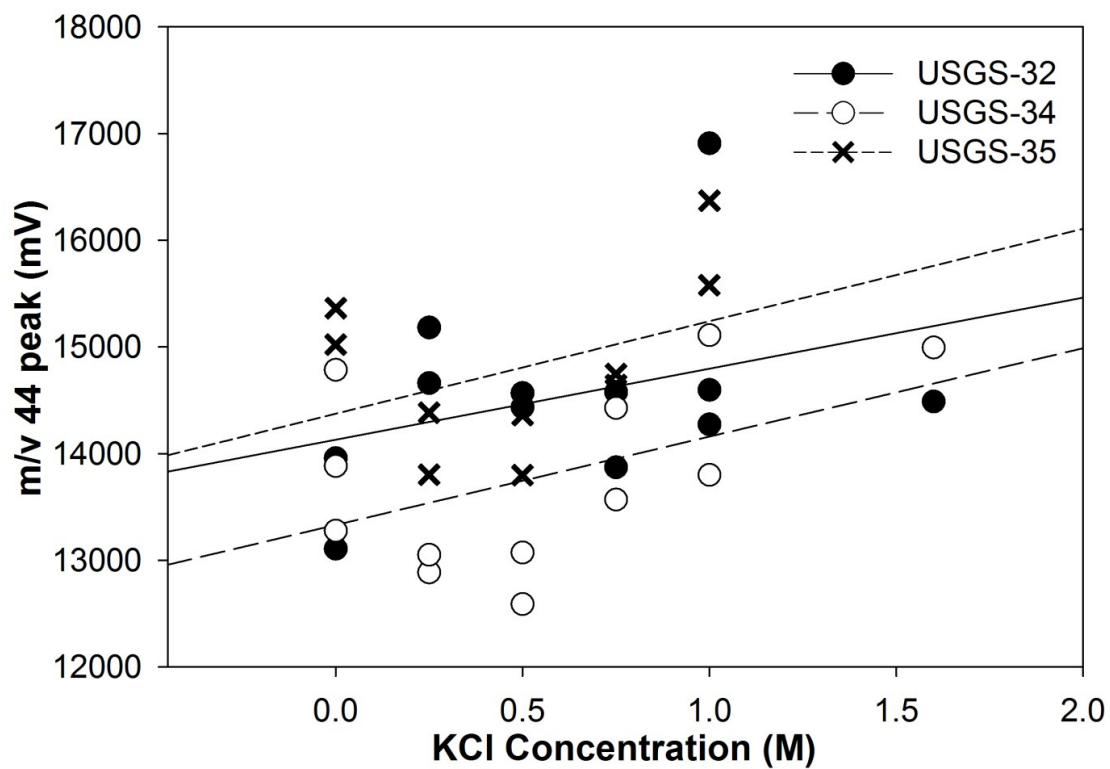


Figure 1.3. The increase in concentration of KCl in standard solutions results in a trend towards an increase in the amount of N_2O produced. The slopes of the correlations are between 666 and 866 mV/M for each standard, but all p values are > 0.1

	Calibrated DDI	Calibrated Fisher- Reagent	±	Calibrated and corrected Fisher-Reagent	±	^H AP _{H₂O}	^H AP _{KCl-CORR}	Δ
δ¹⁵N								
USGS-34	-1.80	-1.80	0.00	-1.80	0.00	0.3659	0.3657	0.0002
	9.53	10.46	-0.93	9.51	0.02	0.3700	0.3693	0.0007
	23.85	26.37	-2.53	23.76	0.09	0.3752	0.3739	0.0013
	47.69	53.55	-5.86	47.83	-0.13	0.3838	0.3816	0.0022
	96.10	107.50	-11.40	96.21	-0.11	0.4012	0.3970	0.0042
	121.21	135.67	-14.46	119.77	1.44	0.4102	0.4045	0.0057
USGS-32	180.00	179.99	0.01	180.00	0.00	0.4314	0.4237	0.0077
δ¹⁸O								
USGS-34	-27.90	-27.90	0.00	-27.90	0.00	0.1945	0.1953	-0.0007
	-24.42	-24.88	0.46	-24.21	-0.21	0.1953	0.1959	-0.0006
	-20.00	-21.12	1.13	-20.10	0.10	0.1961	0.1965	-0.0004
	-12.63	-12.66	0.03	-12.64	0.01	0.1976	0.1978	-0.0002
	2.11	2.42	-0.30	2.02	0.10	0.2005	0.2002	0.0003
	9.48	10.49	-1.00	8.80	0.68	0.2019	0.2013	0.0005
USGS-32	25.70	25.70	0.00	25.70	0.00	0.2053	0.2042	0.0011

Table 1.2. Measured and corrected $\delta^{15}\text{N}$ and $\delta^{18}\text{O}$ for reference standards made in DI water and KCl. Samples were calibrated by regressing measured USGS-32 and USGS-34 values against their expected values. The corrected values were calculated using Eq. 1 to standardize for the input of NO_3^- from the KCl solution. Δ increases for both elements with an increase in the percentage of the heavier isotope.

Chapter 2: Consistency of isotopologues of atmospheric nitric acid in passively collected samples

Abstract

Anthropogenic sources of NO_x have distinct isotopic signatures of oxygen and nitrogen, and might be used to differentiate anthropogenic from natural sources of N. Methods were developed to test the applicability of this approach; Nylon filters are currently used in passive sampling arrays to measure atmospheric nitric acid concentrations to estimate the amount of reactive nitrogen being deposited to the environment. This experiment measures the ability of nylon filters to consistently collect isotopologues of atmospheric nitric acid in the same ratios as they are present in the atmosphere. Samplers were erected in high and low concentration continuous stirred tank reactors (CSTR) as well as high and low deposition field sites in the Colorado Desert, California. Filters were exposed over a four week period with individual filters being subjected to 1-4 week exposure times. Extracts of collected nitric acid were measured for $\delta^{18}\text{O}$ and $\delta^{15}\text{N}$ ratios and compared for consistency based on length of exposure and amount of HNO_3 collected.

Filters within the CSTRs collected HNO_3 at a consistent rate in each of the chambers. After two weeks of exposure, the mean $\delta^{18}\text{O}$ values were within 0.5‰ of the $\delta^{18}\text{O}$ of the source HNO_3 solution. The mean of all weekly exposures were within 0.5‰

of the $\delta^{15}\text{N}$ of the source solution, but after three weeks, the mean $\delta^{15}\text{N}$ of collected HNO_3 was within 0.2‰. The field samplers collected HNO_3 consistent with previously measured values from high deposition sites having three times as much nitric acid as the low deposition sites. The mean $\delta^{18}\text{O}$ of the High sites was 52.2‰ compared to 35.7‰ at the Low sites, consistent with higher anthropogenic loading at the high site. Mean $\delta^{15}\text{N}$ values were similar at both high and low sites. Due to precipitation events occurring during the exposure period, the $\delta^{15}\text{N}$ and $\delta^{18}\text{O}$ of nitric acid were highly variable at all sites. Change in $\delta^{15}\text{N}$ and $\delta^{18}\text{O}$ were linearly correlated at sites with similar deposition levels, but the rate of change was different at the high and low sites. The rates of change of the isotopologues were consistent with a two source mixing model. Direct anthropogenic sources of atmospheric nitric acid were determined to account for 58% of the atmospheric nitric acid at the high sites and 36.5% of the atmospheric nitric acid at the low sites.

The nylon filters proved to be an effective means of collecting isotopologues of HNO_3 consistent with atmospheric concentrations. Length of exposure of two weeks stabilized isotopologue composition and minimized the chance of variable weather events altering atmospheric values. The method can be applied to determine the relative contribution of anthropogenic nitrate along N deposition gradients.

Introduction

Anthropogenic nitrogen (N) deposition has become a global problem because of increased use of fertilizers, increased domestic animal wastes, and N emissions from industry and internal combustion engines (Vitousek et al. 1997, Fenn et al. 2003a, Fenn et al. 2003b, Galloway et al. 2003). The National Atmospheric Deposition Program (NADP) and Environmental Protection Agency Clean Air Status and Trends Network (CASTNET) have national networks designed to measure wet and dry deposition across the continental United States. Both networks' sites are concentrated in the eastern half of the US and have large data gaps in the western United States due to the presence of expansive remote areas (NADP 2012). The US Forest Service has developed a simple and inexpensive passive atmospheric sampling system that allows for large scale monitoring of atmospheric nitric acid in specific areas of interest (Bytnerowicz et al. 2005). These samplers have been used to determine that NADP and CASNET maps have underestimated levels of deposition in the western US by omitting measures of dry deposition and placing samplers far from anthropogenic sources (Allen et al. 2009, Cisneros et al. 2010, Fenn et al. 2010).

Atmospheric N can be deposited to the ecosystem either directly or chemically to surfaces during the dry season or dissolved in precipitation as wet deposition during the rainy season (Seinfeld and Pandis 1998). Due to photochemical reactions, reactive N concentrations fluctuate throughout the year, peaking in the summer and dipping during the winter season (Calvert et al. 1985). The timing of peak atmospheric reactive

N concentration coincides with the dry season in the Colorado Desert of California leading to N primarily being deposited as dry deposition (Fenn et al. 2003b).

Southern California receives and produces some of the highest anthropogenic N deposition rates in the United States, with levels as high as $50 \text{ kg N ha}^{-1} \text{ yr}^{-1}$ just outside of Los Angeles, in the coniferous forests of the San Bernardino Mountains (Fenn et al. 1998, Fenn et al. 2003b, Tonnesen et al. 2003). Onshore winds carry oxidized and reduced N to the eastern edge of the Los Angeles basin where the atmospheric plume passes through the valley between the San Bernardino and the San Jacinto Mountains, and funnels into the Coachella Valley on the leeward side of the mountain range. Deposition decreases in an eastward gradient from the Los Angeles Basin as the N is deposited into the desert system (Tonnesen et al. 2003, Allen et al. 2009, Fenn et al. 2010). A second source of atmospheric nitric acid loading to this area originates from emissions from agriculture within the Coachella Valley. Historically, these operations, which consist of over 70,000 acres of farmland, have relied heavily on pesticides and herbicides that can volatilize reactive N into the atmosphere (Wang et al. 2008). Warm winter temperatures allow crops to be grown and harvested year round, providing a constant flux of anthropogenic N.

In addition to concentrations of N deposited to the ecosystem, it is also possible to measure the isotopic composition of NO_3^- and NH_4^+ to help distinguish the sources that contribute to anthropogenic N (Kendall 1998, Amundson et al. 2003, Scrimgeour and Robinson 2004). Nitrogen and oxygen (O) naturally exist with multiple stable atomic

weights of 14 and 15 for N, and 16, 17, and 18 for O. The change in atomic weight causes very slight differences in the vibration of the atom, and therefore the reactivity of small molecules containing a heavier isotope. These differences result in changes in isotopic composition between chemical reactants and products on the order of one in a thousand during reactions. The percentage of heavier isotopes within a given pool of molecules is then compared to an international standard that has a constant ratio of heavy to light isotopes. The standard notation for reporting the ratio of isotopes within a sample is:

$$\delta X = \left[\left(\frac{R_{\text{Sample}}}{R_{\text{Standard}}} \right) - 1 \right] * 1000$$

Where X = N or O. This is referred to as the delta notation, and is reported in parts per thousand (‰). When there is a large pool of reactants and the kinetic reaction is incomplete, the product tends to have a higher percentage of the light isotope.

Recent research in the eastern United States has shown the utility of using stable isotopes to determine the origins of air pollution (Elliott et al. 2007). NO_x molecules released from anthropogenic sources differ in the ratio of ¹⁸O/¹⁶O relative to those from biological nitrification. Measuring the change in isotopic signature of multiple elements across space can provide understanding of how molecules are moving through the atmosphere. Industrial combustion creates HNO₃ δ¹⁸O values between 20-60‰ while agriculture emissions have been measured between 20-30‰ (Michalski et al. 2004,

Rock and Ellen 2007). Agriculture emissions are a combination of NO_x emissions and volatilized particulate NH_4NO_3 . NO_x molecules released to the atmosphere undergo a series of photolytic reactions with ozone and hydroxyl radicals to produce HNO_3 . The chemical pathway leading to the production of HNO_3 will influence the final $\delta^{18}\text{O}$ of the pollutant (Hastings et al. 2003, Hastings et al. 2004). NO_3^- created through nitrification of NH_4 has a $\delta^{18}\text{O}$ between -5 and 5 due to the addition of two O atoms from water and one from O_2 (Andersson and Hooper 1983).

The $\delta^{15}\text{N}$ - HNO_3 of anthropogenic sources of HNO_3 also provide distinction among N sources, although the offset is not as large as it is for O isotopes. Atmospheric HNO_3 emitted from non fossil fuel sources (combustion of organic material, lightning, and volatilization of N in the soil) generally has a $\delta^{15}\text{N}$ value near 0‰ (Hoering 1957, Li and Wang 2008), and are expected to be below zero due to preferential volatilization of ^{14}N isotopologues. $\delta^{15}\text{N}$ of nitric oxides from vehicle exhaust has been measured between 3.8-5.7 ‰ (Ammann et al. 1999, Pearson et al. 2000). Previous studies have measured a seasonality effect on HNO_3 vapor with samples collected during the winter season being up to 3‰ higher than those collected in summer (Freyer 1991, Hastings et al. 2004).

While using the passive diffusion samplers, Elliot et al. (2009) observed an offset in $\delta^{18}\text{O}$ values between actively and passively collected samples. This offset may have been associated with fractionation of HNO_3 to the filters. Isotopic fractionation can occur when isotopologues of a molecule undergo a kinetic reaction, in this case, the absorption of HNO_3 to a Nylasorb™ filter. The first objective of the study is to determine

if isotopic fractionation of atmospheric HNO_3 is occurring when HNO_3 passively binds to the nylon filters in controlled atmospheric concentrations. I hypothesize that there will be increased fractionation towards a more enriched isotopic sample at higher atmospheric concentrations and at longer exposure times due to increasing saturation of the passive filter. An assessment of the accuracy of passive sampler arrays to measure stable isotopes of atmospheric nitric acid, will enable their use in remote areas yielding better understanding of anthropogenic sources of HNO_3 in the atmosphere. The second objective is to measure variation in isotopic composition of HNO_3 along an anthropogenic nitrogen deposition gradient. I hypothesize that there will be more variation in HNO_3 $\delta^{18}\text{O}$ and $\delta^{15}\text{N}$ in the low deposition sites due to the lower anthropogenic additions and higher percentage of mixing with natural sources. The first objective was tested under experimentally controlled HNO_3 concentrations in chambers, while the second was tested along a N deposition gradient.

Methods

Continuously Stirred Tank Reactors

To determine if fractionation of atmospheric HNO_3 $\delta^{15}\text{N}$ and $\delta^{18}\text{O}$ occurs upon adsorption to Nylasorb™ filters, the filters were exposed in continuously stirred tank reactors (CSTR) set to known HNO_3 concentrations. Ambient air is pumped through an activated charcoal canister and a HEPA filter capsule (model 12144 Gelman Sciences, Ann Arbor, MI, U.S.A.) to remove background atmospheric contaminants before a

concentrated HNO₃ solution is volatilized and mixed with the airstream and pumped into the sealed chambers. For details of the setup, please refer to Padgett et al. (2004). The flow of the HNO₃ enhanced air was controlled into each chamber individually to create three atmospheric concentrations: control, low (10 µg HNO₃/m³), and high (20 µg HNO₃/m³). The air within the chambers was actively circulated and is completely replaced every two minutes.

Filters were first installed in September 2011 in four sets of three replicates. After the first week, one set of filters were collected from the first set and three additional sets were exposed. This pattern continued until four 1-week, three 2-week, two 3-week, and one 4-week exposures were collected. This exposure schedule allowed for comparisons among the filters as they became more saturated. At least 20 µg of NO₃ are needed in solution for accurate values of δ¹⁵N and δ¹⁸O. Due to this limitation, two filters were exposed for each sample in the 1- and 2-week exposures and were combined during extraction.

The filter packs were constructed following the Bytnerowicz (2005) design. A 47mm Pall-Gelman Nylsorb™ filter was used as the collecting surface and was covered by a 47mm Zefluor™ PTFE Membrane filter to prevent particulate contamination. All filters were loaded into the filter packs within a glove-box. The atmosphere within the box was filtered with charcoal to remove reactive nitrogen molecules and eliminate contamination of the filters prior to exposure. The filters were loaded into filter packs constructed out of a Petri dish; allowing them to be capped to prevent contamination

before installation. Upon collection from the chambers, the filters were capped with the Petri dish lid and stored in the freezer at -20°C until all filters were collected and were extracted simultaneously.

Field Survey

Passive sampling arrays were installed in September 2011 at field sites along a nitrogen deposition gradient ranging from high concentration zones of the Los Angeles Air Basin into low concentration zones in the western Sonoran desert. Filters were installed on a crossbar 2.4 meters above the ground, protecting the filters from contamination by soil splash. Of the five sites, one was designated the 'source' site within the Los Angeles air basin [Botanic Gardens at UC Riverside (BG) – NAD83 UTM Zone 11, 470510E 3758845N, elev. 425m], two were in high deposition areas in the western Coachella Valley [Snow Creek (SC) – NAD83 UTM Zone 11, 530029E 3752090N, elev. 367m and Whitewater (WW) – NAD83 UTM Zone 11, 533005E 3756128N, elev. 505m], and two were in low deposition areas within Joshua Tree National Park [Pinto Basin (PB) – NAD83 UTM Zone 11, 614869E 3744147N, elev. 752m, and Sunrise Mill (SM) – NAD83 Zone 11, 620978E 3758602N, elev. 425m] (Figure 2.1). Significant rain events occurred on September 5, 2012 (during Week 1 exposures) and September 14, 2012 (during Week 2 exposures) at all sites. This caused road damage preventing access to the two low N deposition sites for the third week of sampling.

Nitric Acid Analysis

Once all of the air filters were collected, the filters were unloaded from their cases, placed in 125 ml polycarbonate Erlenmeyer flasks, to which 20ml of deionized water was added prior to being shaken on a wrist-action shaker. The resulting filter extract was decanted into a 20 mL HDPE scintillation vial and stored at -20°C. Once all filters were processed, the extracted solutions were analyzed for NO_3^- concentrations on a Technicon® continuous flow autoanalyzer located at UCR using EPA method. The total HNO_3 exposure (Exposure [$\mu\text{g m}^{-3} \text{h}^{-1}$]) was calculated using the NO_3^- concentration and the length of time it was exposed in the field (Bytnerowicz et al. 2005).

The NO_3^- $\delta^{15}\text{N}$ and $\delta^{18}\text{O}$ in solution were measured using a bacterial method to convert NO_3^- into N_2O at the Facility for Isotope Ratio Mass Spectrometer at UCR (Sigman et al. 2001, Casciotti et al. 2002). The bacteria *P. aureofaciens* (ATCC# 13985) lacks nitrous oxide reductase activity and therefore produces nitrous oxide gas as a final product of denitrification which allows the NO_3^- $\delta^{15}\text{N}$ and $\delta^{18}\text{O}$ to be determined. The bacteria was grown in a modified soy broth solution for 7-10 days, concentrated and sealed in a 20ml headspace vial and sparged with He gas for 2 hours. All samples were diluted to a concentration of $1 \mu\text{g ml}^{-1}$ and were added to the vials in 3ml aliquots providing approximately 50 nmols of NO_3^- to the bacteria for conversion. The vials were inverted overnight, before the pH of the solution was raised through the addition of NaOH to stop denitrification. N_2O gas was then cryogenically focused and m/z ratios 44,

45, 46 were measured using a Thermo Delta V isotope ratio mass spectrometer to derive $\delta^{18}\text{O}$ and $\delta^{15}\text{N}$ values for each sample.

Statistical Analysis

The rate of HNO_3 collection in each chamber was determined by regressing the average exposure dose of HNO_3 to the amount of HNO_3 collected by the filters. The slopes of the high and low chambers were compared by ANCOVA using HNO_3 dose as a covariate to isolate if the atmospheric concentration of atmospheric HNO_3 affected the rate of adsorption to the filters. A two-way ANOVA was used to test for the effects of site and exposure length on the amount of HNO_3 collected, and the $\delta^{15}\text{N}$ and $\delta^{18}\text{O}$ values of the extracted NO_3^- .

For the field samples, a correlation analysis was run on the $\delta^{18}\text{O}$ and $\delta^{15}\text{N}$ values from all filters to determine if they co-varied. An Analysis of Covariance Effects test was then run differentiating by site location to evaluate difference in the correlation based on location. Data were analyzed using JMP (Version 9.0 SAS Institute Inc.)

Results

Continuous Stirred Tank Reactors

The amount of nitrogen collected per filter in the high HNO_3 chamber was positively correlated with the amount of nitrogen measured by the inline NO_x analyzer ($r^2=0.93292$, $p < .0001$) (Figure 2.2, open circles). The amount of N- NO_3 collected in the

low HNO₃ chamber was also positively correlated with the amount of N measured by the NOx analyzer, but was more variable at lower N-NO₃ levels ($r^2=0.78$, $p<.0001$) (Figure 2.2, filled circles). ANCOVA analyses on the relationship of the filter nitric acid to exposure (separately for each chamber) indicated that rate of collection of the filters in each chamber was not different ($df=1$, $F=0.94$, $p=0.33$). There was not a significant change in slope based on number of filters per sample in either chamber (Low: $df=23$ $F=0.69$ $p=0.41$; High: $df=23$ $F=2.90$ $p=.10$), so both sets of samples were pooled into the analysis.

The nitric acid used in the chamber had an isotopic signature of $\delta^{15}\text{N}= 0.6 \pm 0.2\%$ and $\delta^{18}\text{O}= 26.0 \pm 0.2\%$. Mean $\delta^{18}\text{O}$ and $\delta^{15}\text{N}$ values of the nitric acid collected from the filters of the high chamber ($\delta^{18}\text{O}= 25.8\pm 0.3\%$ and $\delta^{15}\text{N}=0.32\pm 0.1\%$) were not significantly different from those measured from the filters from the low chamber ($\delta^{18}\text{O}= 25.1\pm 0.9\%$ and $\delta^{15}\text{N}=0.4\pm 0.1\%$) (ANOVA, $p=0.47$). The variance of $\delta^{18}\text{O}$ values was significantly higher ($F= 6.68$ $df=24$, $p<.0001$) in the low chamber (18.73) than the high chamber (2.81), while the variance of $\delta^{15}\text{N}$ was equal in both chambers (0.11) ($F=1.02$ $df=26$, $p=0.96$).

There was no significant difference in either HNO₃ $\delta^{18}\text{O}$ or $\delta^{15}\text{N}$ based on the initial date of exposure in the chamber, although there was a relationship between the length of exposure and measured $\delta^{18}\text{O}$ of HNO₃ on the filter in the low chamber (ANOVA, $df= 3$, $F=4.77$, $p=.01$), but not in the high chamber (ANOVA: $df=3$, $F=0.96$, $p=0.43$). A Student's t test to compare the means indicate that the 1-week exposures

had a lower mean relative to the other samples ($t=2.08$) (Figure 2.3A). The measured $\delta^{15}\text{N}$ values of the extract was significant in both the high (ANOVA: $df=3$, $F=3.18$, $p=0.04$) and the low (ANOVA: $df=3$, $F=3.15$, $p=0.04$) chambers (Figure 2.3B).

Changes in temperature and humidity in the chambers did not affect the isotopic signature of the nitric acid collected by the filters. There was also no correlation between $\delta^{15}\text{N}$ and $\delta^{18}\text{O}$ collected on each filter (Data not shown).

Field Survey

When comparing all exposures, there was a significant relationship between site location and amount of nitrogen collected on the filters (ANOVA: $df=4$, $F=10.29$, $p<.0001$). The Source and High sites collected more nitric acid ($28.7 \mu\text{g m}^{-3} \text{h}^{-1}$) compared to the Low sites ($17.7 \mu\text{g m}^{-3} \text{h}^{-1}$) (Figure 2.4). The variation in of ambient $\text{HNO}_3 \delta^{18}\text{O}$ was between 30 and 80‰ across all sites. There were significant differences in $\text{HNO}_3 \delta^{18}\text{O}$ across the deposition gradient (ANOVA: $df=4$, $F=10.29$, $p<.0001$). The low deposition sites had significantly lower $\text{HNO}_3 \delta^{18}\text{O}$ than the high deposition sites (35.7‰ vs 52.2‰) (Figure 2.5A). The variation of $\text{HNO}_3 \delta^{15}\text{N}$ was between 2 and -10‰ across all sites. There was also an affect of $\delta^{15}\text{N}$ based on location of the samplers (ANOVA: $df=4$, $F=6.24$, $p=.0001$), with the source site having a significantly different mean $\text{HNO}_3 \delta^{15}\text{N}$ relative to the desert sites (Figure 2.5B). The range of $\text{HNO}_3 \delta^{15}\text{N}$ across all filters at each set of sites was different, with the low sites recording the most negative values.

Filters exposed at each site collected HNO_3 with large variation in $\delta^{15}\text{N}$ and $\delta^{18}\text{O}$. The relationship between the two values for all the samples was linearly consistent for the entire sampling period. There was not a significant difference in the relationship between HNO_3 $\delta^{15}\text{N}$ and $\delta^{18}\text{O}$ among filters from the two low sites (ANCOVA: $F=0.92$, $p=0.34$) or filters from the two high sites (ANCOVA: $F=2.31$, $p=0.13$); therefore the low deposition sites and high deposition sites were each combined for analyses (Figure 2.6). There were unique negative linear relationships between HNO_3 $\delta^{15}\text{N}$ and $\delta^{18}\text{O}$ dependent on site location (ANCOVA Effects test: $d=3$, $F=15.12$, $p<.0001$).

The inverse of the amount of HNO_3 collected on each filter was linearly related to its $\delta^{15}\text{N}$ and $\delta^{18}\text{O}$ when regressed independently (Figure 2.7). The slope of the relationships at the two high N deposition sites were not significantly different for $\delta^{18}\text{O}$ (ANCOVA Effects test: $df=1$, $F=.55$, $p=0.46$) but were for $\delta^{15}\text{N}$ (ANCOVA Effects test: $df=1$, $F=4.85$, $p=.03$). The slope of the relationships at the two low sites were not significantly different for $\delta^{18}\text{O}$ (ANCOVA Effects test: $df=1$, $F=2.41$, $p=0.13$) or $\delta^{15}\text{N}$ (ANCOVA Effects Test: $df=1$, $F=3.06$, $p=0.09$). The similar slopes were combined for linear regression analysis.

The high sites had interaction equations of $\delta^{18}\text{O} = 17.77 + 751.56/\text{Exposure}$ ($r^2=.82$, $p<.0001$) and $\delta^{15}\text{N} = 1.63 - 86.94/\text{Exposure}$ ($r^2=.73$, $p<.0001$). The low sites had interaction equations of $\delta^{18}\text{O} = 19.84 + 154.42/\text{Exposure}$ ($r^2=0.76$, $p<.0001$) and $\delta^{15}\text{N} = 0.86 - 35.59/\text{Exposure}$ ($r^2=0.71$, $p<.0001$). There was more variability in the filters collected from the source site than from the desert sites. The interaction between

exposure and isotopic composition of the filters were $\delta^{18}\text{O} = 33.35 + 301.11/\text{Exposure}$ ($r^2=0.54$, $p<.0001$) and $\delta^{15}\text{N} = 0.33 - 17.88/\text{Exposure}$ ($r^2=0.35$, $p<.001$).

A two source mixing model was constructed for each site using two endmembers consisting of the intercept of the above equation and the highest recorded delta value at each site. The two high sites had a mean 'percent anthropogenic HNO_3 ' of $58.4 \pm 3.7\%$ based on $\text{HNO}_3 \delta^{18}\text{O}$ and $60.7 \pm 4.0\%$ based on $\text{HNO}_3 \delta^{15}\text{N}$. The low site was $36.5 \pm 4.1\%$ based on $\text{HNO}_3 \delta^{18}\text{O}$ and $41.4 \pm 4.4\%$ based on $\text{HNO}_3 \delta^{15}\text{N}$. Analysis of Variance indicated a significant difference in mean anthropogenically sourced nitrogen based on ^{18}O ($df=1$, $F=17.66$, $p<.0001$) and ^{15}N ($df=1$, $F=10.49$, $p=.0016$) mixing models.

Discussion

Continuous Stirred Tank Reactors

In both the high and low HNO_3 concentration chambers, the Nylasorb filters collected HNO_3 at a constant rate. The linearity of the nitric acid collected indicates that the filters were not saturated by nitrogen during the exposure period and the rate of collection did not change as the amount of nitric acid on the filter increased. This is consistent with measurements made in previous studies performed in both outdoor and CSTRs (Bytnerowicz et al. 2005).

Comparing the isotopic signature of HNO_3 collected on Nylasorb™ filters to that of the source solution suggests that the filters were an unbiased means of measuring nitrogen and oxygen isotopes of atmospheric nitric acid under stable conditions. The

mean $\delta^{18}\text{O}$ and $\delta^{15}\text{N}$ values of all the samples collected were within 0.3‰ of the HNO_3 input into the chambers. When comparing the average values of weekly exposures, the $\delta^{18}\text{O}$ values were only significantly different during one-week exposures in the low concentration chamber (23.7‰ to 26.3‰). As the length of the exposure increased, the variability in measured $\delta^{18}\text{O}$ decreased in both high and low chambers (Figure 2.2A). The reduction in variability is probably related to the increased loading of the filter with HNO_3 pumped into the system. Given that there was no airflow underneath the collector, the heavier isotopologues may differentiate within the boundary of the collector.

There was more variation and a relatively lower average $\delta^{18}\text{O}$ relative to the differences exhibited in $\delta^{15}\text{N}$ values. The range of the mean value measured from each exposure length was more confined for HNO_3 $\delta^{15}\text{N}$ (0‰ and 0.7‰) than HNO_3 $\delta^{18}\text{O}$ (22.4‰ to 27.0‰). The isotopic values of HNO_3 measured in the control chamber had a mean $\delta^{15}\text{N}$ value 0.6‰ and $\delta^{18}\text{O}$ value of 27.8‰ suggesting that the variation occurring on the filters was not due to mixing with background HNO_3 .

The results of the CSTR portion of the experiment determine that the Nylasorb™ filters effectively capture isotopologues of atmospheric nitric acid at the same ratio that they exist in controlled atmospheric conditions. The filters must be exposed to the atmosphere for at least three consecutive weeks to achieve the highest rate of accuracy for both $\delta^{18}\text{O}$ and $\delta^{15}\text{N}$ of HNO_3 (Figure 2.3B). While rates of dry deposition of atmospheric HNO_3 to soil and plant surfaces are affected by changes in temperature and

humidity (Brook et al. 1999), variations in temperature and humidity in the CSTRs did not have an effect on changes in isotopologue accumulation on the filter. This finding suggests that any changes in accumulation that occurred in the field were the result of changes in atmospheric concentrations associated with shifting air mass mixtures and sources of HNO₃.

Due to the source of HNO₃ remaining unchanged for the entire 4 week exposure, it limits our ability to determine if there is any post adsorption exchange with atmospheric HNO₃. To evaluate if any exchange occurs, it would be necessary to change the source HNO₃ to one with a spiked isotopic signature halfway through the exposure period.

Field Survey

The mean HNO₃ concentrations collected across all filters were higher at the source and high deposition sites compared to the low deposition sites (Figure 2.3). The amount of HNO₃ recorded at each site was relatively similar levels to the previously measured deposition gradient, except that the low sites increased from 2.5 to 3.5 µg-HNO₃ m⁻³ (Allen et al. 2009, Rao et al. 2009). The previous exposure periods did not include precipitation events, which may have altered the amount of atmospheric HNO₃ collected.

The highest HNO₃ concentrations were measured on filters that were exposed during the first two exposure periods. The amount of HNO₃ collected relative to

previous values suggests that there was a source secondary source of HNO_3 that affected the samples. Based on the fact that precipitation occurred during this time, it is assumed that the increased HNO_3 collected was a byproduct of the events. Precipitation events can change many of the factors associated with anthropogenic nitrogen concentration. When air masses come from different directions, they will bring HNO_3 from their source. Precipitation washes HNO_3 and other pollutants out of the air column and decreases atmospheric concentrations (Seinfeld and Pandis 1998), which would lead to an expected decline in ambient HNO_3 . The wetting of dry desert soil, on the other hand, results in pulses of biogenic NO^- emitted into the atmosphere (McCalley and Sparks 2009). All of these factors will vary both the concentration of the HNO_3 as well as the abundance of isotopologues of HNO_3 . The more variation in source of HNO_3 that occurs over the course of the exposure, the more variability there will be in passively collected samples.

The $\delta^{18}\text{O}$ values of nitric acid across all sites ranged from 76.7 – 16.0 ‰. The heaviest $\delta^{18}\text{O}$ values are consistent with fossil fuel combustion measured in previous studies (Hastings et al. 2004, Elliott et al. 2009). The mean $\delta^{18}\text{O}$ values at the source and high sites was 52.2‰ but decreased to 35.7‰ at the low sites (Figure 2.4A). The maximum values of $\delta^{18}\text{O}$ recorded at each site decreased from the high (76.7‰) to low sites (63.4‰) (Figure 2.5). The decrease at low sites is due to a combination of lower amounts of HNO_3 from the LA Basin reaching the area, and mixing in larger amounts with less enriched agricultural HNO_3 . A two source mixing model determined that the

low sites had $36.5 \pm 4.1\%$ of the HNO_3 from the LA Basin compared with $58.4 \pm 3.7\%$ at the high sites.

The $\delta^{15}\text{N}$ values across all the sites ranged from 2.4 – -8.0‰. The mean $\delta^{15}\text{N}$ value at the source site was more enriched in ^{15}N than at all other field sites (Figure 2.4B). The source site sampler was erected 1.5 km from a major freeway where it was exposed to a consistent source of pollution. The source site also did not receive as much precipitation during the exposure period. During the summer, air masses forming in the desert don't tend to travel past the mountain pass just west of the high sites (Figure 2.1) due to cool coastal air moving inland towards the warmer desert, and the drop in elevation from the mountain pass to the Salton Sea. This results in less mixing of agricultural HNO_3 at the source site. The minimum $\delta^{15}\text{N}$ values at each site were consistent with the pattern exhibited by the $\delta^{18}\text{O}$ values; with the lowest values being recorded at the cleanest air sites (Figure 2.5). This may be due to less enriched values being emitted from agricultural sources and mixing at higher rates in low deposition areas.

When comparing the regressions of the isotopic signature of passively collected HNO_3 at each site with the amount of HNO_3 collected on each filter, the lines all intersect at similar values (Figure 2.6). The y-intercept of the regressions of combined low and high sites were within 2‰ of each other for both $\delta^{15}\text{N}$ and $\delta^{18}\text{O}$ (Figure 2.7B). This suggests that the secondary source of nitric acid mixing with the anthropogenic sources was constant at all sites. The lower $\delta^{18}\text{O}$ signature of the high concentration

samples indicated that the majority of HNO_3 collected was from a non-fossil fuel source. The high concentrations of non-combustion HNO_3 sources may be related to the NO_x volatilized from the soil following precipitation events or from the increased humidity/moistening of the filters during precipitation events. Introducing water to the filter surface could alter the rate of collection of the filters during periods where anthropogenic HNO_3 had been removed from the air through wet deposition.

It is clear that the secondary source of HNO_3 present in the filters does not come from a laboratory contaminant, because the lower concentration values present at the low deposition sites would have changed quickly with as the secondary value increased. There was also no contamination during the processing of the CSTR samples, which were performed concurrently with the field samples.

Conclusions

The results of this experiment suggest that Nylasorb™ filters are an effective means of collecting atmospheric HNO_3 for isotopic analysis. Since the filters only passively collect HNO_3 species, they will provide the most consistent measurement when exposed during a consistently dry period.

The rain events that occurred during the study period created variable isotopic ratios of HNO_3 during the length of the exposure period. The mixing of isotopologues was indicative of a two source mixing model. Minor correlations between humidity and the amount of N collected on the filters at high deposition sites corroborate that

changing weather conditions did in fact change the amount of HNO_3 carried to each site. In the CSTR experiment, changing temperature and humidity in the greenhouse did not affect the amount or isotopic ratio of HNO_3 collected. A design change of the protective cup surrounding the filter on the filter holder may reduce impacts of weather. The cup could be extended to prevent water from splattering onto the filter during precipitation events with high winds.

Based on the results, a two week field exposure appears to be the most effective timing to gather accurate isotopic data for a short time period. This length in the CSTRs produced average isotopic ratios within 0.5‰ of the true value for both $\delta^{18}\text{O}$ and $\delta^{15}\text{N}$. Using a two week exposure minimizes the amount of variability in the isotopic ratios data for both elements while increasing the ability to plan the exposure around variable weather patterns. This will allow researchers to gather data from individual air masses and weather events independently.

References

- Allen, E. B., L. E. Rao, R. J. Steers, A. Bytnerowicz, and M. E. Fenn. 2009. Impacts of atmospheric nitrogen deposition on vegetation and soils in Joshua Tree National Park. Pages 78-100 *in* R. H. Webb, L. F. Fenstermaker, J. S. Heaton, D. L. Hughson, E. V. McDonald, and D. M. Miller, editors. *The Mojave Desert: Ecosystem Processes and Sustainability*. University of Nevada Press, Las Vegas.
- Ammann, M., R. Siegwolf, F. Pichlmayer, M. Suter, M. Saurer, and C. Brunold. 1999. Estimating the uptake of traffic-derived NO₂ from N-15 abundance in Norway spruce needles. *Oecologia* 118:124-131.
- Amundson, R., A. T. Austin, E. A. G. Schuur, K. Yoo, V. Matzek, C. Kendall, A. Uebersax, D. Brenner, and W. T. Baisden. 2003. Global patterns of the isotopic composition of soil and plant nitrogen. *Global Biogeochemical Cycles* 17:11.
- Andersson, K. K. and A. B. Hooper. 1983. O₂ and H₂O are each the source of one O in NO₂⁻ produced from NH₃ by Nitrosomonas: ¹⁵N-NMR evidence. *FEBS Letters* 164:236-240.
- Brook, J. R., L. Zhang, Y. Li, and D. Johnson. 1999. Description and evaluation of a model of deposition velocities for routine estimates of dry deposition over North America. Part II: review of past measurements and model results. *Atmospheric Environment* 33:5053-5070.
- Bytnerowicz, A., M. J. Sanz, M. J. Arbaugh, P. E. Padgett, D. P. Jones, and A. Davila. 2005. Passive sampler for monitoring ambient nitric acid (HNO₃) and nitrous acid (HNO₂) concentrations. *Atmospheric Environment* 39:2655-2660.
- Calvert, J. G., A. Lazrus, G. L. Kok, B. G. Heikes, J. G. Walega, J. Lind, and C. A. Cantrell. 1985. Chemical mechanisms of acid generation in the troposphere. *Nature* 317:27-35.
- Casciotti, K. L., D. M. Sigman, M. G. Hastings, J. K. Böhlke, and A. Hilkert. 2002. Measurement of the Oxygen Isotopic Composition of Nitrate in Seawater and Freshwater Using the Denitrifier Method. *Analytical Chemistry* 74:4905-4912.
- Cisneros, R., A. Bytnerowicz, D. Schweizer, S. Zhong, S. Traina, and D. H. Bennett. 2010. Ozone, nitric acid, and ammonia air pollution is unhealthy for people and ecosystems in southern Sierra Nevada, California. *Environmental Pollution* 158:3261-3271.
- Elliott, E. M., C. Kendall, E. B. Boyer, D. A. Burns, G. Lear, H. E. Golden, K. Harlin, A. Bytnerowicz, T. J. Butler, and R. Glatz. 2009. Dual nitrate isotopes in actively and passively collected dry deposition: Utility for partitioning NO_x sources, understanding reaction pathways, and comparison with isotopes in wet nitrate deposition. *Journal of Geophysical Research: Biogeosciences*.

- Fenn, M. E., E. B. Allen, S. B. Weiss, S. Jovan, L. H. Geiser, G. S. Tonnesen, R. F. Johnson, L. E. Rao, B. S. Gimeno, F. Yuan, T. Meixner, and A. Bytnerowicz. 2010. Nitrogen critical loads and management alternatives for N-impacted ecosystems in California. *Journal of Environmental Management* 91:2404-2423.
- Fenn, M. E., J. S. Baron, E. B. Allen, H. M. Rueth, K. R. Nydick, L. Geiser, W. D. Bowman, J. O. Sickman, T. Meixner, D. W. Johnson, and P. Neitlich. 2003a. Ecological effects of nitrogen deposition in the western United States. *Bioscience* 53:404-420.
- Fenn, M. E., R. Haeuber, G. S. Tonnesen, J. S. Baron, S. Grossman-Clarke, D. Hope, D. A. Jaffe, S. Copeland, L. Geiser, H. M. Rueth, and J. O. Sickman. 2003b. Nitrogen emissions, deposition, and monitoring in the western United States. *Bioscience* 53:391-403.
- Fenn, M. E., M. A. Poth, J. D. Aber, J. S. Baron, B. T. Bormann, D. W. Johnson, A. D. Lemly, S. G. McNulty, D. E. Ryan, and R. Stottleyer. 1998. Nitrogen excess in North American ecosystems: Predisposing factors, ecosystem responses, and management strategies. *Ecological Applications* 8:706-733.
- Freyer, H. D. 1991. Seasonal-variation of N¹⁵/N¹⁴ ratios in atmospheric nitrate species. *Tellus Series B-Chemical and Physical Meteorology* 43:30-44.
- Galloway, J. N., J. D. Aber, J. W. Erisman, S. P. Seitzinger, R. W. Howarth, E. B. Cowling, and B. J. Cosby. 2003. The nitrogen cascade. *Bioscience* 53:341-356.
- Hastings, M. G., D. M. Sigman, and F. Lipschultz. 2003. Isotopic evidence for source changes of nitrate in rain at Bermuda. *J. Geophys. Res.* 108:4790.
- Hastings, M. G., E. J. Steig, and D. M. Sigman. 2004. Seasonal variations in N and O isotopes of nitrate in snow at Summit, Greenland: Implications for the study of nitrate in snow and ice cores. *J. Geophys. Res.* 109:D20306.
- Hoering, T. 1957. The isotopic composition of the ammonia and the nitrate ion in rain. *Geochimica Et Cosmochimica Acta* 12:97-102.
- Kendall, C. 1998. Tracing Nitrogen Sources and Cycling in Catchments. Pages 519-576 *in* C. Kendall and J. J. McDonnell, editors. *Isotope Tracers in Catchment Hydrology*. Elsevier Science B.V, Amsterdam.
- Li, D. J. and X. M. Wang. 2008. Nitrogen isotopic signature of soil-released nitric oxide (NO) after fertilizer application. *Atmospheric Environment* 42:4747-4754.
- McCalley, C. K. and J. P. Sparks. 2009. Abiotic Gas Formation Drives Nitrogen Loss from a Desert Ecosystem. *Science* 326:837-840.

- Michalski, G., T. Meixner, M. Fenn, L. Hernandez, A. Sirulnik, E. Allen, and M. Thiemens. 2004. Tracing atmospheric nitrate deposition in a complex semiarid ecosystem using $\Delta^{17}O$. *Environmental Science & Technology* 38:2175-2181.
- NADP. 2012. National Atmospheric Deposition Program 2011 Annual Summary. Illinois State Water Survey.
- Padgett, P. E., A. Bytnerowicz, P. J. Dawson, G. H. Riechers, and D. R. Fitz. 2004. Design, Evaluation and Application of a Continuously Stirred Tank Reactor System for Use in Nitric Acid Air Pollutant Studies. *Water, Air, & Soil Pollution* 151:35-51.
- Pearson, J., D. M. Wells, K. J. Seller, A. Bennett, A. Soares, J. Woodall, and M. J. Ingrouille. 2000. Traffic exposure increases natural N-15 and heavy metal concentrations in mosses. *New Phytologist* 147:317-326.
- Rao, L. E., D. R. Parker, A. Bytnerowicz, and E. B. Allen. 2009. Nitrogen mineralization across an atmospheric nitrogen deposition gradient in Southern California deserts. *Journal of Arid Environments* 73:920-930.
- Rock, L. and B. H. Ellen. 2007. Nitrogen-15 and oxygen-18 natural abundance of potassium chloride extractable soil nitrate using the denitrifier method. *Soil Science Society of America Journal* 71:355-361.
- Scrimgeour, C. M. and D. Robinson. 2004. Stable isotope analyses and applications. Page 576 *in* K. A. Smith and M. S. Cresser, editors. *Soil and environmental analysis modern instrumental techniques*. M. Dekker, New York.
- Seinfeld, J. H. and S. N. Pandis. 1998. *Atmospheric Chemistry and Physics: From Air Pollution to Climate Change*. Wiley-Interscience, Indianapolis.
- Sigman, D. M., K. L. Casciotti, M. Andreani, C. Barford, M. Galanter, and J. K. Bohlke. 2001. A bacterial method for the nitrogen isotopic analysis of nitrate in seawater and freshwater. *Analytical Chemistry* 73:4145-4153.
- Tonnesen, G. S., Z. S. Wang, M. Omary, and C. J. Chien. 2003. Model simulations of formation, transport and deposition of ozone, fine particulates and nitrates in the Sierra Nevada. *in* A. Bytnerowicz, M. Arbaugh, and R. Alonso, editors. *Ozone Air Pollution in the Sierra Nevada - Distribution and Effects on Forests*. Developments in Environmental Sciences. Elsevier Press, Amsterdam, Netherlands.
- Vitousek, P. M., J. D. Aber, R. W. Howarth, G. E. Likens, P. A. Matson, D. W. Schindler, W. H. Schlesinger, and D. G. Tilman. 1997. Human alteration of the global nitrogen cycle: Sources and consequences. *Ecological Applications* 7:737-750.

Wang, G., M. Ngouajio, M. E. McGiffen, Jr, and C. M. Hutchinson. 2008. Summer Cover Crop and In-season Management System Affect Growth and Yield of Lettuce and Cantaloupe. HortScience 43:1398-1403.

Figures

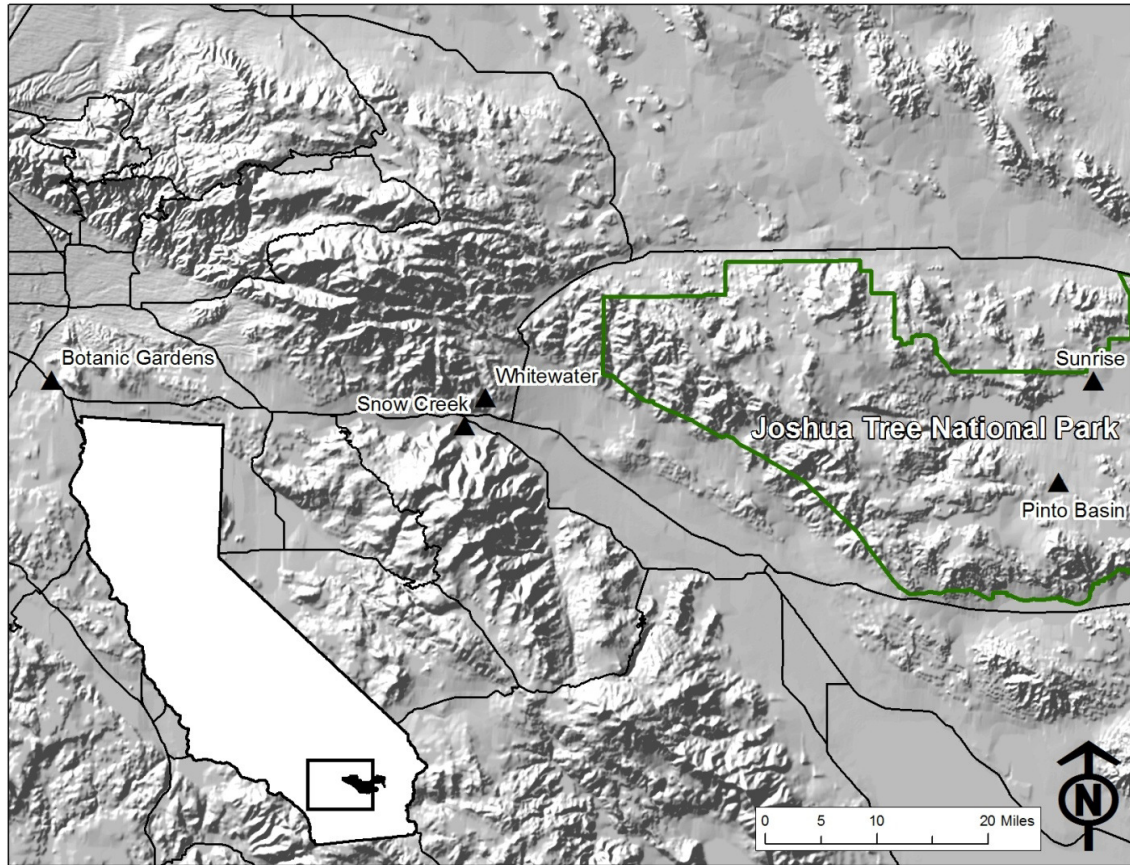


Figure 2.1. Site locations of the 5 field sampling sites.

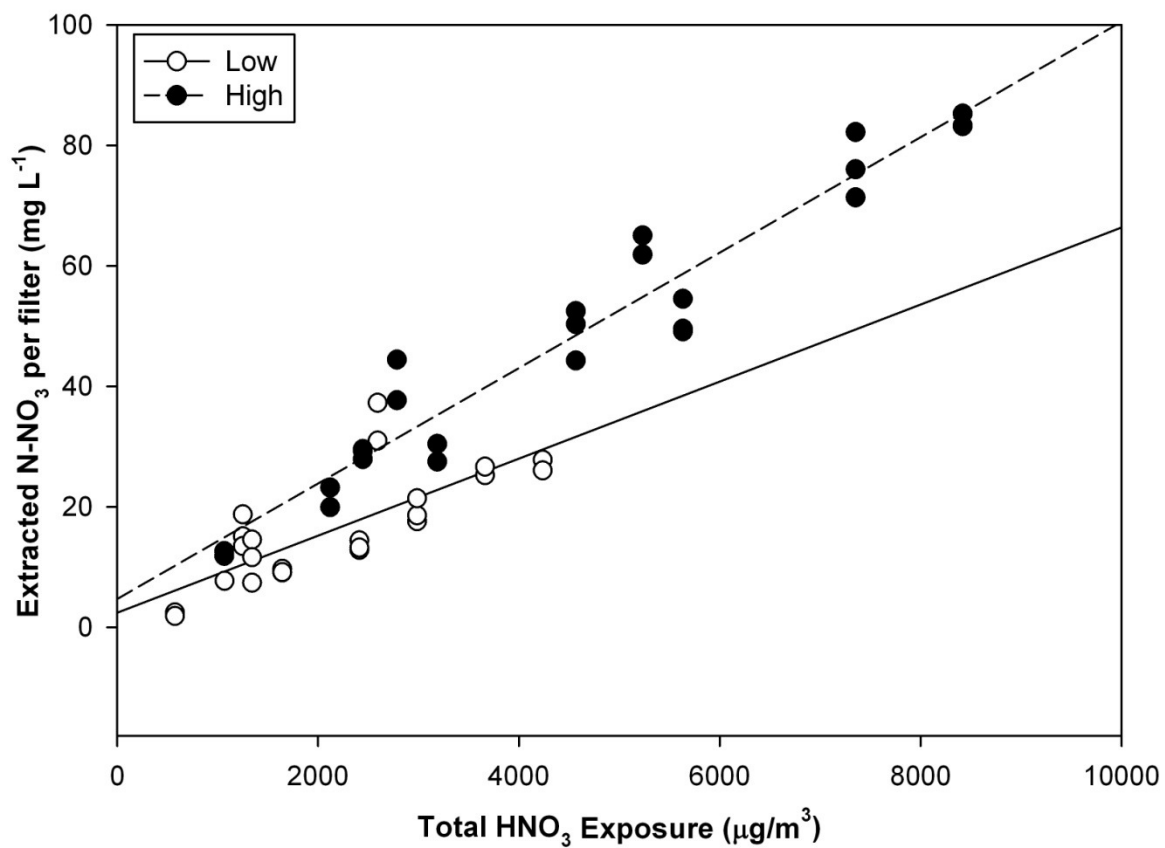


Figure 2.2. Amount of HNO₃ collected on filters in the Continuous Stirred Tank Reactors set to two separate concentrations of HNO₃.

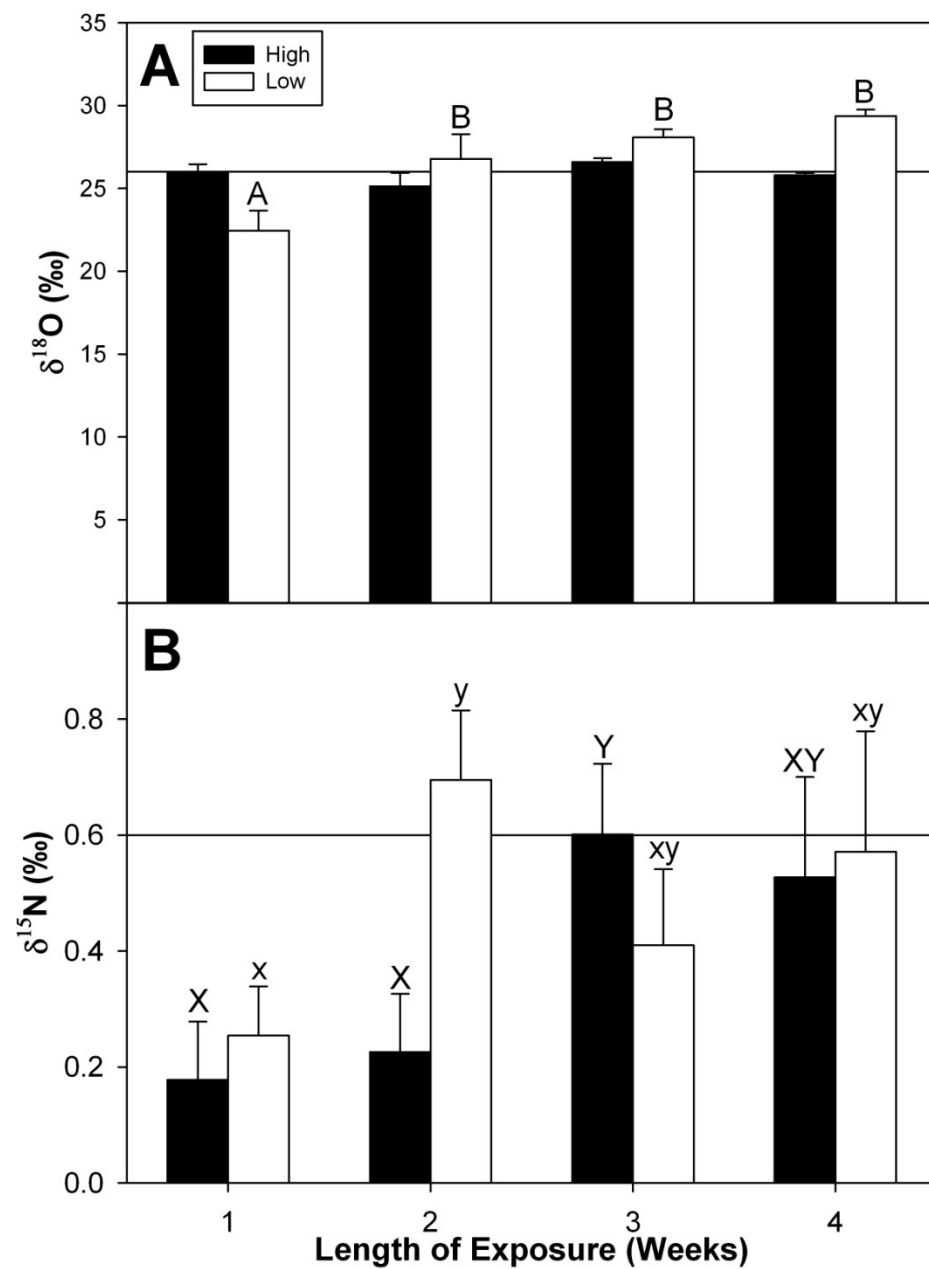


Figure 2.3. Differences in means of $\delta^{18}\text{O}$ (A) and $\delta^{15}\text{N}$ (B) of HNO_3 extracted from filters in the high and low CSTR chambers. Horizontal lines represent $\delta^{18}\text{O}$ and $\delta^{15}\text{N}$ values of the stock HNO_3 solution that was volatilized and pumped into the chamber.

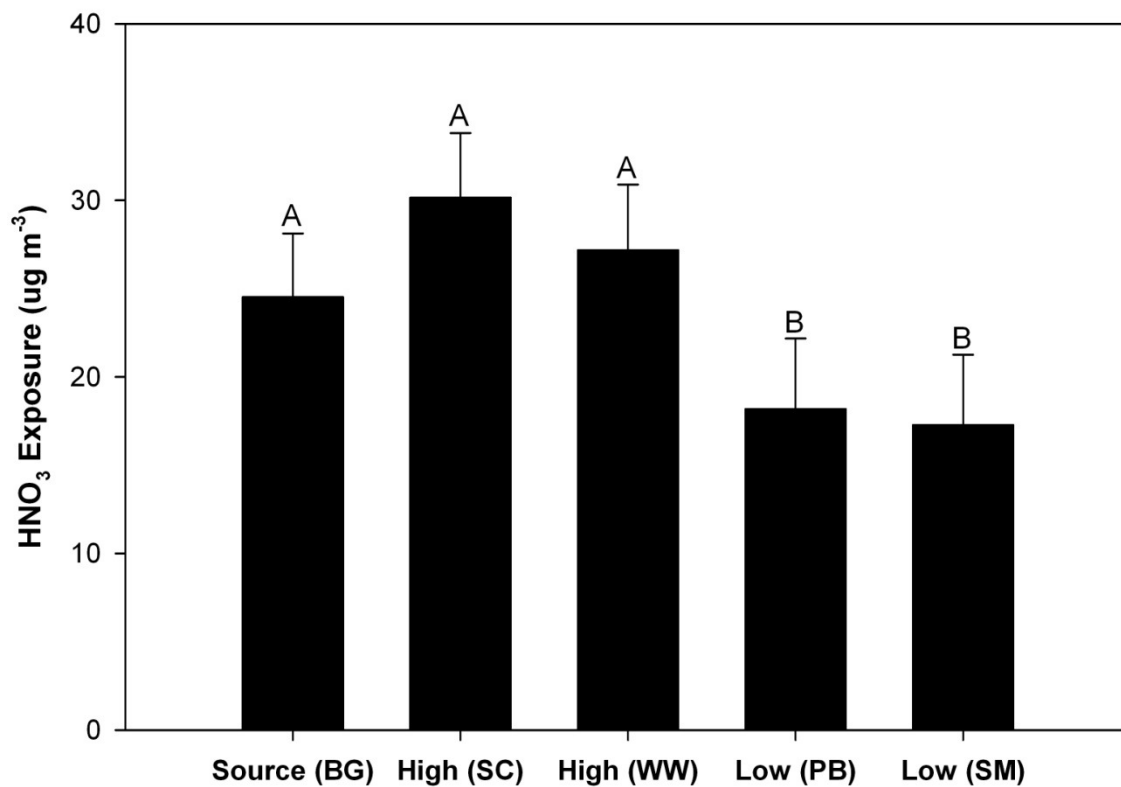


Figure 2.4. Amount of HNO₃ collected per filter calibrated to the amount of time the filters were exposed to the atmosphere. Significance levels were determined using 1/Exposure to normalize the data. Error bars represent the standard error of the mean.

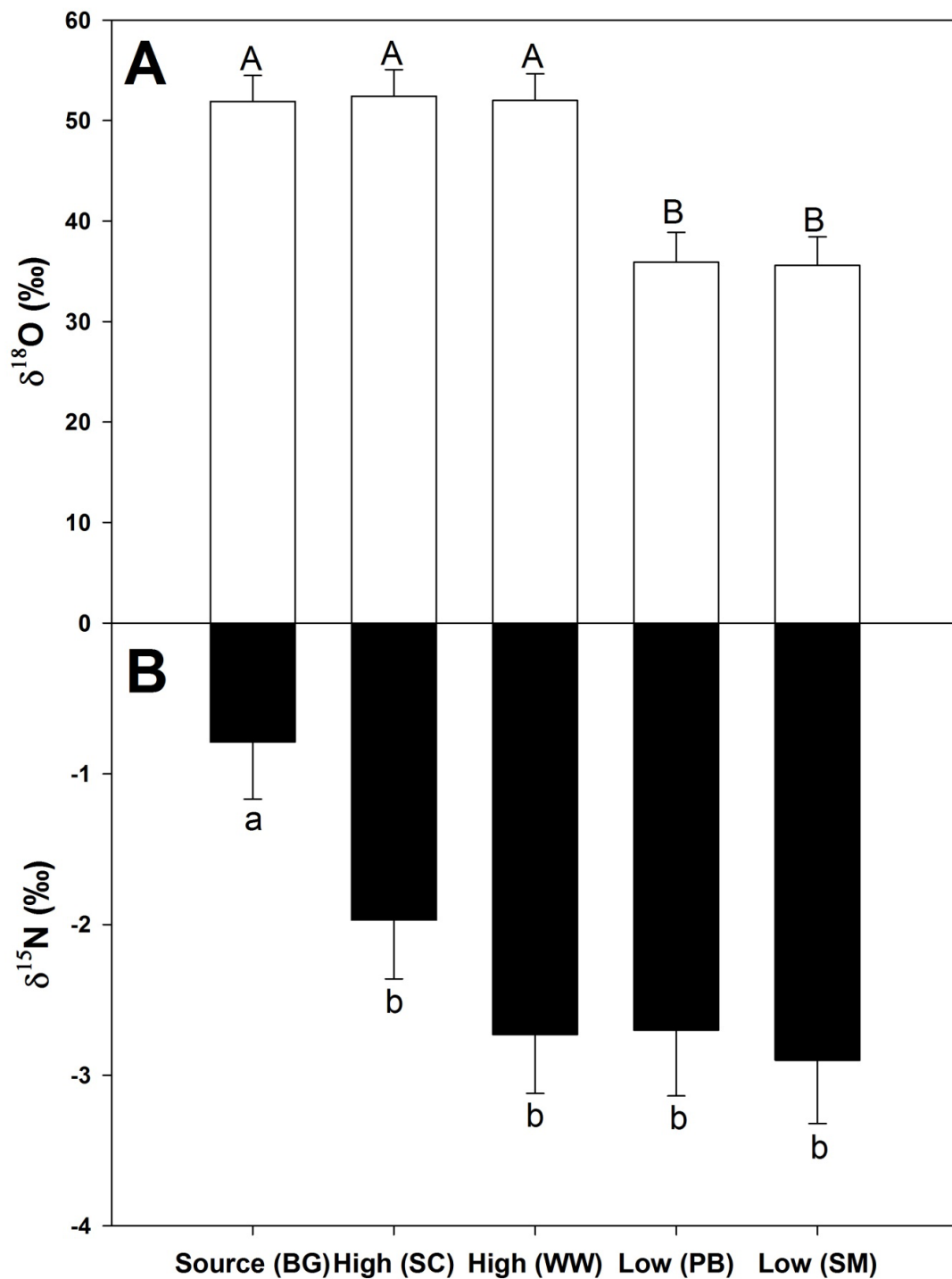


Figure 2.5. The average $\delta^{18}\text{O}$ (A) and $\delta^{15}\text{N}$ (B) values of all passively collected HNO_3 from five field sites over the four week experiment. The Source and High deposition sites had higher average $\delta^{18}\text{O}$ values relative to the low sites. The only difference in $\delta^{15}\text{N}$ values was at the Source site. Error bars represent the standard error of the mean.

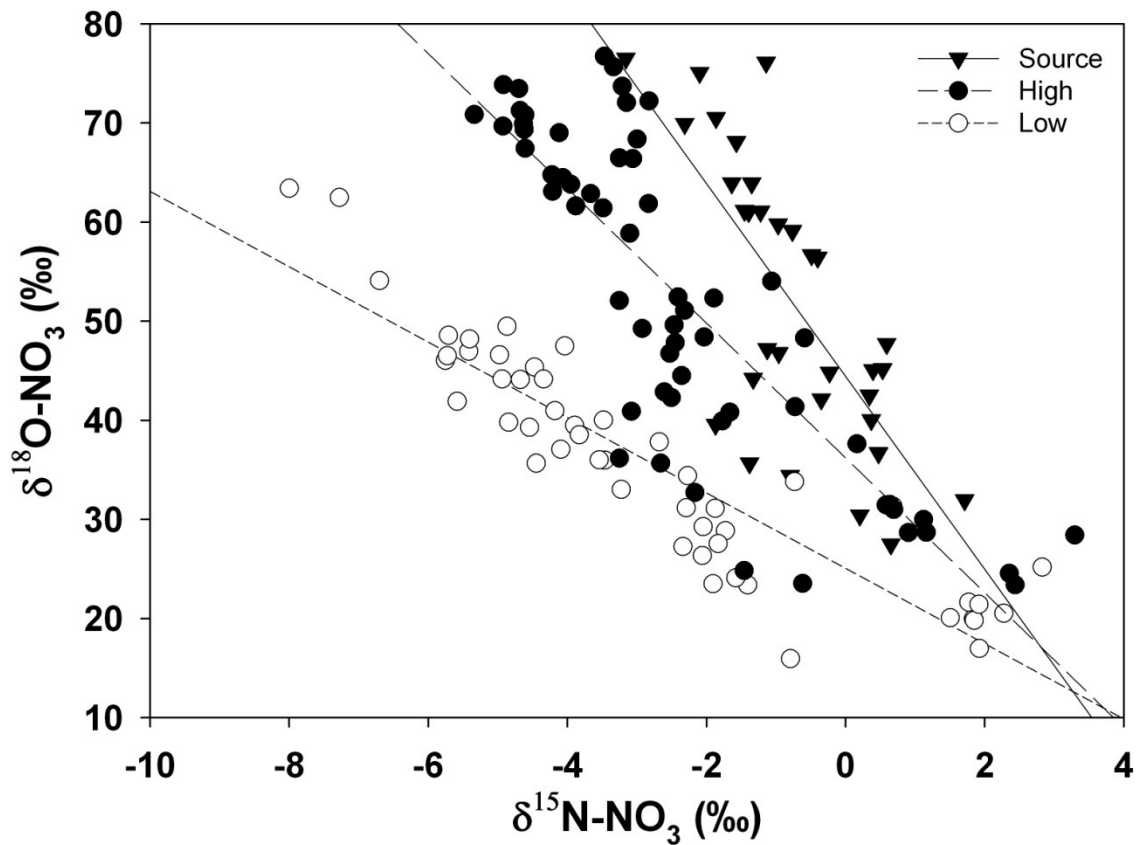


Figure 2.6. The $\delta^{18}\text{O}$ and $\delta^{15}\text{N}$ of passively collected HNO_3 change consistently at each site. The low deposition sites (open circles) have a lower maximum $\delta^{18}\text{O}$ and lower minimum $\delta^{15}\text{N}$ relative to high deposition sites (filled circles), indicating that more enriched isotopes are being deposited faster than less enriched isotopes across the deposition gradient. At all sites, the isotope values are directed towards a similar endpoint indicating a mixing of two sources of HNO_3 .

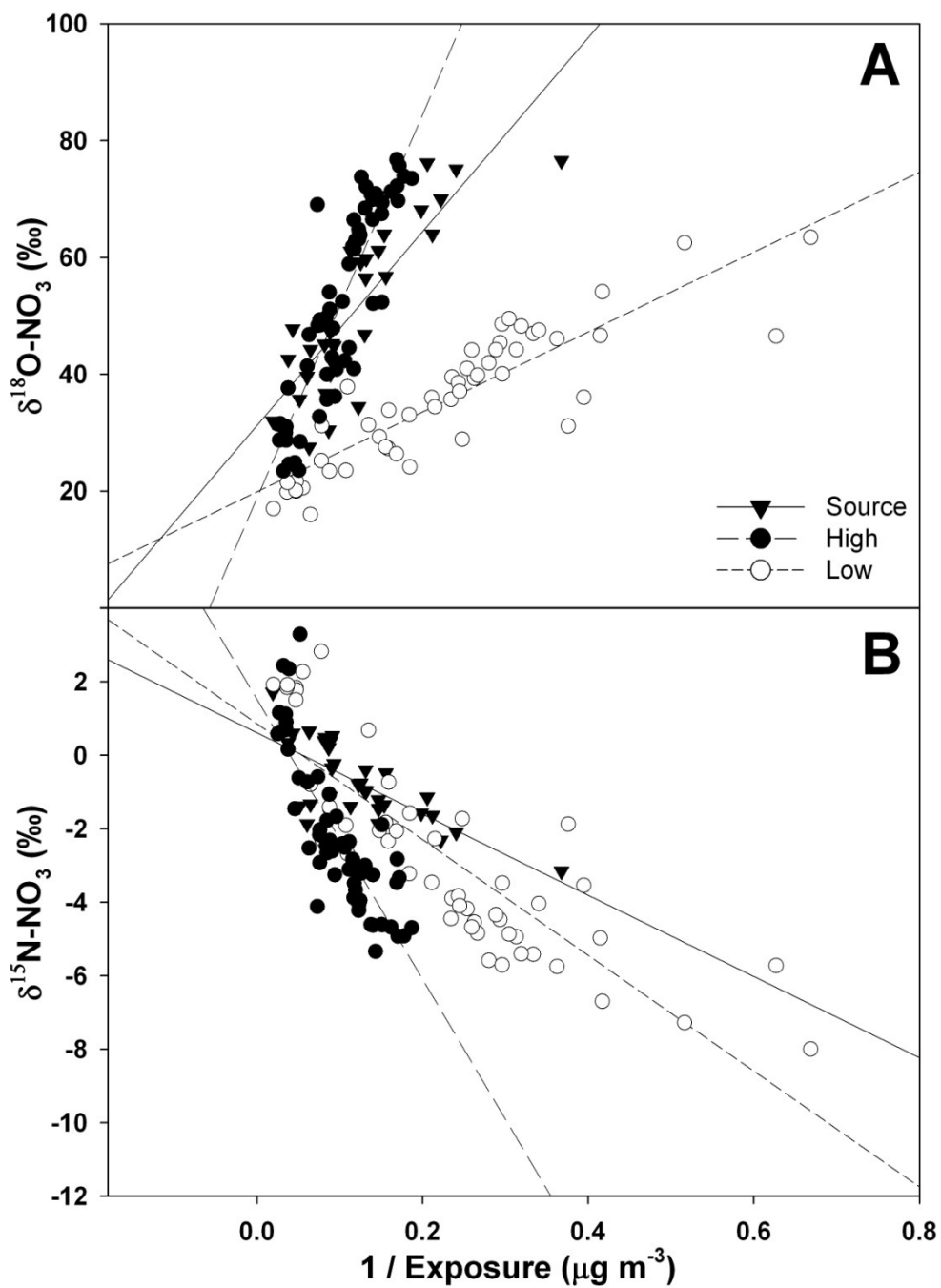


Figure 2.7. The $\delta^{18}\text{O}$ (A) and $\delta^{15}\text{N}$ (B) values of passively collected HNO_3 are correlated with the amount of HNO_3 collected on each filter. As concentrations increased the values at all sites converged on a similar value. The highest levels of HNO_3 collected came from filters exposed during precipitation events during the first two weeks of sampling.

Chapter 3: Evaluation of nitrogen and oxygen isotopes as indicators of nitrate contamination sources across a nitrogen deposition gradient in the Sonoran Desert

Abstract

Gaseous nitrogen (N) in the form of industrial, vehicular, and agricultural emissions, can travel from their source and deposit in wildland areas causing disruption to the nitrogen cycle with deleterious impacts on ecosystem processes. An understanding of the amounts and sources of anthropogenic N is needed to assess and manage these impacts. Reactive N in the atmosphere can be measured using passive air samplers to estimate the amount of N being deposited to a site. Anthropogenic nitric acid collected on these filters can be differentiated from biogenic sources through the analysis of stable isotopes of N and oxygen. Stable isotope ratios can be used to determine the amount of N being added by unique sources. This experiment measured ambient HNO₃ concentrations, $\delta^{18}\text{O}$, and $\delta^{15}\text{N}$ across a N deposition gradient spanning from the Los Angeles Air Basin east into the northwest Sonoran Desert. I established 13 sampling sites across a 120km stretch of creosote bush scrub and exposed Nylasorb filters for 4 week periods during summer 2010, winter 2011, and summer 2011. Extracted NO₃⁻ was converted to N₂O gas to evaluate isotopic composition by using the denitrifying bacteria *Pseudomonas chlororaphis* var. *aureofaciens*.

The atmospheric concentrations measured during the experiment followed spatial patterns similar to those previously measured. The data indicated that not much air flow occurs from the Coachella Valley into Joshua Tree National Park. The HNO_3 $\delta^{15}\text{N}$ values on the east side of the mountains maintained values between -6 to 0‰ for all sampling periods, while samples on the west side of the mountains the HNO_3 $\delta^{15}\text{N}$ changed with the seasons and fluctuated between -6 and 18‰. This suggests that the sites within the park experience less variability over time than sites in the Coachella valley. Even though atmospheric HNO_3 concentrations are highest in the western edge of the study area, isotopic analysis identifies a strong influence by agricultural in the Coachella Valley. HNO_3 concentrations often varied during each sampling period but the ratio of $\delta^{15}\text{N}$ to $\delta^{18}\text{O}$ maintained a linear relationship on each side of the mountains suggesting a mixing of two sources of HNO_3 during each sampling period. The results of this study provide a clearer understanding of how N is moving through the region, and how different sources are seasonally impacting the wildlands.

Introduction

Atmospheric anthropogenic nitrogen (N) pollution is produced through human activities including fossil fuel combustion and emissions from agricultural fertilizer and waste (Vitousek et al. 1997). Reactive N (HNO_3 and NH_3) molecules have short (1-3 day) atmospheric lifespans which allow them to travel downwind from their source with the dominant air mass flow (Neuman et al. 2006). These molecules are then deposited to

plant and soil surfaces through wet and dry deposition (Seinfeld and Pandis 1998).

Anthropogenic inputs of N can be differentiated from biogenic N through the analysis of stable isotopes of N and O (Kendall et al. 2007). Increasing anthropogenic inputs causes predictable shifts in the isotopic signature of available HNO_3 and NH_4^+ which can be used to calculate anthropogenic N present, and allows researchers to determine where inputs are accumulating within the ecosystem (Voss et al. 2006, Wankel et al. 2006, Granger et al. 2008).

In the western United States, the main sources of atmospheric inputs originate from metropolitan areas and agricultural zones (Fenn et al. 2003b). The proximity of these sources to wilderness areas puts many undisturbed ecosystems at risk of shift in vegetation diversity and community structure (Fenn et al. 2003a, Johnson et al. 2003, Fenn et al. 2010, Ochoa-Hueso et al. 2011, Pardo et al. 2011). The Los Angeles air basin exposes local forests to some of the highest levels of deposition in the United States ($50 \text{ kg N ha}^{-1} \text{ yr}^{-1}$) (Bytnerowicz and Fenn 1996). The air basin empties to the east into the Sonoran Desert depositing N at rates as high as ($12 \text{ kg h}^{-1} \text{ yr}^{-1}$) into a nitrogen deficient ecosystem (Allen et al. 2009). The main nitrogen species that affect this region are HNO_3 and NH_3 (EPA, 2012). HNO_3 is a byproduct of atmospheric reactions with NO_x emissions, 90% of which come from automobiles (EPA, 2008). NH_4^+ emissions stem from agricultural activities (12%) as well as an increasing percentage from automobiles due to emissions from catalytic converters (25%) (EPA, 2008). A second source of atmospheric N loading to the Sonoran Desert originates from emissions from agricultural operations

within the Coachella Valley. Historically, these operations, which consist of over 70,000 acres of farmland, have relied heavily on pesticides and herbicides that can volatilize reactive N into the atmosphere (Krupa 2003, Wang et al. 2008). Warm winter temperatures allow crops to be grown and harvested year round, providing a constant flux of anthropogenic N, but with peak agricultural production occurring during the wet winter season.

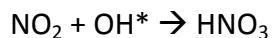
As anthropogenic N inputs are deposited to undisturbed areas, they cause shifts in measureable isotopologue ratios due to isotopic differences of biologically and anthropogenically created molecules (Kendall et al. 2007). Nitrogen and oxygen (O) naturally exist with multiple stable atomic weights of 14 and 15 for N, and 16, 17, and 18 for O. Increasing the amount of heavy isotopes in a molecule can cause very slight differences in the vibration of the atom, and therefore the reactivity of small molecules containing the heavier isotope relative to their depleted isotopologues (Peterson and Fry 1987). These differences result in changes in isotopic composition between chemical reactants and products on the order of one in a thousand during reactions. The percentage of heavier isotopes within a given pool of molecules can be compared to an international standard that has a constant ratio of heavy to light isotopes. The standard notation for reporting the ratio of isotopes within a sample is:

$$\delta X = \left[\left(\frac{R_{\text{Sample}}}{R_{\text{Standard}}} \right) - 1 \right] * 1000$$

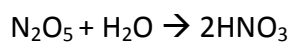
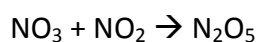
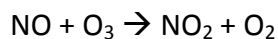
Where X = ^{15}N or ^{18}O . This is referred to as the delta notation, and is reported in parts per thousand (‰).

Recent research across the United States has shown the utility of using stable isotopes to determine the origins of air pollution (Elliott et al. 2007). NO_x molecules released from anthropogenic sources differ in the ratio of $^{18}\text{O}/^{16}\text{O}$ relative to those from biological sources. Measuring the change in isotopic signature of multiple elements across space will give a clearer image of how molecules are moving through the atmosphere. Combustion creates NO_x $\delta^{18}\text{O}$ between 60-90‰ (Elliott et al. 2007, Elliott et al. 2009) while soil emissions NO_x $\delta^{18}\text{O}$ have been measured between 20-30‰ (Michalski et al. 2004, Rock and Ellen 2007).

NO_x molecules released to the atmosphere undergo a series of photolytic reactions with ozone and hydroxyl radicals to produce HNO_3 . Daytime reactions are dominated by atmospheric oxidation reactions with ozone and OH^* :



While at night reactions favor this pathway:



to form HNO_3 . Winter reactions are commonly dominated by the night time reactions due to decreased day length, increased humidity, and reduced light intensity (Seinfeld and Pandis 1998). The chemical pathway leading to the production of HNO_3 will influence the final $\delta^{18}\text{O}$ of the pollutant (Hastings et al. 2003, Hastings et al. 2004). The different pathways lead to winter HNO_3 $\delta^{18}\text{O}$ averaging $\sim 10\text{‰}$ higher than summer values coming from the same source (Hastings et al. 2003, Hastings et al. 2004).

Anthropogenic N emissions also vary in $\delta^{15}\text{N}$ and generally range between -15 to 15‰ (Elliott et al. 2007, Kendall et al. 2007). Studies have consistently shown a seasonal change in $\delta^{15}\text{N}$ values with higher values being measured in the winter relative to the summer (Russell et al. 1998, Hastings et al. 2004, Elliott et al. 2009). This pattern can change if the source of HNO_3 shifts with the season, such as an increase in lightning storms (Hastings et al. 2003). While most studies have measured wet deposition due to the accessibility of rain water, $\delta^{15}\text{N}$ of dry deposition have been recorded as being higher than wet deposition (Heaton et al. 1997).

Atmospheric nitrogen species are commonly measured through passive and active collectors. Passive collectors using Nylasorb™ and Ogawa™ filter discs allow for the accurate measurement of pollutants in remote areas. Exposure periods of 2-4 weeks allow passive samplers to integrate atmospheric chemistry over time. Chapter 1 showed these filters are effective and unbiased at measuring HNO_3 $\delta^{15}\text{N}$ and $\delta^{18}\text{O}$. HNO_3 collected on the filters had a standard error of 0.2‰ for $\delta^{15}\text{N}$ and 0.6‰ for $\delta^{18}\text{O}$ relative the source HNO_3 . A two week exposure was enough to stabilize measurements at high

deposition sites, while the low deposition site required three weeks to decrease variability in measurements. Increasing the length of the exposure in field conditions induces variability in atmospheric patterns that can lead to changes in atmospheric concentration and isotopic ratios of HNO₃. In field conditions on the east coast, HNO₃ ambient samplers had a slight difference in $\delta^{15}\text{N}$ relative to active samplers (0.6‰), but $\delta^{18}\text{O}$ was more variable (6.4‰).

The first objective of this study is to evaluate HNO₃ concentrations across a HNO₃ gradient extending from the Los Angeles Air Basin and into Joshua Tree National Park (JOTR) in the Sonoran Desert. I hypothesize that the agricultural zone near the Salton Sea will produce additional N emissions especially in the winter, during peak agricultural activity. The second objective is to measure the isotopic composition of HNO₃ along the gradient to determine if multiple sources of nitrogen are contributing to atmospheric inputs to the study area. I hypothesize that the two main sources of N inputs will be the Los Angeles air basin and the agricultural zone, and these should be identifiable by the difference in $\delta^{18}\text{O}$ of HNO₃. I hypothesize that a larger percentage of N will be from anthropogenic sources on the western edge of the gradient.

Methods

Site Location

Ambient atmospheric passive samplers were installed at 13 sites in September 2010, January 2010, and September 2011 along a previously identified nitrogen

deposition gradient extending from high concentration zones at the edge of the Los Angeles Air Basin near Banning, CA into low concentration zones 120km east in the Sonoran desert, spanning north into Joshua Tree National Park and south to the Salton Sea (Figure 1) (Allen et al. 2009). All samplers were erected in creosote bush scrubland in the interspace between the shrubs. For more information on the vegetation at the sites, see Chapter 3. Each sampler was positioned at least 100m from the nearest road to minimize direct influence from automobiles.

Sampler Design

The filter packs were constructed following the methods of Bytnerowicz (2005). A 47mm Pall-Gelman Nylsorb™ filter was used as the collecting surface and was covered by a 47mm Zefluor™ PTFE Membrane filter to prevent particulate contamination. All filters were loaded into the filter packs within a glove-box. The atmosphere within the box was filtered with charcoal to remove reactive nitrogen molecules and eliminate contamination of the filters prior to exposure. The filters were loaded into filter packs constructed out of a Petri dish; allowing them to be capped to prevent contamination before installation. Filters were installed on a crossbar 2.5m above the ground, reducing the direct saltation of dust and debris to the filter. Three replicates of HNO₃ filter packs were installed at each site and exposed for a 4 week period. Upon collection from the field, the filters were capped with the Petri dish lid and stored in the freezer at -20°C before being extracted simultaneously.

Nitric Acid Analysis

Once all of the air filters were collected, the filters were unloaded from their cases, placed in 125 ml polycarbonate Erlenmeyer flasks, to which 20ml of deionized water was added prior to being shaken on a wrist-action shaker. The resulting filter extract was decanted into a 20 mL HDPE scintillation vial and stored at -20°C. Once all filters were processed, the extracted solutions were analyzed for NO_3^- concentrations on a Technicon® continuous flow autoanalyzer located at UCR using EPA method. The total HNO_3 exposure (Exposure [$\mu\text{g m}^{-3} \text{h}^{-1}$]) was calculated using the NO_3^- concentration and the length of time it was exposed in the field (Bytnerowicz et al. 2005).

The NO_3^- $\delta^{15}\text{N}$ and $\delta^{18}\text{O}$ in solution were measured using a bacterial method to convert NO_3^- into N_2O at the Facility for Isotope Ratio Mass Spectrometer at UCR (Sigman et al. 2001, Casciotti et al. 2002). The bacteria *Pseudomonas chlororaphis var. aureofaciens* (ATCC# 13985) lacks nitrous oxide reductase activity and therefore produces nitrous oxide gas as a final product of denitrification which allows NO_3^- $\delta^{15}\text{N}$ and $\delta^{18}\text{O}$ to be determined (Greenberg and Becker 1977). The bacteria was grown in a modified soy broth solution for 7-10 days, concentrated and sealed in a 20ml headspace vial and sparged with He gas for 2 hours. All samples were diluted to a concentration of $1 \mu\text{g ml}^{-1}$ and were added to the vials in 3ml aliquots providing approximately 50 nmols of NO_3^- to the bacteria for conversion. The vials were inverted overnight, before the pH of the solution was raised through the addition of NaOH to stop denitrification. N_2O gas was then cryogenically focused and m/z ratios 44, 45, 46 were measured using a

Thermo Delta V isotope ratio mass spectrometer to derive $\delta^{18}\text{O}$ and $\delta^{15}\text{N}$ values for each sample.

HYSPLIT

The HYbrid Single Particle Lagrangian Integrated Trajectory Model (HYSPLIT) (NOAA 2012) was used to model air mass back trajectories at the western, southern, and eastern boundaries of the sampling area. 48-hour back trajectories were modeled at 6-hour intervals (0600, 1200, 1800, 2400) at 10m for each sampling period. Mean path length and directions were analyzed with TrajStat (Wang et al. 2009) to create five cluster trajectories per sampling period. Trajectories are reported as percentage of air movement following a single pathway.

Spatial Interpolation

Regional atmospheric variables were interpolated using Simple Kriging analysis in ArcGIS (Version 9.3) using mean site HNO_3 concentration, HNO_3 $\delta^{15}\text{N}$, and HNO_3 $\delta^{18}\text{O}$ for each sampling period.

Results

Summer HNO₃ Characteristics

2010

Summer ambient atmospheric HNO₃ concentrations followed a similar distribution pattern in 2010 as had previously been measured in the region (Allen et al. 2009, Rao et al. 2009), with the highest concentrations on the western edge of the study area before decreasing to the east. The mean site values ranged from 2.5 µg/m³ and 9.5 µg/m³ (Figure 3.2A).

Ambient δ¹⁸O values ranged from 34.8‰ and 71.5‰ (Figure 3.2B). The most enriched samples occurred on the western and eastern boundaries of the study area. No significant relationship was observed between HNO₃ concentration and HNO₃ δ¹⁸O. Instead I observed a large decrease in δ¹⁸O with minimal change in HNO₃ concentration in the first 30km of the gradient. From that point towards the Salton Sea, as the HNO₃ concentration decreased, the δ¹⁸O increased on the eastern side of the Little San Bernardino Mountains (LSBM).

Atmospheric δ¹⁵N ranged from -8.1‰ to 19‰ (Figure 3.2C). The samples collected on the west side of the LSBM had positive values, while the samples on the eastern side of the LSBM all had negative values. Geographically, the samplers on the western side of the mountains had a strong association with the samplers near the agricultural zone on the southern region of the sampling area (Figure 3.2C). Comparing HNO₃ concentration with δ¹⁸O (Figure 3.3A) and HNO₃ (Figure 3.3B) produced two

distinct groups of points on the east and west sides of the LSBM. Regressing $\delta^{18}\text{O}$ with $\delta^{15}\text{N}$ independently on each side of the mountains produced positive linear interactions on the west (Figure 3.3C, open circles) ($r^2=0.88$, $p<0.001$) and east (Figure 3.3C, filled circles) ($r^2=0.98$, $p<0.0001$).

Due to complications accessing a field site, filters at one site on the western edge of the study area were not exposed until 2 weeks after the rest of the samplers. The short exposure filter had an atmospheric concentration relatively similar to nearby sites, but the mean $\delta^{18}\text{O}$ (71.4‰) was more enriched and $\delta^{15}\text{N}$ (1.1‰) was less enriched than adjacent measurements. Even though their values were different for these short exposures, the relationship between $\delta^{18}\text{O}$ and $\delta^{15}\text{N}$ was consistent with the rest of the samples (Figure 3.3C).

2011

Atmospheric ambient HNO_3 concentration measurements from summer 2011 ranged from $3.3 \mu\text{g}/\text{m}^3$ to $11.9 \mu\text{g}/\text{m}^3$ and followed the same spatial pattern as in 2010 with the highest concentrations on the western edge of the study area (Figure 3.4A). A spatial pattern emerged that was linearly consistent between 2010 and 2011 (Figure 3.5) ($r^2=0.342$, $p=0.0588$); with the western most site having recorded more HNO_3 relative to the general trend. This site experiences higher wind than the other sites and, upon collection, the Zefluor™ filters covering the Nylasorb™ filter had more dust relative to other sites, suggesting that additional soil-derived N may have contaminated the

filter. Removing this point from the regression improved the significance of the interaction ($r^2=0.496$, $p<0.05$).

Mean 2011 $\delta^{18}\text{O}$ across sites ranged from 34.5‰ to 69.3‰ and followed a west to east gradient similar to HNO_3 concentrations (Figure 3.4B). The $\delta^{18}\text{O}$ at west sites (Figure 3.6A, open circles) ($r^2=.183$, $p<0.05$) and east sites (Figure 3.6A, filled circles) ($r^2=0.662$, $p<0.005$) had negative linear relationships when regressed with HNO_3 concentration. The HNO_3 $\delta^{18}\text{O}$ at the eastern sites also decreased with increasing ambient HNO_3 concentration. Both of these relationships were driven by a few filters from two sites on the edge of the gradient. There was no consistent spatial pattern between mean $\delta^{18}\text{O}$ from 2010 and 2011 ($p=0.2829$).

Mean 2011 $\delta^{15}\text{N}$ across sites ranged from -6.5 ‰ to -0.2‰ (Figure 3.4C). The most enriched sites were on the western and eastern borders and $\delta^{15}\text{N}$ decreased moving towards the center of the study area. There was a positive linear relationship between HNO_3 concentration and $\delta^{15}\text{N}$ of the eastern (Figure 3.6B, open circles) ($r^2=0.89$, $p<0.0001$) and western (Figure 3.6B, filled circles) ($r^2=0.90$, $p<0.001$) sites. ANCOVA analyses on the change in $\delta^{15}\text{N}$ with HNO_3 concentration indicated that rate of mixing was different on each side of the LSBM ($df=1$, $F=76.78$, $p<0.0001$). There was no relationship between $\delta^{15}\text{N}$ from 2010 and 2011 ($p=0.5233$).

I observed separate strong negative relationship between the $\delta^{15}\text{N}$ and $\delta^{18}\text{O}$ present on the western side of the LSBM (Figure 3.6C, open circles) ($r^2=0.469$, $p<0.0005$) and eastern side of the LSBM (Figure 3.6C, filled circles) ($r^2=0.904$, $p<0.0001$). ANCOVA

analysis of the rate of change between $\delta^{15}\text{N}$ and HNO_3 $\delta^{18}\text{O}$ determined that there was no difference in mixing rates based on location relative to the LSBM (df=1, F=0.078, p=0.78).

Winter HNO₃ Characteristics

2011

Mean atmospheric HNO_3 concentrations were lower during the winter sampling period relative to the summer samples and ranged from $0.29 \mu\text{g}/\text{m}^3$ to $1.9 \mu\text{g}/\text{m}^3$ across the study area (Figure 3.7A). The highest concentrations were observed near the agricultural zone on the southern boundary of the study area. These higher values were limited to the sites within the Coachella Valley and did not spread over the LSBM into JOTR. This is consistent with the HYSPLIT model which showed that the dominant air masses for sites east of the LSBM came from the north, while less than half of the air masses moving toward the agricultural zone came from the west (Figure 3.8).

Mean $\delta^{18}\text{O}$ ranged from 70 to 83‰ and were highest along the western side of the Coachella Valley (Figure 3.7B). The $\delta^{18}\text{O}$ values at the west sites decreased linearly with increasing HNO_3 concentration (Figure 3.9A, open circles) ($r^2=0.231$, $p<0.05$). The same pattern existed on the east side of the LSBM (Figure 3.9A, filled circles) ($r^2=0.537$, $p<0.01$). The relationships between HNO_3 concentration and its $\delta^{15}\text{N}$ and $\delta^{18}\text{O}$ separate sites on the east and west sides of the LSBM into non-overlapping groups (Figure 3.9).

Mean $\delta^{15}\text{N}$ ranged from -3.7‰ to 1.5‰ (Figure 3.7C). There was a positive linear relationship between HNO_3 concentration and its $\delta^{15}\text{N}$ values at the west sites (Figure 3.9B, open circles) ($r^2=0.640$, $p<0.0001$), but there was no relationship for the sites east of the LSBM ($p=0.536$).

The relationship between $\delta^{15}\text{N}$ and $\delta^{18}\text{O}$ across all of the sites separated the sites into non-overlapping groups, although there was no consistent relationship within an individual group.

Discussion

Summer Mixing Dynamics

Ambient HNO_3 concentrations were higher in the summer sampling period relative to the winter which was expected due to changes in the pathway of atmospheric HNO_3 formation (Seinfeld and Pandis 1998), the removal of atmospheric HNO_3 from precipitation (Seinfeld and Pandis 1998), and a change in air mass trajectories (Figures 3.8,3.10,3.11). At JOTR, the modeled direct atmospheric contribution from the Los Angeles air basin dropped during the winter sampling period. The HNO_3 concentration measured in both summer and winter were similar to those measured during previous studies in the JOTR region (Allen et al. 2009). There was a relative increase of ambient HNO_3 across most sites during the 2011 sampling period. I hypothesize that this is attributed to the release of abiotic emissions of NO_x molecules following summer precipitation (McCalley and Sparks 2009). During the 4 week

exposure period there were 2 rain events totaling between 1.5cm and 7.5cm within a one week period. These events kept the soil wet consistently for a week as temperatures returned to highs above 100°F (personal observation). McCalley and Sparks measured an increase in soil emissions under these conditions which could account for the increase in ambient HNO₃ measured. Further research must be done to measure the isotopic signature of these emissions to verify if this source is being picked up by the samplers.

The range of summer $\delta^{18}\text{O}$ stayed between 30‰ to 70‰ in both 2010 and 2011, but the distributions were unique. The change in distribution may be due to the influence of abiotic NO_x emissions. As seen in the weekly exposures from Chapter 2, there was a mixing of three apparent sources across the study area, with the shared source contributing highest in samples that were exposed during the precipitation events. On the western edge of the study area the rain caused flooding that closed many of the roads in the area, therefore reducing vehicular emissions during the summer 2011 exposure. I hypothesize that the reduction in local emissions combined with a possible increase in soil emissions would account for reduced $\delta^{18}\text{O}$ in the sites east of the LSBM. For sites on the west side of the LSBM, the spatial relationship with the agricultural zone was less apparent as the dominant spatial trend came from the western sites. Without the change in airflow due to a storm moving through the area, it appears that there is surface air flow from the agricultural sites north towards Palm

Springs. During the summer this is visible as a low elevation inversion layer of smog observed from the west.

The distribution of $\delta^{15}\text{N}$ in summer 2010 creates a fast transition from enriched to depleted values along the LSBM, suggesting that there was not very much transport of atmospheric HNO_3 over the range. The $\delta^{15}\text{N}$ measured at the farthest east sites (-3‰ to -5‰) are within the range that has previously been measured from automobile exhaust inputs (Freyer 1991, Ammann et al. 1999, Hastings et al. 2003). Based on the similarity of values and the differences between the eastern and western sites, I hypothesize that most of the anthropogenic nitrogen measured during the sampling period was sourced from local vehicular traffic. The western sites had $\delta^{15}\text{N}$ between 7.7‰ and 19.5‰ and the highest values were measured in the center of the study area where air from the Los Angeles air basin and the agricultural zone mix. Most atmospheric $\delta^{15}\text{N}$ measurements have been made through the analysis of wet deposition and have ranged from -11‰ to 3.5‰ (Elliott et al. 2007). A study in the northwestern United States used similar passive samplers to measure ambient HNO_3 and observed values between -1‰ and 11‰ (Elliott et al. 2009), but the dominant NO_x emissions were from stationary sources. The modeled back trajectories for the sampling sites near agricultural zones showed that air masses passing over the San Bernardino National Forest, south of the Banning pass connecting the desert to the Los Angeles Air Basin (Figure 3.10). The individual linear relationships between the 2010 $\delta^{18}\text{O}$ and $\delta^{15}\text{N}$

(Figure 3.3C) suggests that there are two independent sources from each side of the LSBMs mixing with a single source from the agricultural zone.

The sampling site at Whitewater, which was set up 2 weeks into the experiment, had values on one end of the western LSBM mixing line suggesting that there was a shift in air flow between the first two weeks and the second two weeks of the exposure. There was less influence on these samples by the agricultural emissions coming from the east, and I hypothesize that this collector represents the HNO_3 isotope values from the Los Angeles air basin.

Mean summer 2011 $\delta^{15}\text{N}$ ranged from -0.2‰ and -5.4‰ . The lowest values were measured on the east and west boundaries of the study area similar to the $\delta^{18}\text{O}$ measurements from 2010. The relationships between HNO_3 concentration and $\delta^{15}\text{N}$ on both sides of the LSBM suggest that there were three sources mixing across all sites (Figure 3.6B). As with 2010, it is assumed that there are two independent sources on the east and western LSBM, but with the changing weather patterns over the course of the exposures, more mixing took place among the sources than in 2010. The relationship between $\delta^{15}\text{N}$ and $\delta^{18}\text{O}$ among the east and west sites were consistent with the previous pattern, and based on the analysis of weekly exposures from two of the high deposition sites and two of the low deposition sites (Chapter 2), the secondary source appears to be derived from soil emissions, based on the two mixing lines crossing at $\delta^{15}\text{N}=0.3\text{‰}$ and $\delta^{18}\text{O}=33\text{‰}$.

Winter Mixing Dynamics

The mean HNO₃ concentrations during the winter ranged from 0.29 to 1.8 µg/m³. The highest values were recorded at the southern sampling sites near the agricultural zone and spread up the valley toward Palm Springs. The eastern sites in the interior of the park had very low HNO₃ concentrations which were expected due to the modeled air trajectory (Figure 3.8). The dominant source of the air flow to the interior sites was from the north, which bypassed the relatively high emission zones of the Los Angeles air basin and the Coachella Valley.

The δ¹⁵N values followed a similar geographic pattern as the HNO₃ concentration with values ranging from -3.7‰ to 2.14‰. The depleted δ¹⁵N values all occurred at the western sites while the positive values occurred east of the LSBM. The pattern is similar to that observed in summer 2010 with change from positive to negative values when crossing the LSBM. This finding suggests that the majority of nitrogen deposition occurring during the winter months is due to agricultural emissions that remain within the valley.

The winter δ¹⁸O values ranged from 70‰ to 83‰ and are, on average, more enriched than their summer counterparts. This temporal pattern is consistent with samples collected in other environments (Hastings et al. 2003, Hastings et al. 2004) and consistent with the reduction of NO_x degassing during cooler, continuous wet periods (Davidson 1992, Smart et al. 1999). Without admixtures of soil NO, atmospheric HNO₃ maintains its anthropogenic source signature. Both the eastern and western sites' δ¹⁸O

were negatively related to increasing atmospheric HNO₃ concentration (Figure 9A). The consistent linear relationship suggests a mixing of two sources dominated by a source with a less enriched δ¹⁸O to the east. The winter δ¹⁵N values were not significantly related to δ¹⁸O on either side of the mountains (Figure 9C), suggesting that there were more than two sources of HNO₃ collected by the filters. Due to the lower HNO₃ concentrations present during the winter, smaller, local HNO₃ additions would make up a larger percentage of measurements, while in the summer time, if present, they would be less noticeable as ambient HNO₃ was dominated by two main sources.

Variability in measurements

One of the most interesting outcomes from this seasonal study was that during the summer sampling periods the relationship between δ¹⁵N and δ¹⁸O was consistent and unique on each side of the LSBM. At some of the sites there was high variability in the amount of HNO₃ present on filters, while the isotopic composition of the HNO₃ remained consistent for the area. This suggests that the HNO₃ sources mixing at a site remained the same throughout the exposure, but certain filters on the sampler may have been prone to collecting HNO₃ during discrete times during the exposure period. These discrete events may have been caused by changing weather patterns combined with wind gusts that were measured at over 50 mph at some sites during the filter

exposure period. There is also the possibility that if dust settles on the filters, it may reduce the flow of HNO_3 to the collection filter.

While this field survey used four week exposures to ensure that enough HNO_3 was collected for isotopic analysis, new methods have been developed to reduce the amount of NO_3^- necessary to produce accurate isotopic results (McIlvin and Casciotti 2011). Therefore, I recommend only exposing the filters in 2 week intervals in areas that experience highly variable extreme weather conditions and are subject to high amounts of dust.

Conclusions

Passive samplers were an effective tool to measure the $\delta^{18}\text{O}$ and $\delta^{15}\text{N}$ of HNO_3 along a deposition gradient from the LA basin to JOTR. Variations in measured HNO_3 on the filters were associated with changes in the source of HNO_3 . The isotopic analyses suggest that, during the summer, there are two unique anthropogenic sources on the east and west sides of the LSBM, each mixing with a third source originating from the agricultural zone of the Coachella Valley. On the west side of the LSBM, the second source comes from the Los Angeles air basin, while on the east side of the LSBM, the second source appears to be from local emissions from automobiles in the park.

During the summer, variations in $\delta^{18}\text{O}$ and $\delta^{15}\text{N}$ of HNO_3 were recorded at each site, but the relationship between the two isotopes was unique on each side of the LSBM. The isotopic signature of HNO_3 appeared to be affected by changes in weather

patterns. High winds and changing sources of air masses influenced the amount of HNO_3 accumulation varied on individual filters. Different storms have been measured with unique isotopic signatures based on the path that the air mass travels and how much rain was dropped prior to reaching a site (Moore 1977). Simple changes to the sampler design, such as increasing the length of the outer cover, may reduce the impact of these variable weather conditions.

The isotopic signature helps to define the movement of HNO_3 through this complex ecosystem. Efforts are currently underway to assess critical loads of N on ecosystem processes for regulatory purposes (Pardo et al. 2011). A better understanding of sources and movement of anthropogenic nitrogen will allow regulators to reduce N emissions and the source and search for solutions to reduce their impact.

References

- Allen, E. B., L. E. Rao, R. J. Steers, A. Bytnerowicz, and M. E. Fenn. 2009. Impacts of atmospheric nitrogen deposition on vegetation and soils in Joshua Tree National Park. Pages 78-100 in R. H. Webb, L. F. Fenstermaker, J. S. Heaton, D. L. Hughson, E. V. McDonald, and D. M. Miller, editors. *The Mojave Desert: Ecosystem Processes and Sustainability*. University of Nevada Press, Las Vegas.
- Ammann, M., R. Siegwolf, F. Pichlmayer, M. Suter, M. Saurer, and C. Brunold. 1999. Estimating the uptake of traffic-derived NO₂ from N-15 abundance in Norway spruce needles. *Oecologia* 118:124-131.
- Bytnerowicz, A. and M. E. Fenn. 1996. Nitrogen deposition in California forests: A review. *Environmental Pollution* 92:127-146.
- Bytnerowicz, A., M. J. Sanz, M. J. Arbaugh, P. E. Padgett, D. P. Jones, and A. Davila. 2005. Passive sampler for monitoring ambient nitric acid (HNO₃) and nitrous acid (HNO₂) concentrations. *Atmospheric Environment* 39:2655-2660.
- Casciotti, K. L., D. M. Sigman, M. G. Hastings, J. K. Böhlke, and A. Hilkert. 2002. Measurement of the Oxygen Isotopic Composition of Nitrate in Seawater and Freshwater Using the Denitrifier Method. *Analytical Chemistry* 74:4905-4912.
- Davidson, E. A. 1992. Sources of Nitric Oxide and Nitrous Oxide following Wetting of Dry Soil. *Soil Sci. Soc. Am. J.* 56:95-102.
- Elliott, E. M., C. Kendall, E. B. Boyer, D. A. Burns, G. Lear, H. E. Golden, K. Harlin, A. Bytnerowicz, T. J. Butler, and R. Glatz. 2009. Dual nitrate isotopes in actively and passively collected dry deposition: Utility for partitioning NO_x sources, understanding reaction pathways, and comparison with isotopes in wet nitrate deposition. *Journal of Geophysical Research: Biogeosciences*.
- Elliott, E. M., C. Kendall, S. D. Wankel, D. A. Burns, E. W. Boyer, K. Harlin, D. J. Bain, and T. J. Butler. 2007. Nitrogen isotopes as indicators of NO_x source contributions to atmospheric nitrate deposition across the Midwestern and northeastern United States. *Environmental Science & Technology* 41:7661-7667.

- Fenn, M. E., E. B. Allen, S. B. Weiss, S. Jovan, L. H. Geiser, G. S. Tonnesen, R. F. Johnson, L. E. Rao, B. S. Gimeno, F. Yuan, T. Meixner, and A. Bytnerowicz. 2010. Nitrogen critical loads and management alternatives for N-impacted ecosystems in California. *Journal of Environmental Management* 91:2404-2423.
- Fenn, M. E., J. S. Baron, E. B. Allen, H. M. Rueth, K. R. Nydick, L. Geiser, W. D. Bowman, J. O. Sickman, T. Meixner, D. W. Johnson, and P. Neitlich. 2003a. Ecological effects of nitrogen deposition in the western United States. *Bioscience* 53:404-420.
- Fenn, M. E., R. Haeuber, G. S. Tonnesen, J. S. Baron, S. Grossman-Clarke, D. Hope, D. A. Jaffe, S. Copeland, L. Geiser, H. M. Rueth, and J. O. Sickman. 2003b. Nitrogen emissions, deposition, and monitoring in the western United States. *Bioscience* 53:391-403.
- Freyer, H. D. 1991. Seasonal-variation of N¹⁵/N¹⁴ ratios in atmospheric nitrate species. *Tellus Series B-Chemical and Physical Meteorology* 43:30-44.
- Granger, S. J., T. H. E. Heaton, R. Bol, G. S. Bilotta, P. Butler, P. M. Haygarth, and P. N. Owens. 2008. Using delta N-15 and delta O-18 to evaluate the sources and pathways of NO₃⁻ in rainfall event discharge from drained agricultural grassland lysimeters at high temporal resolutions. *Rapid Communications in Mass Spectrometry* 22:1681-1689.
- Greenberg, E. P. and G. E. Becker. 1977. Nitrous oxide as end product of denitrification by strains of fluorescent pseudomonads. *Canadian Journal of Microbiology* 23:903-907.
- Hastings, M. G., D. M. Sigman, and F. Lipschultz. 2003. Isotopic evidence for source changes of nitrate in rain at Bermuda. *J. Geophys. Res.* 108:4790.
- Hastings, M. G., E. J. Steig, and D. M. Sigman. 2004. Seasonal variations in N and O isotopes of nitrate in snow at Summit, Greenland: Implications for the study of nitrate in snow and ice cores. *J. Geophys. Res.* 109:D20306.
- Heaton, T. H. E., B. Spiro, S. Madeline, and C. Robertson. 1997. Potential canopy influences on the isotopic composition of nitrogen and sulphur in atmospheric deposition. *Oecologia* 109:600-607.

- Johnson, N. C., D. L. Rowland, L. Corkidi, L. M. Egerton-Warburton, and E. B. Allen. 2003. Nitrogen enrichment alters mycorrhizal allocation at five mesic to semiarid grasslands. *Ecology* 84:1895-1908.
- Kendall, C., E. M. Elliott, and S. D. Wankel. 2007. Tracing Anthropogenic Inputs of Nitrogen. *in* R. Michener and K. Lajtha, editors. *Stable Isotopes in Ecology and Environmental Science*. Wiley-Blackwell, Malden, MA.
- Krupa, S. V. 2003. Effects of atmospheric ammonia (NH₃) on terrestrial vegetation: a review. *Environmental Pollution* 124:179-221.
- McCalley, C. K. and J. P. Sparks. 2009. Abiotic Gas Formation Drives Nitrogen Loss from a Desert Ecosystem. *Science* 326:837-840.
- McIlvin, M. R. and K. L. Casciotti. 2011. Technical Updates to the Bacterial Method for Nitrate Isotopic Analyses. *Analytical Chemistry* 83:1850-1856.
- Michalski, G., T. Meixner, M. Fenn, L. Hernandez, A. Sirulnik, E. Allen, and M. Thiemens. 2004. Tracing atmospheric nitrate deposition in a complex semiarid ecosystem using Delta(17)O. *Environmental Science & Technology* 38:2175-2181.
- Moore, H. 1977. Isotopic composition of ammonia, nitrogen-dioxide, and nitrate in atmosphere. *Atmospheric Environment* 11:1239-1243.
- Neuman, J. A., D. D. Parrish, M. Trainer, T. B. Ryerson, J. S. Holloway, J. B. Nowak, A. Swanson, F. Flocke, J. M. Roberts, S. S. Brown, H. Stark, R. Sommariva, A. Stohl, R. Peltier, R. Weber, A. G. Wollny, D. T. Sueper, G. Hubler, and F. C. Fehsenfeld. 2006. Reactive nitrogen transport and photochemistry in urban plumes over the North Atlantic Ocean. *J. Geophys. Res.* 111:D23S54.
- NOAA. 2012. HYSPLIT (HYbrid Single-Particle Lagrangian Integrated Trajectory) Model. NOAA Air Resources Laboratory, Silver Spring, Md.
- Ochoa-Hueso, R., E. B. Allen, C. Branquinho, C. Cruz, T. Dias, M. E. Fenn, E. Manrique, M. E. Pérez-Corona, L. J. Sheppard, and W. D. Stock. 2011. Nitrogen deposition effects on Mediterranean-type ecosystems: An ecological assessment. *Environmental Pollution* 159:2265-2279.

- Pardo, L. H., M. E. Fenn, C. L. Goodale, L. H. Geiser, C. T. Driscoll, E. B. Allen, J. S. Baron, R. Bobbink, W. D. Bowman, C. M. Clark, B. Emmett, F. S. Gilliam, T. L. Greaver, S. J. Hall, E. A. Lilleskov, L. Liu, J. A. Lynch, K. J. Nadelhoffer, S. S. Perakis, M. J. Robin-Abbott, J. L. Stoddard, K. C. Weathers, and R. L. Dennis. 2011. Effects of nitrogen deposition and empirical nitrogen critical loads for ecoregions of the United States. *Ecological Applications* 21:3049-3082.
- Peterson, B. J. and B. Fry. 1987. Stable Isotopes in Ecosystem Studies. *Annual Review of Ecology and Systematics* 18:293-320.
- Rao, L. E., D. R. Parker, A. Bytnerowicz, and E. B. Allen. 2009. Nitrogen mineralization across an atmospheric nitrogen deposition gradient in Southern California deserts. *Journal of Arid Environments* 73:920-930.
- Rock, L. and B. H. Ellen. 2007. Nitrogen-15 and oxygen-18 natural abundance of potassium chloride extractable soil nitrate using the denitrifier method. *Soil Science Society of America Journal* 71:355-361.
- Russell, K. M., J. N. Galloway, S. A. Macko, J. L. Moody, and J. R. Scudlark. 1998. Sources of nitrogen in wet deposition to the Chesapeake Bay region. *Atmospheric Environment* 32:2453-2465.
- Seinfeld, J. H. and S. N. Pandis. 1998. *Atmospheric Chemistry and Physics: From Air Pollution to Climate Change*. Wiley-Interscience, Indianapolis.
- Sigman, D. M., K. L. Casciotti, M. Andreani, C. Barford, M. Galanter, and J. K. Bohlke. 2001. A bacterial method for the nitrogen isotopic analysis of nitrate in seawater and freshwater. *Analytical Chemistry* 73:4145-4153.
- Smart, D. R., J. M. Stark, and V. Diego. 1999. Resource limitations to nitric oxide emissions from a sagebrush-steppe ecosystem. *Biogeochemistry* 47:63-86.
- U.S. Environmental Protection Agency. *2008 National Emission Inventory (NEI) Documentation and Data, Version 2*. Office of Air Quality Planning and Standards, U.S. EPA: Research Triangle Park, NC, 2004.

- U.S. Environmental Protection Agency (U.S. EPA), 2011. Clean Air Status and Trends Network, JOT403. <http://www.epa.gov/castnet/sites/jot403.html> (accessed 10.10.12)
- Vitousek, P. M., J. D. Aber, R. W. Howarth, G. E. Likens, P. A. Matson, D. W. Schindler, W. H. Schlesinger, and D. G. Tilman. 1997. Human alteration of the global nitrogen cycle: Sources and consequences. *Ecological Applications* 7:737-750.
- Voss, M., B. Deutsch, R. Elmgren, C. Humborg, P. Kuuppo, M. Pastuszak, C. Rolff, and U. Schulte. 2006. Source identification of nitrate by means of isotopic tracers in the Baltic Sea catchments. *Biogeosciences* 3:663-676.
- Wang, G., M. Ngouajio, M. E. McGiffen, Jr, and C. M. Hutchinson. 2008. Summer Cover Crop and In-season Management System Affect Growth and Yield of Lettuce and Cantaloupe. *HortScience* 43:1398-1403.
- Wang, Y. Q., X. Y. Zhang, and R. R. Draxler. 2009. TrajStat: GIS-based software that uses various trajectory statistical analysis methods to identify potential sources from long-term air pollution measurement data. *Environmental Modelling & Software* 24:938-939.
- Wankel, S. D., C. Kendall, C. A. Francis, and A. Paytan. 2006. Nitrogen sources and cycling in the San Francisco Bay Estuary: A nitrate dual isotopic composition approach. *Limnology and Oceanography* 51:1654-1664.

Figures

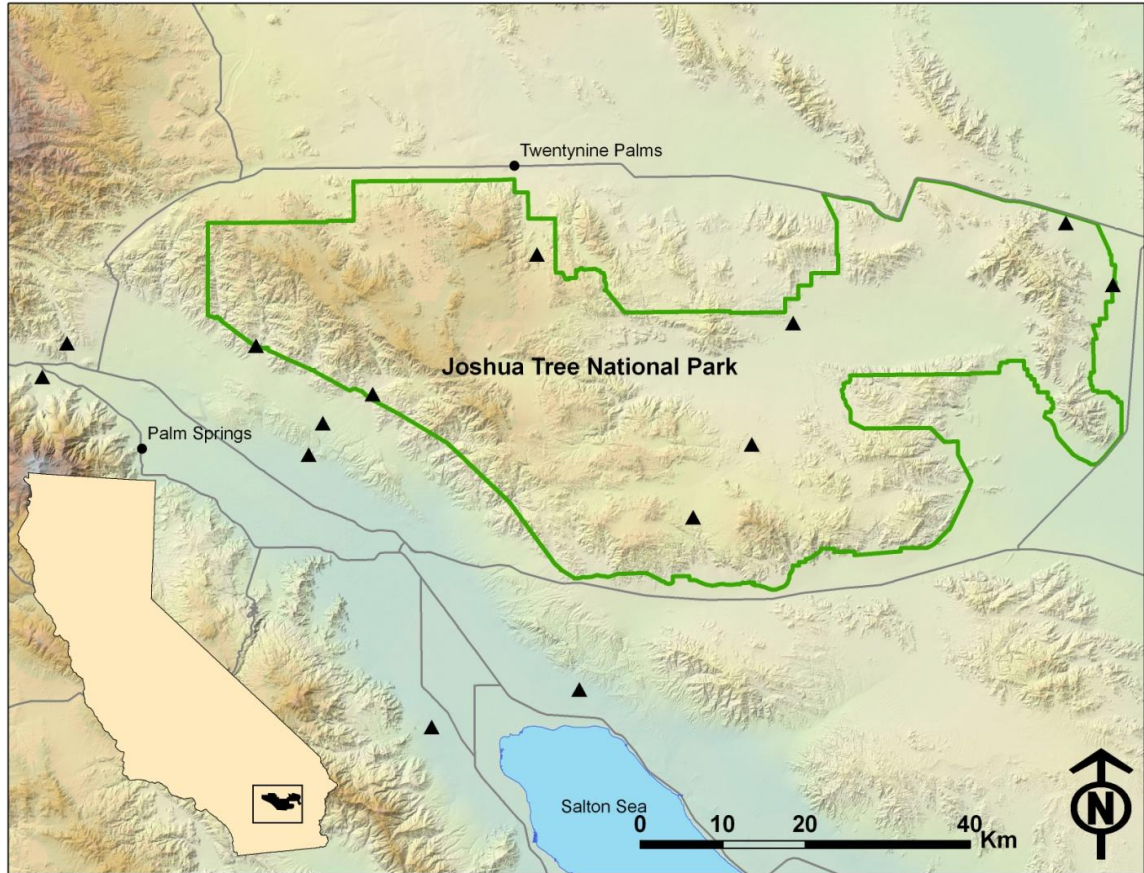


Figure 3.1. Site locations of atmospheric samplers relative to major cities and Joshua Tree National Park.

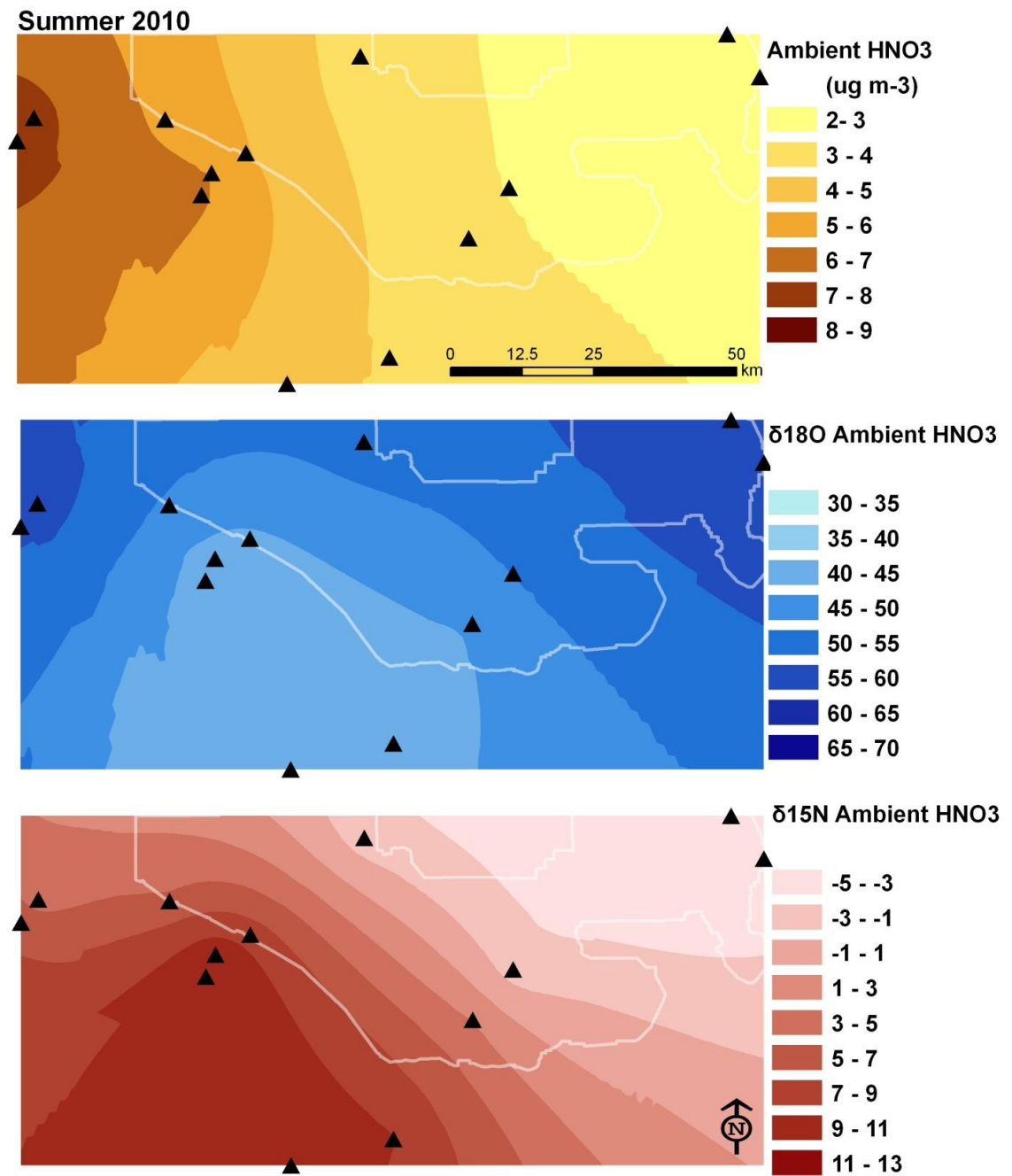


Figure 3.2. Field measurements of (A) ambient atmospheric concentration of HNO₃, (B) ambient HNO₃ δ¹⁸O, and (C) ambient HNO₃ δ¹⁵N from the exposure period between August 26, 2010 to September 21, 2010. Contours generated using an original Kriging analysis based on mean values from each site.

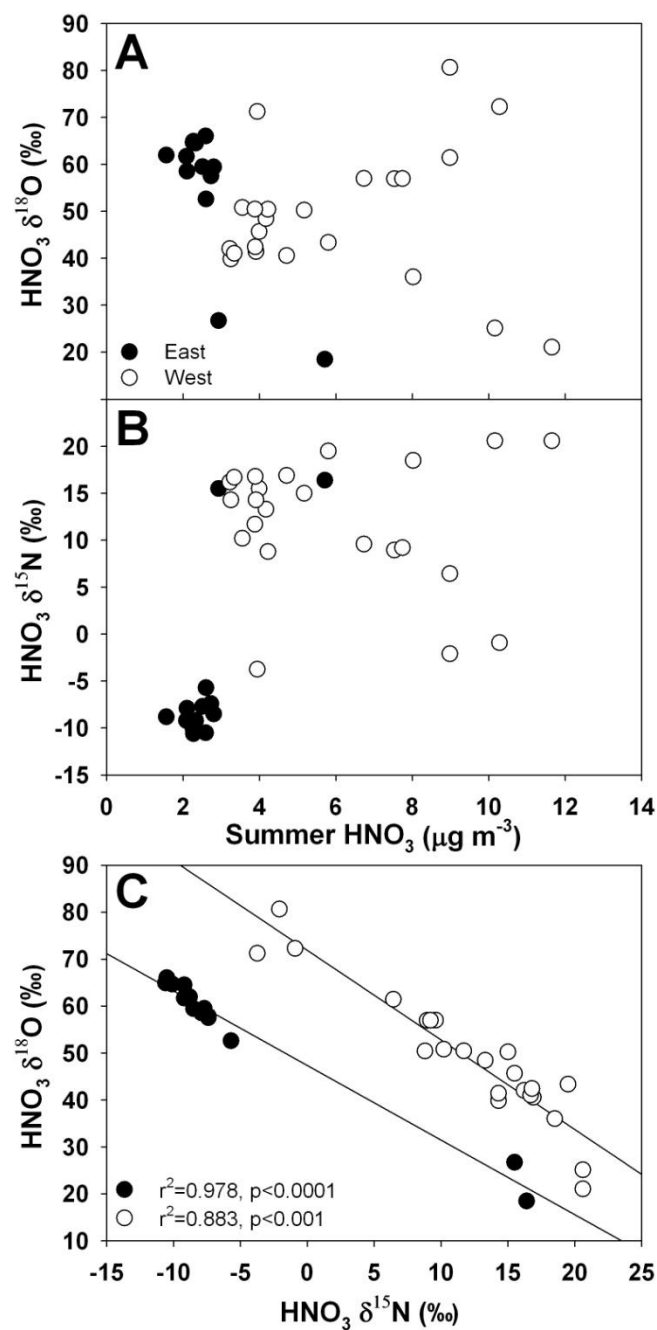


Figure 3.3. There is not a linear relationship between summer ambient HNO_3 concentration and (A) $\text{HNO}_3 \delta^{18}\text{O}$ or (B) $\text{HNO}_3 \delta^{15}\text{N}$ from samplers on the east (filled circles) or west (open circles) of the Little San Bernardino Mountains for summer exposures between August 26, 2010 and September 21, 2010. When $\text{HNO}_3 \delta^{15}\text{N}$ is regressed against $\text{HNO}_3 \delta^{18}\text{O}$ (C) there are linear relationships present on each side of the mountains.

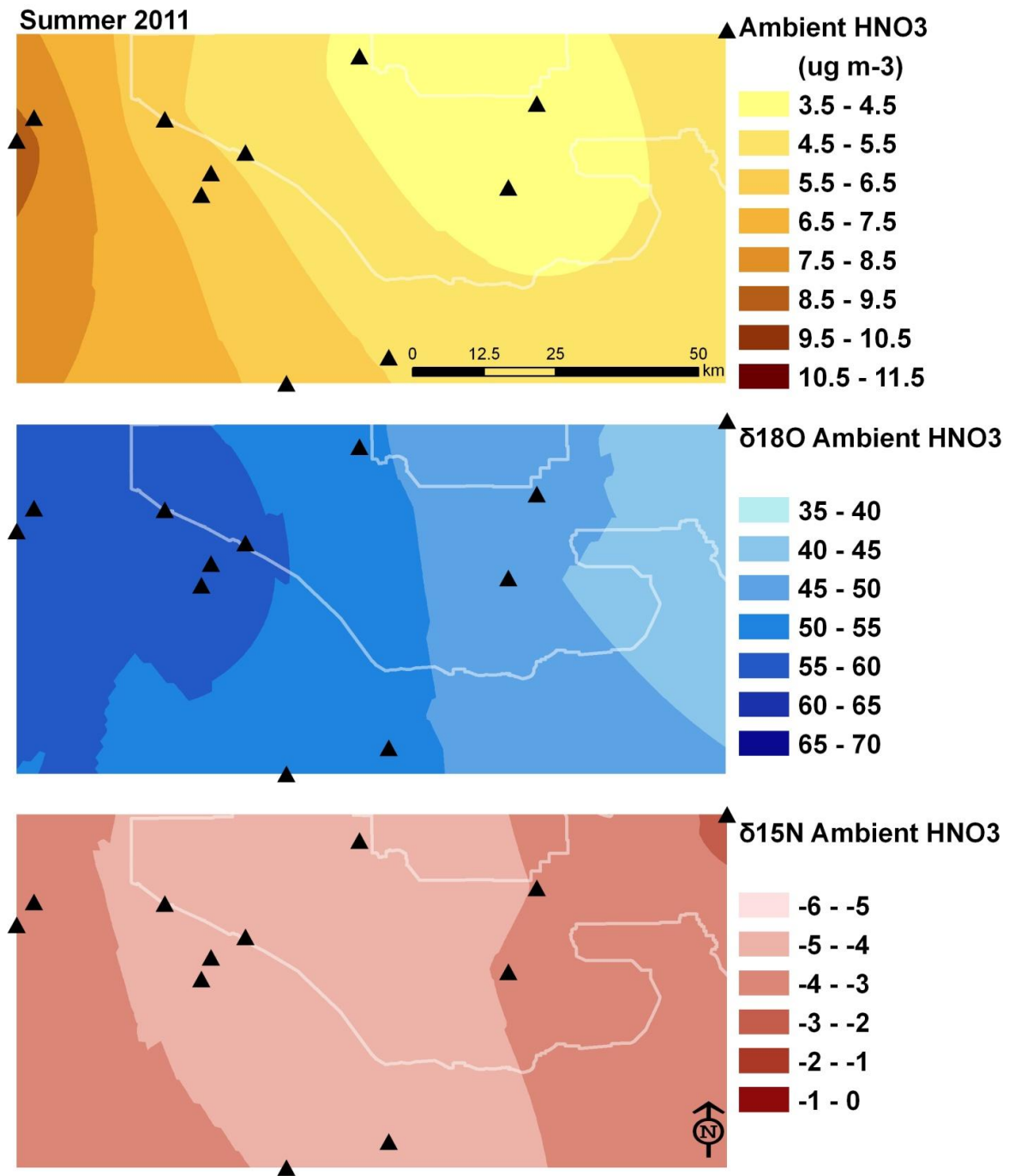


Figure 3.4. Field measurements of (A) ambient atmospheric concentration of HNO₃, (B) ambient HNO₃ δ¹⁸O, and (C) ambient HNO₃ δ¹⁵N from the exposure period between August 31, 2011 to September 28, 2011. Contours generated using an original Kriging analysis based on mean values from each site.

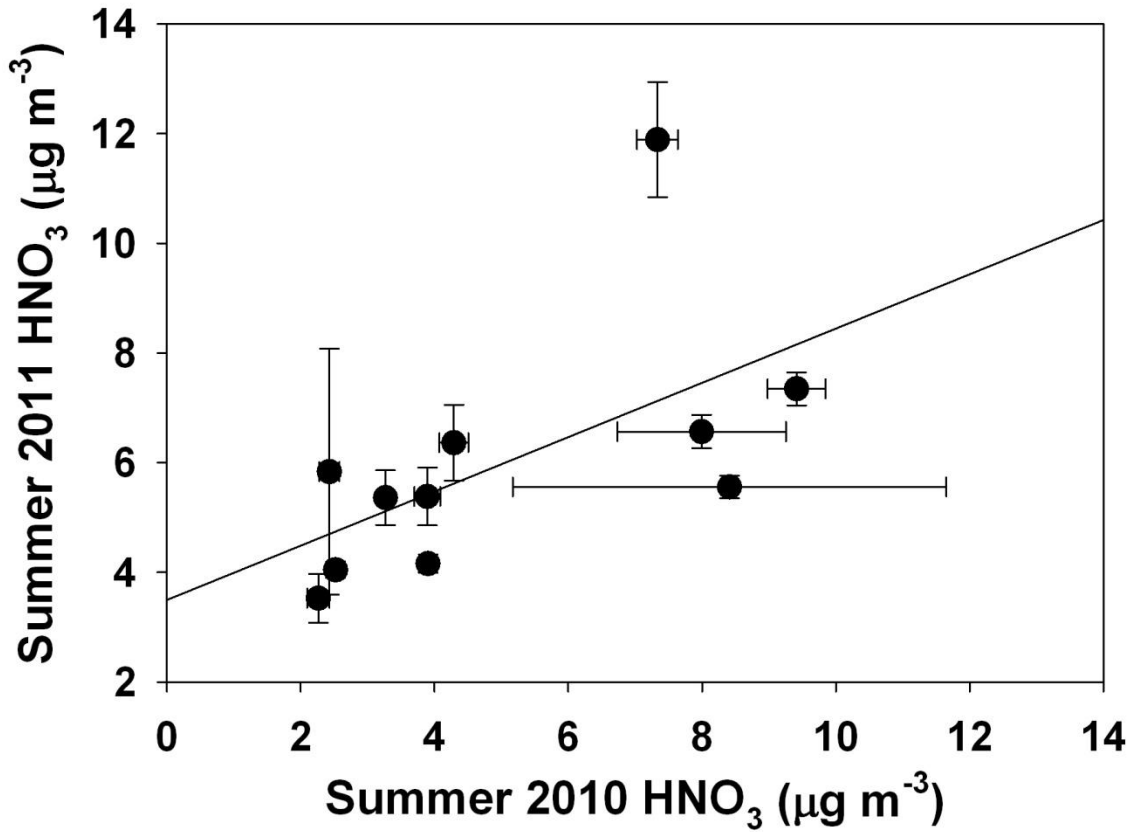


Figure 3.5. Regression between mean ambient HNO₃ values from the summer 2010 exposure period and the summer 2011 exposure period.

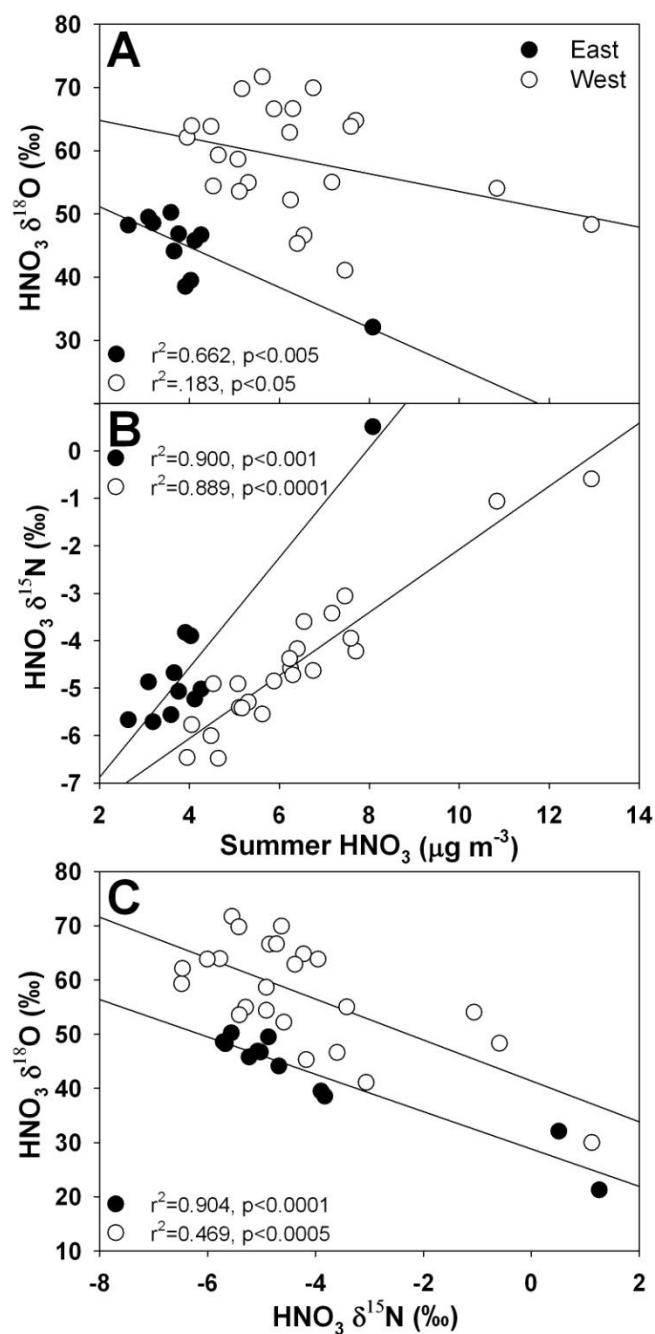


Figure 3.6. Relationships between summer ambient HNO_3 concentration and (A) $\text{HNO}_3 \delta^{18}\text{O}$ and (B) $\text{HNO}_3 \delta^{15}\text{N}$ from samplers on the east (filled circles) or west (open circles) of the Little San Bernardino Mountains for samples exposed between August 31, 2011 and September 28, 2011. When $\text{HNO}_3 \delta^{15}\text{N}$ is regressed against $\text{HNO}_3 \delta^{18}\text{O}$ (C) there are significant relationships on each side of the mountains.

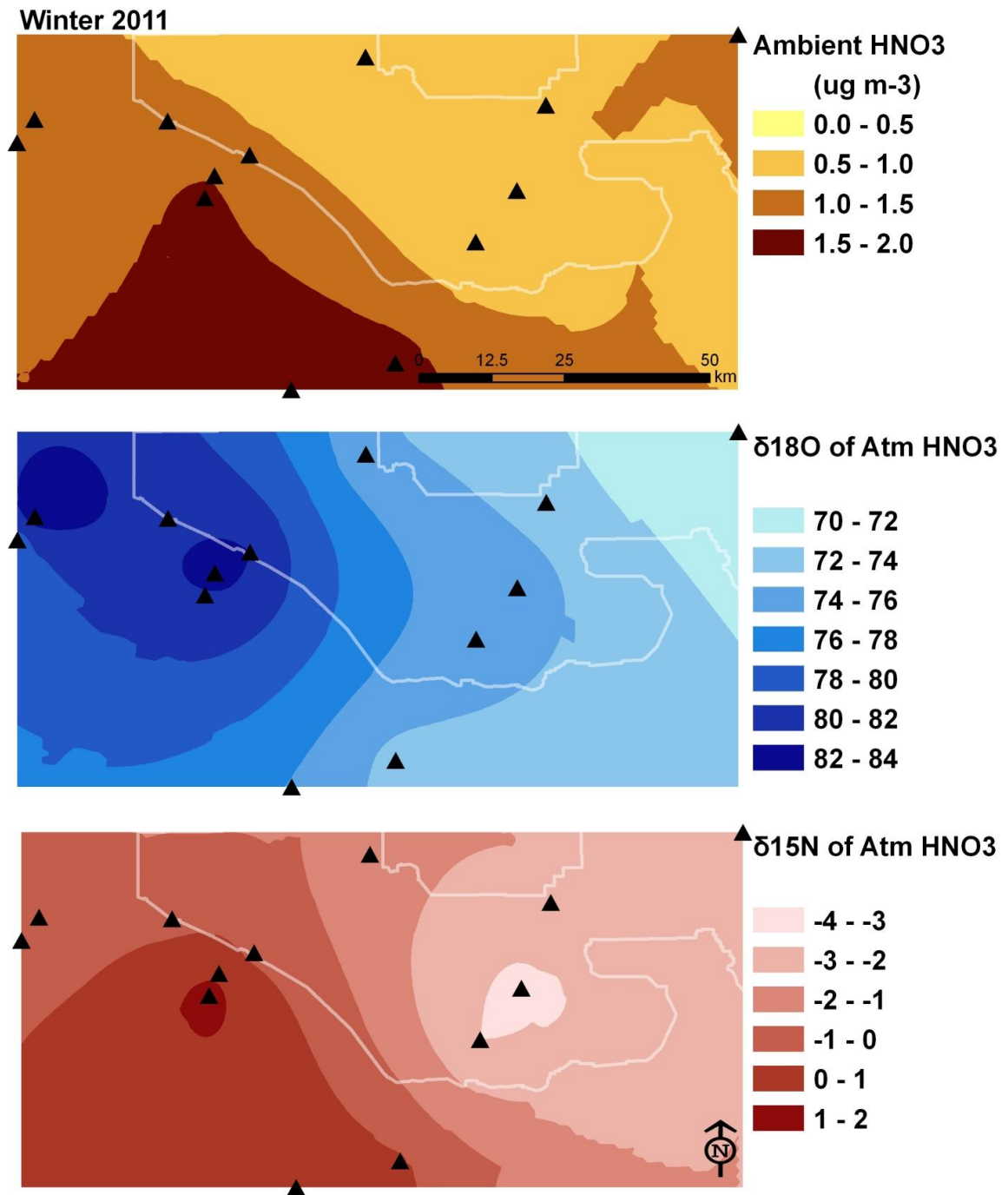


Figure 3.7. Field measurements of (A) ambient atmospheric concentration of HNO₃, (B) ambient HNO₃ δ¹⁸O, and (C) ambient HNO₃ δ¹⁵N from the exposure period between January 6, 2011 to February 1, 2011. Contours generated using an original Kriging analysis based on mean values from each site.

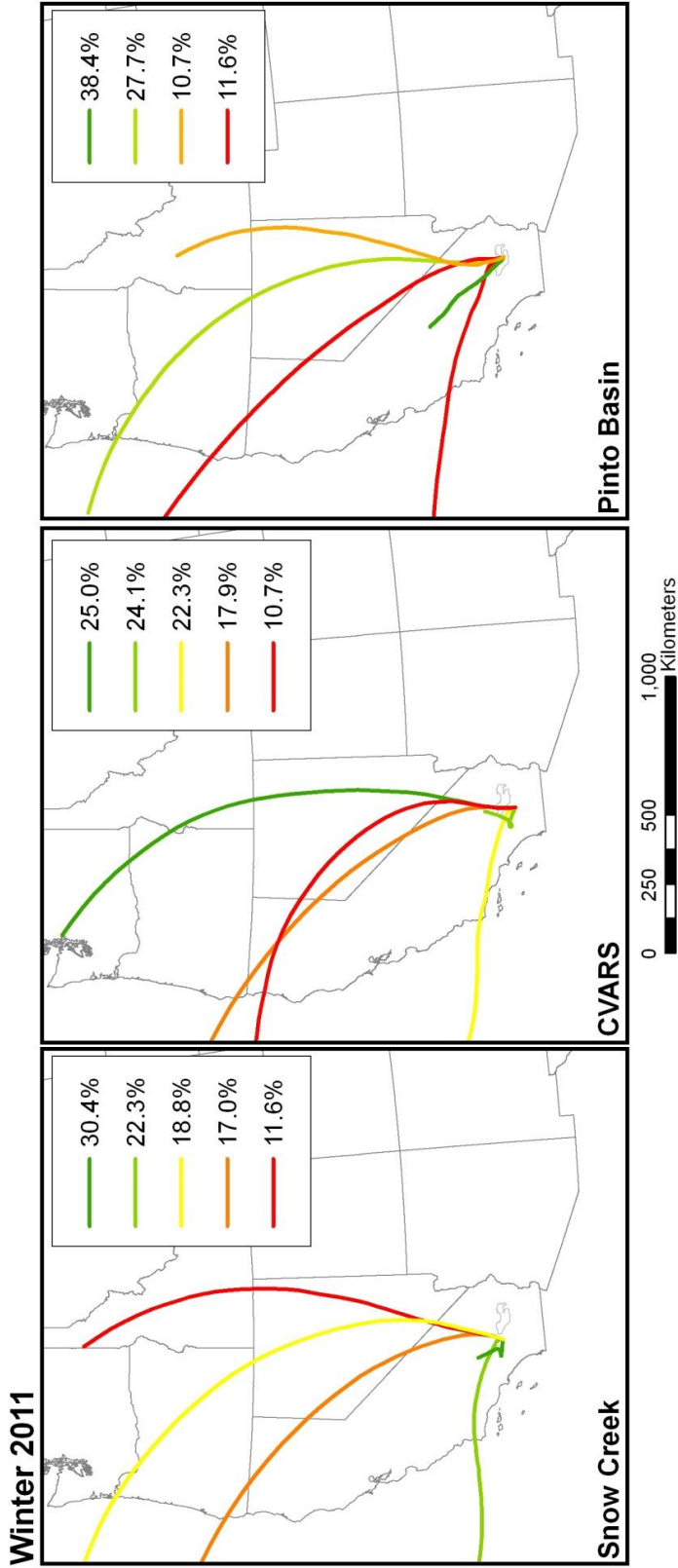


Figure 3.8. The five dominant particle movement paths of 48-hour HYSPLIT air mass back trajectories during the winter 2011 ambient HNO₃ exposure period, identified by percentage of air movement that followed a single path. Trajectories were taken every 6 hours (0600h, 1200h, 1800h, 2400h) from particles with a final elevation of 10m.

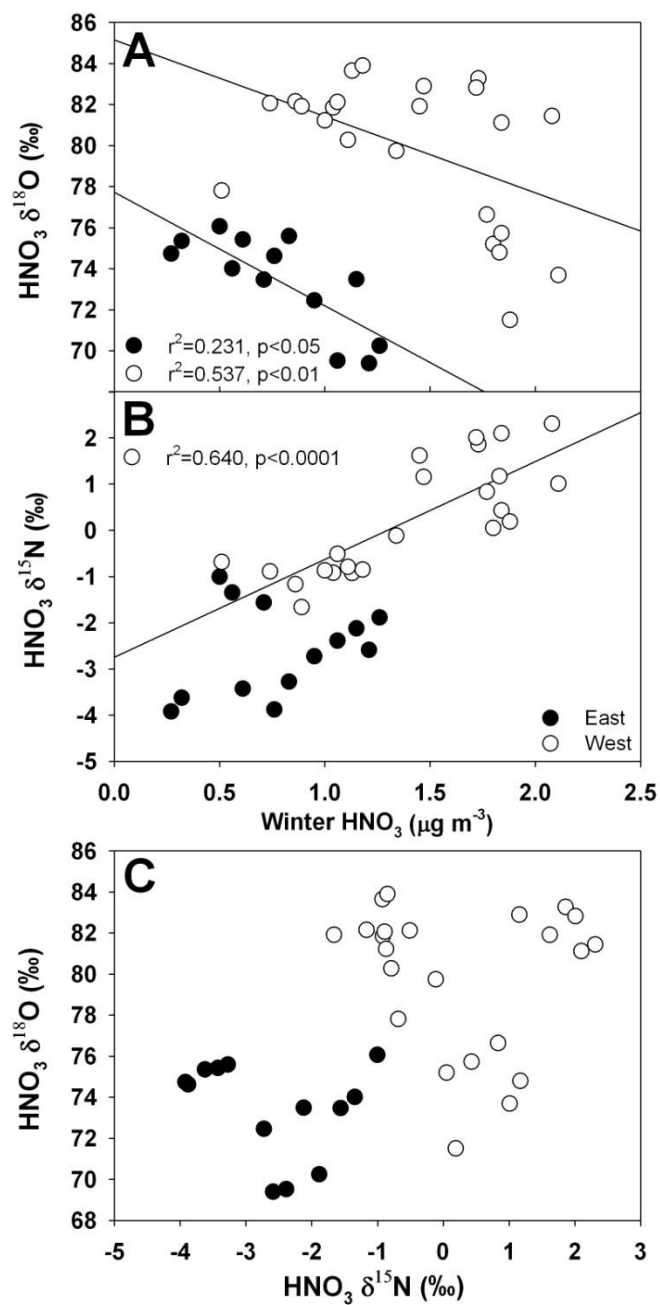


Figure 3.9. Regressions between summer ambient HNO_3 concentration and (A) $\text{HNO}_3 \delta^{18}\text{O}$ and (B) $\text{HNO}_3 \delta^{15}\text{N}$ from winter samplers on the east (filled circles) or west (open circles) of the Little San Bernardino Mountains exposed between January 6, 2011 to February 1, 2011. When $\text{HNO}_3 \delta^{15}\text{N}$ is regressed against $\text{HNO}_3 \delta^{18}\text{O}$ (C) there are significant relationships on each side of the mountains.

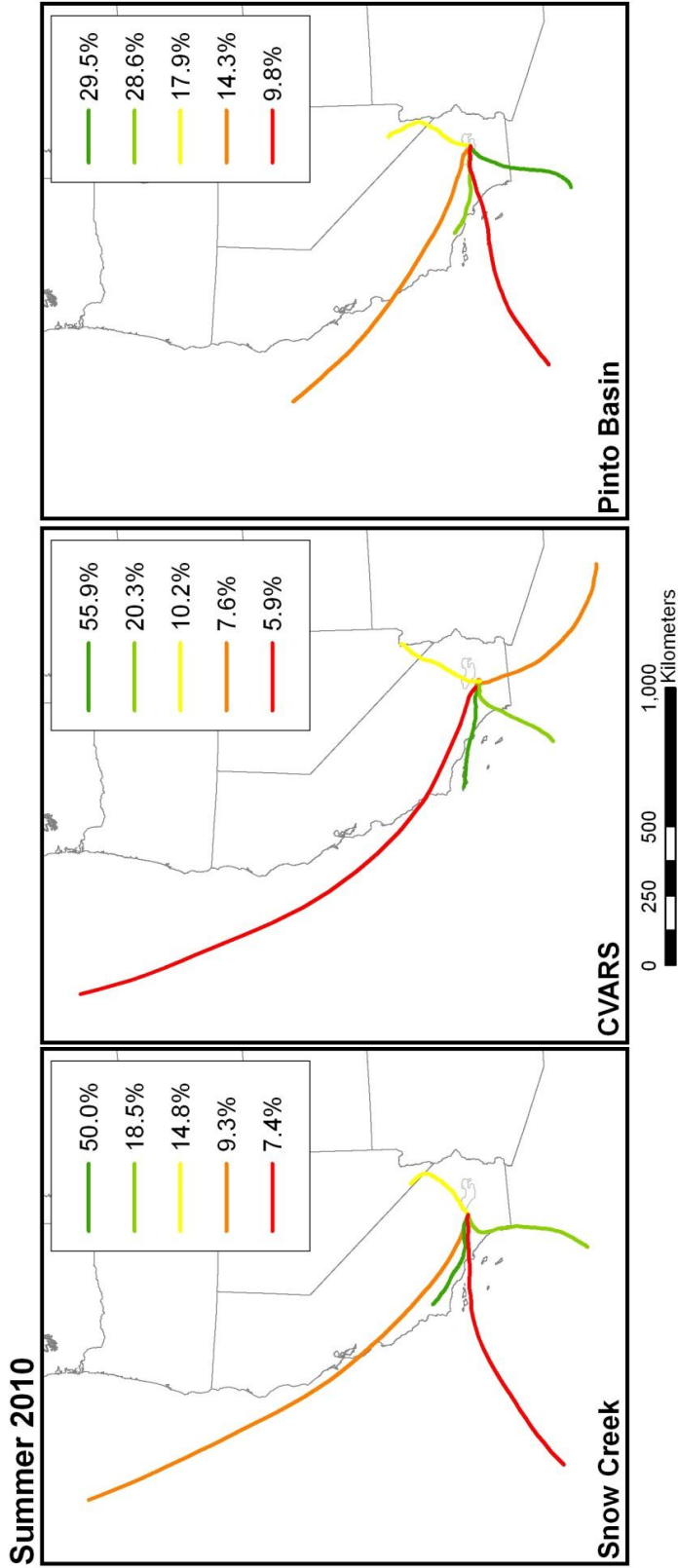


Figure 3.10. The five dominant particle movement paths of 48-hour HYSPLIT air mass back trajectories during the summer 2010 ambient HNO₃ exposure period, identified by percentage of air movement that followed a single path. Trajectories were taken every 6 hours (0600h, 1200h, 1800h, 2400h) from particles with a final elevation of 10m.

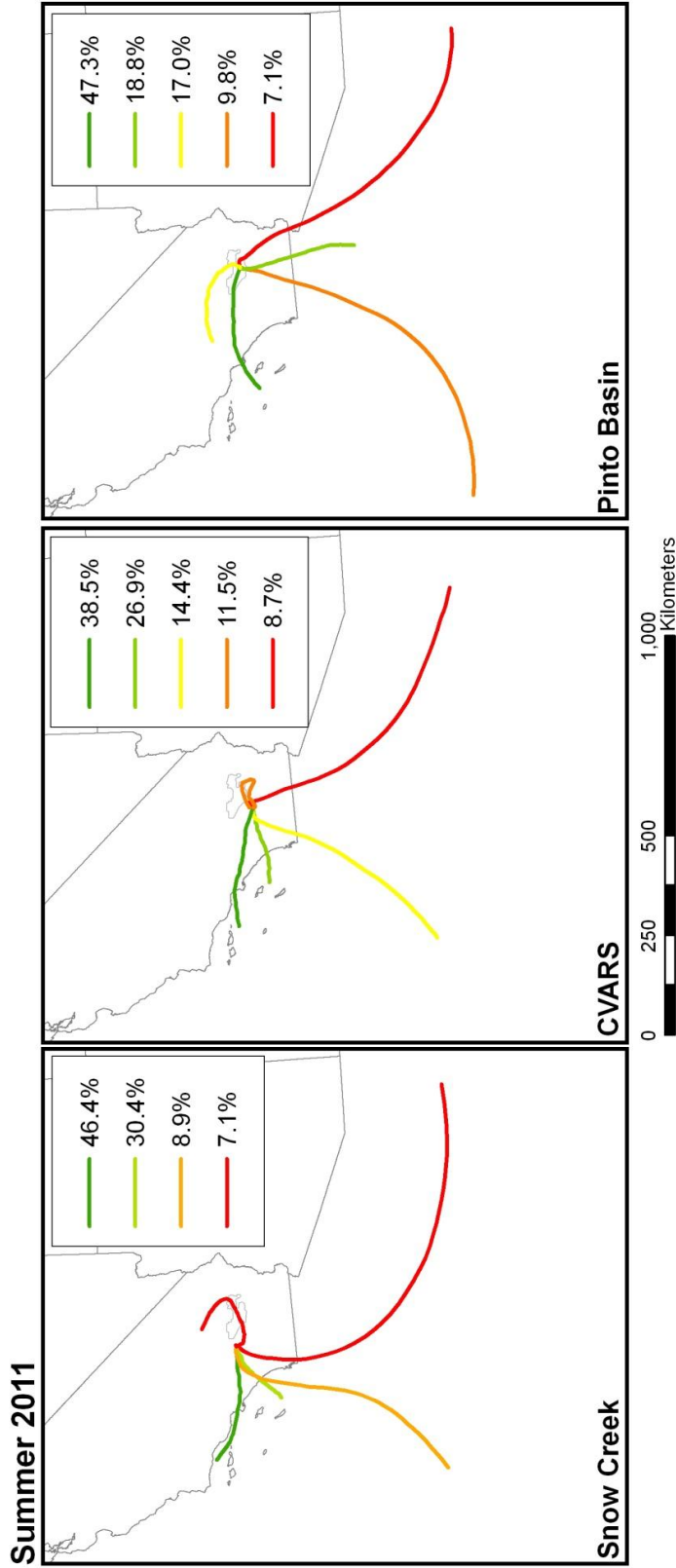


Figure 3.11. The five dominant particle movement paths of a 48-hour HYSPLIT air mass back trajectories during the summer 2011 ambient HNO_3 exposure period, identified by percentage of air movement that followed a single path. Trajectories were taken every 6 hours (0600h, 1200h, 1800h, 2400h) from particles with a final elevation of 10m.

Chapter 4: Isotopes of nitrogen and oxygen in soil and plant material as indicators of anthropogenic nitrogen additions to the Sonoran Desert

Abstract

Anthropogenic nitrogen (N) inputs to undisturbed ecosystems can cause vegetation responses in the form of increased biomass and community composition shifts. Anthropogenic inputs often have consistent ratios of N and oxygen (O) isotopes which allow them to be identified when mixing with natural N sources. This research measures extractable soil NO_3^- $\delta^{15}\text{N}$ and $\delta^{18}\text{O}$ and leaf tissue $\delta^{15}\text{N}$ across a N deposition gradient in the western Sonoran Desert with the goal of using stable isotopes as tracers to identify anthropogenic sources and amounts of N added to the region. Surface soil samples were taken in the summer and winter from thirteen sites spanning a 100 km N deposition gradient in creosote bush scrub vegetation. From each site, leaf tissue from *Larrea tridentata* was collected in the summer, and *Schismus arabicus* and *Chaenactis fremontii* tissue were collected in early winter and early spring where available. Surface soil NO_3^- concentration and $\delta^{18}\text{O}$ were positively linearly correlated with summer ambient atmospheric N concentration. *Larrea tridentata* leaf tissue $\delta^{15}\text{N}$ had a negative linear correlation with soil NO_3^- $\delta^{18}\text{O}$, consistent with the relationship between soil NO_3^- $\delta^{15}\text{N}$ and $\delta^{18}\text{O}$. Early winter annual vegetation changed consistently with summer soil

$\text{NO}_3^- \delta^{18}\text{O}$, but only *C. fremontii* maintained a relationship with deposition in the late spring. The results of this research suggest that summer surface soil NO_3^- can be used as an indicator of the amount of atmospheric HNO_3 deposition to a site. It is most effective when samples are collected prior to summer precipitation events, allowing a detailed understanding of deposition patterns for a large region.

Introduction

Anthropogenic nitrogen (N) deposition to undisturbed ecosystems can alter vegetation community composition by decreasing richness while increasing productivity (Stevens et al. 2004, Cleland and Harpole 2010, Pardo et al. 2011), which in turn can lead to increased frequency of disturbance by altering the fire cycle (Brooks et al. 2004, Henry et al. 2006, Ochoa-Hueso et al. 2011). Measuring direct anthropogenic N inputs to ecosystems can be time and resource intensive, especially in remote areas (Bytnerowicz et al. 2005). Detecting anthropogenic sources at increasing distances from their origin is complicated due to dilution and mixing of multiple sources. Stable isotopes of N and oxygen (O) have been used to detect anthropogenic sources and influences along environmental gradients (Kendall et al. 2007). Isotopic analysis is common in atmospheric, rainfall, watershed samples, and agricultural soil samples (Vitoria et al. 2004, Wankel et al. 2006, Granger et al. 2008, Elliott et al. 2009, Rock et al. 2011). The rate of change of these isotopes along an environmental gradient enables

determination of anthropogenic source contribution relative to natural variation (Kohl et al. 1971, Kellman and Hillaire-Marcel 2003, Pardo et al. 2004, Elliott et al. 2007).

Reactive N (NH_3 and HNO_3) is currently being produced through anthropogenic activities (e.g., fossil fuel combustion, fertilizers, N-fixing crops) at a global rate more than double the preindustrial rate (Galloway et al. 1995, Galloway et al. 2004). This has led to increased N deposition to natural areas located near urban and agricultural zones (Vitousek et al. 1997, Fenn et al. 2003). In southern California, deposition zones downwind from the Los Angeles air basin have some of the highest annual levels of deposition in the United States (Bytnerowicz and Fenn 1996). The amount of reactive N that induces a negative biological response, the critical load, is dependent on the type of ecosystem and the species of organism being evaluated (Fenn et al. 2010, Pardo et al. 2011). Additional responses to surpassing these critical loads include the change in soil nitrogen processing (Vitousek et al. 1997), loss of sensitive species (Jovan and McCune 2005), increase in exotic invasive plants (Allen et al. 2009), and changes in insect populations (Throop and Lerdau 2004). In order for managers to mitigate for the additions of nitrogen, it is necessary to understand how inputs vary across a region and to easily determine where they are highest.

The proposed study examines the sources and sinks of anthropogenic nitrogen being deposited in the Sonoran Desert located east of the Los Angeles air basin. Nitrogen inputs of $12 \text{ kg ha}^{-1} \text{ yr}^{-1}$ have been measured using throughfall data collectors for the desert on the western edge of the Coachella Valley on the boundary of Joshua

Tree National Park (JOTR) (Allen et al. 2009). Most of the N deposition in dry climates tends to occur in the hot, dry summer season as dry deposition (Fenn and Bytnerowicz 1993, Bytnerowicz and Fenn 1996, Allen et al. 2009). Dry atmospheric N particles can readily deposit on any surface and therefore contribute to N inputs into soils (Eilers et al. 1992). In semi-arid and arid habitats, deposited N can accumulate during the dry season in the upper 2cm of the soil profile in high deposition areas (Padgett et al. 1999), before entering the rhizosphere in a pulse with the initial precipitation event of the season (James et al. 2006). Recent research at JOTR demonstrated that atmospheric N deposition contributes to increased N availability in soils and stimulates the growth of biomass of both native and exotic, invasive plant species (Brooks 2003, Allen et al. 2009, Rao et al. 2009, Rao and Allen 2010, Rao et al. 2010). The increase in invasive plant biomass has the possibility of fueling wildfires, increasing their size and intensity relative to historic events, and creating large scale ecosystem changes (D'Antonio and Vitousek 1992, Brooks 1999, Brooks et al. 2004).

As most vegetation growth is limited by N, anthropogenic inputs of N to the soil profile are expected to change nutrient dynamics (Vitousek 1994). The majority of N assimilated by plants is in the form of NO_3^- and NH_4^+ , while DIN and amino acids make up lower proportions (Schimel and Bennett 2004, Harrison et al. 2007). ^{15}N uptake tends to mimic the pool in which it originates (Evans et al. 1996), although the correlation between soil $\delta^{15}\text{N}$ and vegetation $\delta^{15}\text{N}$ is often muddled by various pools of N available for uptake (Hogberg 1997, Evans 2001). Discrimination of isotopologues during uptake

can vary within species and can be dependent on the type and pathway in which it is assimilated (Evans 2001). Plants can also absorb gaseous N molecules directly through their stomata for use within leaf tissue, altering the isotopic signature of vegetation towards the atmospheric signature (Frank et al. 2004, Vallano and Sparks 2008).

The pools of soil nitrogen that are influencing plant tissue $\delta^{15}\text{N}$ under the natural abundance range can be imprecise due to transformations of NH_4^+ and NO_3^- being subjected to competing reactions within the soil profile (Schimel and Bennett 2004). Each of these reactions (e.g., denitrification and nitrification) will have a unique fractionation of isotopologues between the source and product pools, which can obfuscate isotopic changes. In sandy desert soils, microbial activity decreases in the dry summer months as many of the soil microorganisms are dormant and activity can be undetectable (Gallardo and Schlesinger 1992), although high soil temperatures can cause minor abiotic volatilization of reactive N from the surface (McCalley and Sparks 2009). Microorganisms have a rapid increase in activity in response to changes in abiotic conditions such as a precipitation event (Shamir and Steinberger 2007). The lack of microbial activity during the summer suggests that the isotopic signature of deposited N may be measured at the soil surface because deposition accumulates and does not undergo biological transformation.

The accumulation of anthropogenic nitrogen may allow plants to serve as effective bioindicators of an N gradient, if they occur throughout the gradient. Perennial plants may be effective indicators because, although they may reabsorb tissue N from

previous years, their roots are already in the ground during initial precipitation events allowing them to assimilate nitrogen deposited on the soil surface. Annual plants may be useful indicators as they take up new N each year. Desert annual plants are inherently variable due to their adaptation to specific soil conditions and timing of annual rain events (Barbour and Diaz 1973). Native plants have germination requirements that are specific to local environmental conditions, which may not make them the best indicators of landscape level changes (Venable et al. 1993, Adondakis and Venable 2004). However, *Schismus arabicus* and *Schismus barbatus* (together *Schismus*) are invasive grasses that have increased in dominance in southern California since the 1970s (Johnson et al. 1975), occur widely across the desert, and are potential bioindicators of N deposition. They have an earlier phenology than native annual forbs, which will potentially allow them to integrate anthropogenic N into early tissue before it is leached from the surface and processed by microorganisms (Burk 1982, Brooks 1999, Jennings 2001).

The objectives of this study were to compare ambient atmospheric HNO₃, extractable soil NO₃⁻, plant tissue N, and stable isotopes of N and O along a N deposition gradient in the Sonoran Desert in the summer and winter. I tested three hypotheses: 1) the isotopic signature of atmospheric nitric acid will be conserved in soil samples taken during the summer due to deposited N remaining on the soil surface with minimal microbial activity occurring. Annual and perennial plants were collected at each site to determine if the species' ¹⁵N is altered by increased levels of deposition. 2) Perennial

plants will have a high correlation with ^{15}N due to constant exposure to deposition and their ability to uptake soil N as soon as it is available after a winter storm. 3) *Schismus* will also be an effective bioindicator due to its early phenology and access to accumulated N solubilized during early precipitation events.

Methods

Site locations

The study area was in the western Sonoran Desert including the Coachella Valley and Joshua Tree National Park in both Riverside and San Bernardino Counties, California (Figure 4.1). This area is in the Colorado Desert, a subregion of the Sonoran Desert that lies in the rain shadow of the Peninsular Mountain Ranges. The vegetation of this area is predominately creosote bush scrub, dominated by *Larrea tridentata* (DC.) Coville with *Ambrosia dumosa* (A. Gray) Payne as a common associate.

Primary production in the California deserts is limited by precipitation and nutrient availability (Hooper and Johnson 1999, Yahdjian et al. 2011). The alluvial fans and bajadas of the Sonoran desert are dominated by a mosaic of *Larrea tridentata* shrubs with interspaces that are barren during the summer and fill with annual plants during the winter (Barbour et al. 2007). The shrubs act as islands of fertility where litter and debris collects under the shaded canopy. Microbial biomass is concentrated under the shrubs relative to the interspaces (Schlesinger and Pilmanis 1998). Based on 100yr

records from Palm Springs, average annual precipitation is 139mm, with 115mm occurring in the winter growing season, from October through April, (WRCC 2012).

Atmospheric HNO₃ collection

Twelve ambient HNO₃ samplers were erected in the western Sonoran Desert along a previously measured N deposition gradient (Allen et al. 2009). A detailed description of samplers and methods are covered in Chapter 3 of this document. Filters were exposed for four week intervals in September 2010 and 2011 and January 2011.

Soil collection

Soil samples were collected from the same 12 sites when the air samplers were erected in September 2010 and 2011 and January 2011. Cores were taken 5cm deep in the interspaces between shrubs. A composite sample of three cores was collected in triplicate at each site. Samples were air dried and sieved to remove coarse fragments (>2mm). Samples were extracted using 1N KCl and ammonium (NH₄⁺) and nitrate (NO₃⁻) were measured colorimetrically using a Technicon Autoanalyzer. The KCl extracts were used in the bacterial denitrification method described below, followed by measurements of stable isotopes of extracted NO₃⁻

Vegetation collection

In July 2010, leaves (~1 g dwt) from *L. tridentata* were collected from all 12 sites. In winter 2010-2011, the first significant rain event occurred in early December. The sites were visited 3 weeks later to collect early germinating seedlings of annuals. Due to the high amount of diversity that exists within the study area, many species were not consistently present across all sites. The most common annual species were the native forbs desert pincushion (*Chaenactis fremontii* A. Gray) and desert dandelion (*Malacothrix glabrata* (A. Gray ex D. C. Eaton) A. Gray), and the exotic invasive Mediterranean splitgrass (*Schismus barbatus* (L.) Thell and *S. arabicus* Nees). A second set of leaf tissue was collected from annual vegetation in March 2010 when plants were at peak biomass. *Schismus* root tissue was collected as well as leaf tissue in March. After collection, all plant material was rinsed with DI water to remove dust and deposited N and dried at 40°C to constant mass. Tissue was then ground with a mortar and pestle and analyzed with an elemental analyzer attached to a Thermo Delta V isotope ratio mass spectrometer. Species nomenclature follows Baldwin et al. (2012).

Nitrate isotope analysis

To determine the $\delta^{15}\text{N}$ and $\delta^{18}\text{O}$ values of NO_3^- , a bacterial method was used to convert NO_3^- into N_2O (Sigman et al. 2001, Casciotti et al. 2002). KCl-extracted samples were calibrated for contamination by NO_3^- within the KCl solution (Chapter 1). The bacteria *Pseudomonas chlororaphis* ssp. *aureofaciens* (ATCC# 13985) lacks nitrous oxide

reductase activity and therefore produces nitrous oxide gas as a final product of denitrification which allows NO_3^- $\delta^{15}\text{N}$ and $\delta^{18}\text{O}$ to be measured. The bacteria was grown in a modified soy broth solution for 7-10 days, concentrated and sealed in a 20ml headspace vial and sparged with He gas for 2 hours. Samples were then added to the vials which were inverted overnight to allow for complete conversion of nitrate while minimizing N_2O loss. The following day 0.1 ml 10N NaOH was added to each vial to raise the pH of solution, lysing the bacteria to stop denitrification and immobilizing CO_2 gas as dissolved inorganic carbon. Samples were loaded on a PAL GC and sparged with He gas forcing N_2O gas in the headspace to be cryogenically concentrated in a liquid N_2 trap. After separating gases in a GC column, the m/z ratios 44, 45, 46 were measured using a Thermo Delta V isotope ratio mass spectrometer to derive $\delta^{18}\text{O}$ and $\delta^{15}\text{N}$ values for each sample. International standards USGS-32, USGS-34, and USGS-35 were used as samples of known isotopic composition to correct for instrumental error in isotopic measurements, USGS-32 and USGS-34 were used to create a first order calibration curve for N, and USGS-34 and USGS-35 were used to create a first order equation to calibrate for O.

Data Analysis

To determine the relationship between atmospheric nitric acid and extractable soil N, linear regressions were developed with data from all sites. The mean atmospheric nitric acid concentration and their isotopic signatures were individually

regressed against individual soil sample concentration and isotopic signature. Linear regressions of mean soil N values (N-NO_3^- , $\delta^{15}\text{N}$, $\delta^{18}\text{O}$) were then run against $\delta^{15}\text{N}$ and N concentration of leaf tissue across all sites where plant material was collected. All statistical analyses were performed with JMP[®] 9.0.2 (SAS Institute, Inc. Cary, NC) at $\alpha = 0.05$.

Results

Soil

In summer 2010, extractable soil NO_3^- was linearly correlated with ambient atmospheric HNO_3 concentration across all sites ($r^2=0.394$, $p < 0.0001$) (Figure 4.2A). The high deposition sites had 2-3 times (1 to 3.5 mg N kg^{-1}) more extractable soil NO_3^- than low deposition sites. The 2010 extractable soil NO_3^- $\delta^{18}\text{O}$ was also positively related with the soil NO_3^- ($r^2=0.208$, $p<0.05$) (Figure 4.2B). The r^2 of both of these regressions was reduced due to four points at two sites. When ambient HNO_3 exposure was regressed against soil NO_3^- $\delta^{18}\text{O}$, there was a positive relationship that corrected for the two sets of outliers that were present in the first two relationships ($r^2=0.538$, $p<.0001$) (Figure 4.2C).

There was not a significant relationship between ambient air HNO_3 concentrations and soil NO_3^- concentration, nor soil N-NO_3^- concentration and soil NO_3^- $\delta^{18}\text{O}$ in the summer of 2011 (Figure 4.2D,E), likely because of high soil N-NO_3^- heterogeneity at lower deposition sites. There was a relationship between ambient

HNO₃ exposure with soil NO₃⁻ δ¹⁸O ($r^2 = 0.412$, $p < 0.001$) (Figure 4.2F). The slopes of the relationships were similar for 2010 and 2011 suggesting a similar relative rate of input of anthropogenic N across the sites. There was a decrease in the δ¹⁸O of soil NO₃⁻ from 2010 to 2011 that may have been caused by a 1.3cm precipitation event 2 weeks prior to soil sampling. Comparing mean soil NO₃⁻ δ¹⁸O at each site from 2010 to 2011 produced a positive relationship with a slope of 0.945 suggesting the same relative contribution of anthropogenic N to each site over time (Figure 4.3). The intercept of the relationship was -4.67 indicating that there was more anthropogenic NO₃⁻ in the soil in 2010 relative to 2011.

Summer soil NO₃⁻ δ¹⁵N was not related to soil NO₃⁻ concentration in either 2010 or 2011 and had weakly positively relationships with increasing concentrations of ambient HNO₃ ($r^2 = 0.253$, $p < 0.05$) and ambient HNO₃ δ¹⁵N ($r^2 = 0.143$, $p = 0.059$) in 2010. Due to the rain events during atmospheric sampling the 2011 soil samples were compared , the 2011 soil samples were compared with 2010 atmospheric values, where there was a positive relationship between 2011 soil NO₃⁻ δ¹⁵N and 2010 ambient HNO₃ δ¹⁵N ($r^2 = 0.380$, $p < 0.001$).

Winter soil NO₃⁻ concentration had a minor relationship with winter ambient δ¹⁸O HNO₃ ($r^2 = 0.148$, $p < 0.0012$), suggesting that the slight increase in measured anthropogenic HNO₃ in the atmosphere resulted in more NO₃⁻ deposition to the soil. While there was no relationship between atmospheric HNO₃ loading and soil δ¹⁵N, there

was a geographic relationship where higher enriched soil $\text{NO}_3^- \delta^{15}\text{N}$ was located closer to agricultural areas on the southern region of the study area (Figure 4.4).

Vegetation

Larrea tridentata has an average leaf life span of 12 months (Reich et al. 1998). Young (bright green) and old (dark green to brownish) leaves were compared with no difference in leaf $\delta^{15}\text{N}$ between leaf ages at either a high or low deposition site (Data not shown). There was no relationship between leaf %N and summer ambient HNO_3 exposure ($p=0.924$), although there was a linear decline in leaf $\delta^{15}\text{N}$ with increasing ambient air HNO_3 concentration ($r^2=0.547$, $p<0.0001$) (Figure 4.5A). The decrease in leaf tissue $\delta^{15}\text{N}$ was consistent with the trend measured between increasing soil $\text{NO}_3^- \delta^{15}\text{N}$ and increasing ambient $\text{HNO}_3 \delta^{15}\text{N}$ ($r^2=0.179$, $p<0.05$) (Figure 4.5B). There was no correlation between *L. tridentata* leaf tissue and winter soil values.

The first significant winter precipitation event did not occur until December 17, 2010 when over 6cm of rain fell over six days. Due to the late rainfall, *Schismus* did not get its customary head start in germination. Upon collection in early January, *Schismus* seedlings were only present at 4 of the 13 sites and *C. fremontii* was only present at 3 sites. The subsequent winter precipitation was sparse and contained long (over 1 month) dry periods resulting in low annual plant richness and few species in common among sites. In early spring, when annual vegetation was flowering, *Schismus* was the

most common annual plant, growing at all 12 sites; *C. fremontii* was the most common native annual, present at 5 sites, followed by *M. glabrata*, 4 sites.

Winter *Schismus* leaf tissue $\delta^{15}\text{N}$ had a positive linear relationship with summer soil $\text{NO}_3^- \delta^{18}\text{O}$ ($r^2=0.8518$, $p<0.01$) (Figure 4.6A) with a variation between -0.83 to 4.4%. There was no relationship between any of the winter soil variables and seedling $\delta^{15}\text{N}$. Spring shoot %N decreased linearly with increasing summer soil $\delta^{18}\text{O}$ ($r^2=0.395$, $p<.01$) (Figure 4.6B), but there was no relationship between leaf tissue $\delta^{15}\text{N}$ and atmospheric or soil N variables. There was also no relationship between individual *Schismus* leaf $\delta^{15}\text{N}$ and the root $\delta^{15}\text{N}$.

Early season *C. fremontii* seedlings had a negative linear relationship with soil $\text{NO}_3^- \delta^{18}\text{O}$ ($n=6$, $r^2=0.885$, $p<.01$) (Figure 4.7A). The dry period following the initial collection period caused many of the early germinating native annuals to die prematurely. The spring collection sites only overlapped with the winter sites at one high N deposition site. The relationship of spring leaf $\delta^{15}\text{N}$ remained linear and negative when compared to summer soil NO_3^- ($n=8$, $r^2=0.928$, $p<0.0001$) (Figure 4.7B).

There were no relationships between *M. glabrata* $\delta^{15}\text{N}$ and soil and atmospheric N variables.

Discussion

Soil

The increases in soil extractable nitrate in 2010 summer soil samples at areas of high ambient HNO₃ concentration are consistent with previous data collected in semi-arid coastal sage scrub (Padgett et al. 1999). The relationship between summer soil NO₃⁻ concentration and its δ¹⁸O suggests that the increase in available soil NO₃⁻ is due to the deposition of anthropogenic HNO₃. The enriched soil NO₃⁻ δ¹⁸O is consistent with anthropogenic sources of HNO₃ created through combustion processes (Kendall et al. 2007). Measured ambient HNO₃ δ¹⁸O ranged from 35-80‰ along the deposition gradient (Chapter 2).

Two sites had soil NO₃⁻ concentrations falling far outside the general relationship of the other sites (Fig. 2). Two samples with low soil NO₃⁻ concentration occurred at high atmospheric HNO₃ concentration and were taken from sandy soils near a wash, compared with the finer textured soils collected on the raised interspaces surrounding the *L. tridentata* shrubs. Since sand has a larger particle size than silt or clay it binds fewer ionic particles than soil and has increased porosity which promotes free drainage of water as well as air movement. These characteristics may make it an ideal candidate for analysis of N deposition to a desert site. Minimizing the mixing with local signals will provide a better signal of anthropogenic inputs to the system. The second set of outlier points (Fig. 2) were from an intermediate deposition zone in a small drainage with more annual biomass than sites in the same area. The increased organic matter in

combination with variable surface roughness may have resulted in soil nutrient heterogeneity.

The lack of relationship between soil NO_3^- concentration and ambient HNO_3 concentration in summer 2011 samples may be due to the rain event that occurred two weeks before soil collection. By the time samples were collected from the field, the surface soils were dry, but after a precipitation event, abiotic soil losses may be increased by as much as two orders of magnitude (McCalley and Sparks 2009). This loss is driven by temperature and increases with the size of the precipitation pulse (Harms and Grimm 2012). Wetting of the soil also increases microbial activity which can release nitrogen held by microbes in their dormant state and produce increased transformation among pools. The relationship between soil $\delta^{15}\text{N}$ and ambient HNO_3 $\delta^{15}\text{N}$ is maintained when comparing the summer 2011 soil sample to the summer 2010 air sample. This suggests that while the atmospheric patterns were different during the sampling period, they may have been similar leading up to it. Although even with the changes in the amount of N present at the sites between years, the isotopic signature of anthropogenic inputs is preserved.

Comparing soil NO_3^- $\delta^{18}\text{O}$ from summer 2010 strengthened the relationship between soil NO_3^- and ambient HNO_3 concentration (Figure 4.1C). The NO_3^- $\delta^{18}\text{O}$ corrected for the outliers that were present in NO_3^- concentration measurements. Summer 2011 extractable NO_3^- $\delta^{18}\text{O}$ also maintained a correlation with the deposition gradient (Figure 4.1F). The consistency of the NO_3^- $\delta^{18}\text{O}$ relationship between years

suggests relative contribution of anthropogenic N across the gradient remains the same (Figure 4.3). The offset of the intercept between years may be related to increased biologically sourced N in the soil due to increased soil activity due to increased soil moisture.

These results suggest that the top 2-5 centimeters of soil in arid regions that experience high levels of dry deposition are an effective means to measure the amount of anthropogenic HNO_3 being deposited during the dry season. Collecting soil samples prior to and after a summer rain event will provide the clearest indication of inputs due to the lack of biological activity occurring in the soils. Further studies need to evaluate the effects of soil texture and surface roughness on the accumulation of anthropogenic HNO_3 in the soil. My current hypothesis is that sand from washes may act as the most accurate determinant of deposition based on the lack of organic material in the soil and the porosity to allow increased air flow. These soils are also the most likely to lose deposited N during a rain event, as NO_3^- particles would easily be washed from the surface.

The precipitation events that cause abiotic degassing of NO_x molecules during the heat of the summer did not impact the ratio of NO_3^- isotopologues in the soil. This is consistent with the isotopic signature of the secondary source of HNO_3 collected in Chapter 1. The atmospheric HNO_3 collected on the filters in the field had consistent HNO_3 $\delta^{15}\text{N}$ and $\delta^{18}\text{O}$ in both high and low sites. If the volatilized N was linked to the amount deposited to the soil, it would have removed the anthropogenic signature

present in 2011 soil $\text{NO}_3^- \delta^{18}\text{O}$ after the rain event occurring weeks before soil collection.

Vegetation

I predicted that *L. tridentata* would show the most consistent relationship between atmospheric and tissue N, as it occurs consistently across the study area and is alive during the period of peak of atmospheric deposition. The lack of correlation between ambient atmospheric HNO_3 or soil $\delta^{18}\text{O}$ and *L. tridentata* leaf tissue %N suggests that anthropogenic deposition did not have an effect on the amount of N assimilated in the leaves, although it could have produced an overall growth response that was not measured. This is consistent with a previous fertilization experiments that recorded no change in summer N uptake rates in fertilized plots under simulated rain events (BassiriRad et al. 1999, Barker et al. 2006). Leaf samples were all taken in the summer, prior to monsoon precipitation events, when leaf N reabsorption is greatest (Lajtha 1987).

While there was no change in the amount of N in the leaf, the leaf tissue $\delta^{15}\text{N}$ declined with increasing soil $\delta^{18}\text{O}$ suggests that the relationship is related to increasing anthropogenic inputs to the soil. Soil $\text{NO}_3^- \delta^{18}\text{O}$ acts as an indicator of HNO_3 deposition to the soil surface, and the change in leaf $\delta^{15}\text{N}$ is consistent with the linear negative trend observed in soil $\text{NO}_3^- \delta^{15}\text{N}$ as $\delta^{18}\text{O}$ increased across sites. The range of $\delta^{15}\text{N}$ was similar in both soil and leaf samples. Dry deposition of atmospheric HNO_3 occurs on *L.*

tridentata leaves primarily during the dry season and is washed towards the base of the plant during precipitation events to provide a pulse of nitrate of greater magnitude relative to the interspace when uptake will be greatest. This corroborates a previous study indicating that *L. tridentata* leaf tissue $\delta^{15}\text{N}$ mimics soil pools following precipitation events (BassiriRad et al. 1999, Barker et al. 2006). The response of leaf tissue $\delta^{15}\text{N}$ to the combination of N deposition and precipitation events makes it important to collect samples prior to the beginning of monsoon season, or to only collect from sites that have been subjected to a particular event.

Alternatively, desert winter annuals obtain most of their N from the upper soil profile. The consistency of soil NO_3^- $\delta^{18}\text{O}$ relative to atmospheric HNO_3 concentration in summer 2011 (Figure 4.2F) suggests that after initial precipitation begins, the anthropogenic NO_3^- is still accessible in the upper soil profile. Thus, early germinating seeds at high deposition sites will have access to soil NO_3^- with altered $\delta^{15}\text{N}$. Winter *Schismus* seedling leaf $\delta^{15}\text{N}$ had a positive relationship with soil NO_3^- $\delta^{18}\text{O}$ suggesting that anthropogenic inputs are influencing the soil N pools available to early germinating seedlings. The relationship was in the opposite direction from *L. tridentata*, suggesting that *Schismus* may acquiring its N from a different source than the native species measured. Further tests on soil NH_4^+ $\delta^{15}\text{N}$ have to be run in order to determine the value of the anthropogenic inputs.

Soil NH_4^+ concentrations are equal to NO_3^- in these desert soils (Rao et al. 2009), as is the relative atmospheric concentration of NO_3^- and NH_3 across the gradient

(Chapter 2). NO_3^- was chosen as an indicator based on the distinct anthropogenic signature present in anthropogenic forms. The correlations present between $\delta^{15}\text{N}$ of plant tissue are related to the anthropogenic inputs measured as soil $\text{NO}_3^- \delta^{18}\text{O}$. As plant tissue $\delta^{15}\text{N}$ is consistent with the $\delta^{15}\text{N}$ of the pool that it gets its nitrogen from (Evans et al. 1996), the knowledge of $\delta^{15}\text{N}$ NH_4^+ will help determine the pool each species assimilates its nitrogen from.

The spring *Schismus* seedlings unexpectedly decreased in leaf %N as soil $\delta^{18}\text{O}$ increased. Previous research has tied N fertilization to an increase in *Schismus* biomass production (Allen et al. 2009, Rao et al. 2011). Due to sporadic rain events during the season, *Schismus* plants may have translocated N from their leaf tissue into seed production. At the time of collection, the plants had already started producing seed at all sites. The lack of correlation between *Schismus* root $\delta^{15}\text{N}$ and leaf $\delta^{15}\text{N}$ strengthens this argument, as there would be increased mixing from both leaf and root sources of N with redistribution. The variability of *Schismus* leaf $\delta^{15}\text{N}$ at each site and along the N deposition gradient suggests that *Schismus* does not have preferential uptake from a single soil N pool, but instead assimilates N in relation to its abundance, anthropogenic vs. mineralized N sources. Collecting samples earlier in the season before the grass goes to seed may provide a better signal of deposition for the only annual plant that was found consistently across the region.

Due to the first major rain event occurring in December 2011, there was a late start to the annual plant growing season for 2011/2012. In response to this, the exotic

annuals did not have a phenological head start on the native annuals during the sampling period. *Schismus* typically germinates with the first fall rains, while many native annuals are delayed in their phenology (Kimball et al. 2011). The seedlings of *C. fremontii* emerged at approximately the same time as *Schismus* seedlings; having access to the same pools of N. Winter *C. fremontii* seedling leaf $\delta^{15}\text{N}$ followed the same pattern as *L. tridentata* leaves, having a linear relationship with soil $\text{NO}_3^- \delta^{18}\text{O}$. This suggests that the anthropogenic NO_3^- inputs were accessible and preferentially used by seedlings.

Spring *C. fremontii* plants maintained the same relationship with soil $\text{NO}_3^- \delta^{18}\text{O}$ as was measured in the winter seedlings. The consistency of the leaf $\delta^{15}\text{N}$ across seasons may be related to the extended growing season of *C. fremontii* relative to *Schismus*. *C. fremontii* plants had yet to set seed before collection and were still actively growing. The late growing season allowed the plant to incorporate spring deposition which began to increase at the change of the season (Chapter 3).

Conclusions

Summer surface soil $\text{NO}_3^- \delta^{18}\text{O}$ had a consistent relationship with ambient summer atmospheric HNO_3 concentration, suggesting that it is a strong indicator of HNO_3 deposition in a desert ecosystem. Soil $\text{NO}_3^- \delta^{18}\text{O}$ values are consistent with previously measured values of anthropogenic inputs (Kendall et al. 2007), as well as ambient HNO_3 values measured across the study area (Chapter 3). The relationship between the atmospheric HNO_3 concentration gradient and soil $\text{NO}_3^- \delta^{18}\text{O}$ provided an

assay for measuring the percent of anthropogenic nitrogen present at a site. Soil NO_3^- concentration can also be used to determine the amount of N being deposited to the site as long as soil type and surface cover are kept constant and the samples are collected prior to a summer rain event. This can be used as a strong environmental indicator to trace N deposition to the region.

Leaf $\delta^{15}\text{N}$ of *L. tridentata* shrubs responded to high levels of anthropogenic inputs even while changes in leaf N concentration did not occur. There was high variability in leaf $\delta^{15}\text{N}$ across low deposition sites, but at sites where the dominant source of NO_3^- originated from anthropogenic sources, there was a decline in leaf $\delta^{15}\text{N}$ related to observed reduction in soil NO_3^- $\delta^{15}\text{N}$. *Schismus* has the most potential to be used as a bioindicator of deposition, due to its consistent presence in the shrub interspaces across the Sonoran Desert, but samples may need to be acquired prior to seed development. Comparisons of annual and perennial plant tissue $\delta^{15}\text{N}$ and $\delta^{18}\text{O}$ across sites may be used to detect sources and amounts of anthropogenic inputs of N.

Using stable isotopes of soil N and O has the potential to provide a spatial model of deposition across a desert region using considerably fewer resources than to measure atmospheric conditions. Remote areas can be analyzed without having to set up equipment and return to collect filters.

References

- Adondakis, S. and D. L. Venable. 2004. Dormancy and germination in a guild of Sonoran desert annuals. *Ecology* 85:2582-2590.
- Allen, E. B., L. E. Rao, R. J. Steers, A. Bytnerowicz, and M. E. Fenn. 2009. Impacts of atmospheric nitrogen deposition on vegetation and soils in Joshua Tree National Park. Pages 78-100 *in* R. H. Webb, L. F. Fenstermaker, J. S. Heaton, D. L. Hughson, E. V. McDonald, and D. M. Miller, editors. *The Mojave Desert: Ecosystem Processes and Sustainability*. University of Nevada Press, Las Vegas.
- Baldwin, B. G., D. H. Goldman, D. J. Keil, R. Patterson, and T. J. Rosatti. 2012. *The Jepson Manual: Vascular Plants of California*. Second Edition. Second edition. University of California Press, Berkeley, CA.
- Barbour, M. G. and D. V. Diaz. 1973. Larrea Plant Communities on Bajada and Moisture Gradients in the United States and Argentina. *Vegetatio* 28:335-352.
- Barbour, M. G., T. Keeler-Wolf, and A. A. Schoenherr, editors. 2007. *Terrestrial Vegetation of California*. 3rd Edition edition. University of California Press, Berkeley, CA.
- Barker, D. H., C. Vanier, E. Naumburg, T. N. Charlet, K. M. Nielsen, B. A. Newingham, and S. D. Smith. 2006. Enhanced monsoon precipitation and nitrogen deposition affect leaf traits and photosynthesis differently in spring and summer in the desert shrub *Larrea tridentata*. *New Phytologist* 169:799-808.
- BassiriRad, H., D. C. Tremmel, R. A. Virginia, J. F. Reynolds, A. G. de Soyza, and M. H. Brunell. 1999. Short-term patterns in water and nitrogen acquisition by two desert shrubs following a simulated summer rain. *Plant Ecology* 145:27-36.
- Brooks, M. L. 1999. Alien annual grasses and fire in the Mojave Desert. *Madroño* 45:13-19.
- Brooks, M. L. 2003. Effects of increased soil nitrogen on the dominance of alien annual plants in the Mojave Desert. *Journal of Applied Ecology* 40:344-353.

- Brooks, M. L., C. M. D'Antonio, D. M. Richardson, J. B. Grace, J. E. Keeley, J. M. DiTomaso, R. J. Hobbs, M. Pellant, and D. Pyke. 2004. Effects of Invasive Alien Plants on Fire Regimes. *Bioscience* 54:677-688.
- Burk, J. H. 1982. Phenology, germination, and survival of desert ephemerals in Deep Canyon, Riverside County, California. *Madroño* 29:154-163.
- Bytnerowicz, A. and M. E. Fenn. 1996. Nitrogen deposition in California forests: A review. *Environmental Pollution* 92:127-146.
- Bytnerowicz, A., M. J. Sanz, M. J. Arbaugh, P. E. Padgett, D. P. Jones, and A. Davila. 2005. Passive sampler for monitoring ambient nitric acid (HNO₃) and nitrous acid (HNO₂) concentrations. *Atmospheric Environment* 39:2655-2660.
- Casciotti, K. L., D. M. Sigman, M. G. Hastings, J. K. Böhlke, and A. Hilkert. 2002. Measurement of the Oxygen Isotopic Composition of Nitrate in Seawater and Freshwater Using the Denitrifier Method. *Analytical Chemistry* 74:4905-4912.
- Cleland, E. E. and W. S. Harpole. 2010. Nitrogen enrichment and plant communities. *Annals of the New York Academy of Sciences* 1195:46-61.
- D'Antonio, C. M. and P. M. Vitousek. 1992. Biological Invasions by Exotic Grasses, the Grass/Fire Cycle, and Global Change. *Annual Review of Ecology and Systematics* 23:63-87.
- Eilers, G., R. Brumme, and E. Matzner. 1992. Aboveground N-uptake from wet deposition by Norway spruce (*Picea-abies karst*). *Forest Ecology and Management* 51:239-249.
- Elliott, E. M., C. Kendall, E. B. Boyer, D. A. Burns, G. Lear, H. E. Golden, K. Harlin, A. Bytnerowicz, T. J. Butler, and R. Glatz. 2009. Dual nitrate isotopes in actively and passively collected dry deposition: Utility for partitioning NO_x sources, understanding reaction pathways, and comparison with isotopes in wet nitrate deposition. *Journal of Geophysical Research: Biogeosciences*.
- Elliott, E. M., C. Kendall, S. D. Wankel, D. A. Burns, E. W. Boyer, K. Harlin, D. J. Bain, and T. J. Butler. 2007. Nitrogen isotopes as indicators of NO_x source contributions to atmospheric nitrate deposition across the Midwestern and northeastern United States. *Environmental Science & Technology* 41:7661-7667.

- Evans, R. D. 2001. Physiological mechanisms influencing plant nitrogen isotope composition. *Trends in Plant Science* 6:121-126.
- Evans, R. D., A. J. Bloom, S. S. Sukrapanna, and J. R. Ehleringer. 1996. Nitrogen isotope composition of tomato (*Lycopersicon esculentum* Mill. cv. T-5) grown under ammonium or nitrate nutrition. *Plant, Cell & Environment* 19:1317-1323.
- Fenn, M. E., E. B. Allen, S. B. Weiss, S. Jovan, L. H. Geiser, G. S. Tonnesen, R. F. Johnson, L. E. Rao, B. S. Gimeno, F. Yuan, T. Meixner, and A. Bytnerowicz. 2010. Nitrogen critical loads and management alternatives for N-impacted ecosystems in California. *Journal of Environmental Management* 91:2404-2423.
- Fenn, M. E. and A. Bytnerowicz. 1993. Dry deposition of nitrogen and sulfur to Ponderosa and Jeffrey pine in the San Bernardino national forest in Southern California. *Environmental Pollution* 81:277-285.
- Fenn, M. E., R. Haeuber, G. S. Tonnesen, J. S. Baron, S. Grossman-Clarke, D. Hope, D. A. Jaffe, S. Copeland, L. Geiser, H. M. Rueth, and J. O. Sickman. 2003. Nitrogen emissions, deposition, and monitoring in the western United States. *Bioscience* 53:391-403.
- Frank, D. A., R. D. Evans, and B. F. Tracy. 2004. The role of ammonia volatilization in controlling the natural N-15 abundance of a grazed grassland. *Biogeochemistry* 68:169-178.
- Gallardo, A. and W. Schlesinger. 1992. Carbon and nitrogen limitations of soil microbial biomass in desert ecosystems. *Biogeochemistry* 18:1-17.
- Galloway, J. N., F. J. Dentener, D. G. Capone, E. W. Boyer, R. W. Howarth, S. P. Seitzinger, G. P. Asner, C. C. Cleveland, P. A. Green, E. A. Holland, D. M. Karl, A. F. Michaels, J. H. Porter, A. R. Townsend, and C. J. Vorosmarty. 2004. Nitrogen cycles: past, present, and future. *Biogeochemistry* 70:153-226.
- Galloway, J. N., W. H. Schlesinger, H. Levy, A. Michaels, and J. L. Schnoor. 1995. Nitrogen-fixation - Anthropogenic Enhancement - Environmental Response. *Global Biogeochemical Cycles* 9:235-252.

- Granger, S. J., T. H. E. Heaton, R. Bol, G. S. Bilotta, P. Butler, P. M. Haygarth, and P. N. Owens. 2008. Using delta N-15 and delta O-18 to evaluate the sources and pathways of NO₃⁻ in rainfall event discharge from drained agricultural grassland lysimeters at high temporal resolutions. *Rapid Communications in Mass Spectrometry* 22:1681-1689.
- Harms, T. K. and N. B. Grimm. 2012. Responses of trace gases to hydrologic pulses in desert floodplains. *J. Geophys. Res.* 117:G01035.
- Harrison, K. A., B. Roland, and R. D. Bardgett. 2007. Preferences for Different Nitrogen Forms by Coexisting Plant Species and Soil Microbes. *Ecology* 88:989-999.
- Henry, H., N. Chiariello, P. Vitousek, H. Mooney, and C. Field. 2006. Interactive Effects of Fire, Elevated Carbon Dioxide, Nitrogen Deposition, and precipitation on a California Annual Grassland. *Ecosystems* 9:1066-1075.
- Hogberg, P. 1997. Tansley review No 95 - N-15 natural abundance in soil-plant systems. *New Phytologist* 137:179-203.
- Hooper, D. U. and L. Johnson. 1999. Nitrogen limitation in dryland ecosystems: Responses to geographical and temporal variation in precipitation. *Biogeochemistry* 46:247-293.
- James, J. J., Z. T. Aanderud, and J. H. Richards. 2006. Seasonal timing of N pulses influences N capture in a saltbush scrub community. *Journal of Arid Environments* 67:688-700.
- Jennings, W. B. 2001. Comparative flowering phenology of plants in the western Mojave Desert. *Madroño* 48:162-171.
- Johnson, H. B., F. C. Vasek, and T. Yonkers. 1975. Productivity, Diversity and Stability Relationships in Mojave Desert Roadside Vegetation. *Bulletin of the Torrey Botanical Club* 102:106-115.
- Jovan, S. and B. McCune. 2005. Air-Quality Bioindication in the Greater Central Valley of California, with Epiphytic Macrolichen Communities. *Ecological Applications* 15:1712-1726.

- Kellman, L. M. and C. Hillaire-Marcel. 2003. Evaluation of nitrogen isotopes as indicators of nitrate contamination sources in an agricultural watershed. *Agriculture, Ecosystems & Environment* 95:87-102.
- Kendall, C., E. M. Elliott, and S. D. Wankel. 2007. Tracing Anthropogenic Inputs of Nitrogen. *in* R. Michener and K. Lajtha, editors. *Stable Isotopes in Ecology and Environmental Science*. Wiley-Blackwell, Malden, MA.
- Kimball, S., A. L. Angert, T. E. Huxman, and D. L. Venable. 2011. Differences in the timing of germination and reproduction relate to growth physiology and population dynamics of Sonoran Desert winter annuals. *American Journal of Botany* 98:1773-1781.
- Kohl, D. H., G. B. Shearer, and B. Commoner. 1971. Fertilizer Nitrogen: Contribution to Nitrate in Surface Water in a Corn Belt Watershed. *Science* 174:1331-1334.
- Lajtha, K. 1987. Nutrient reabsorption efficiency and the response to phosphorus fertilization in the desert shrub *Larrea tridentata* (DC.) Cov. *Biogeochemistry* 4:265-276.
- McCalley, C. K. and J. P. Sparks. 2009. Abiotic Gas Formation Drives Nitrogen Loss from a Desert Ecosystem. *Science* 326:837-840.
- Ochoa-Hueso, R., E. B. Allen, C. Branquinho, C. Cruz, T. Dias, M. E. Fenn, E. Manrique, M. E. Pérez-Corona, L. J. Sheppard, and W. D. Stock. 2011. Nitrogen deposition effects on Mediterranean-type ecosystems: An ecological assessment. *Environmental Pollution* 159:2265-2279.
- Padgett, P. E., E. B. Allen, A. Bytnerowicz, and R. A. Minich. 1999. Changes in soil inorganic nitrogen as related to atmospheric nitrogenous pollutants in southern California. *Atmospheric Environment* 33:769-781.
- Pardo, L. H., M. E. Fenn, C. L. Goodale, L. H. Geiser, C. T. Driscoll, E. B. Allen, J. S. Baron, R. Bobbink, W. D. Bowman, C. M. Clark, B. Emmett, F. S. Gilliam, T. L. Greaver, S. J. Hall, E. A. Lilleskov, L. Liu, J. A. Lynch, K. J. Nadelhoffer, S. S. Perakis, M. J. Robin-Abbott, J. L. Stoddard, K. C. Weathers, and R. L. Dennis. 2011. Effects of nitrogen deposition and empirical nitrogen critical loads for ecoregions of the United States. *Ecological Applications* 21:3049-3082.

- Pardo, L. H., C. Kendall, J. Pett-Ridge, and C. C. Y. Chang. 2004. Evaluating the source of streamwater nitrate using $\delta^{15}\text{N}$ and $\delta^{18}\text{O}$ in nitrate in two watersheds in New Hampshire, USA. *Hydrological Processes* 18:2699-2712.
- Rao, L. and E. Allen. 2010. Combined effects of precipitation and nitrogen deposition on native and invasive winter annual production in California deserts. *Oecologia* 162:1035-1046.
- Rao, L., R. Steers, and E. Allen. 2011. Effects of natural and anthropogenic gradients on native and exotic winter annuals in a southern California Desert. *Plant Ecology* 212:1079-1089.
- Rao, L. E., E. B. Allen, and T. Meixner. 2010. Risk-based determination of critical nitrogen deposition loads for fire spread in southern California deserts. *Ecological Applications* 20:1320-1335.
- Rao, L. E., D. R. Parker, A. Bytnerowicz, and E. B. Allen. 2009. Nitrogen mineralization across an atmospheric nitrogen deposition gradient in Southern California deserts. *Journal of Arid Environments* 73:920-930.
- Reich, P. B., M. B. Walters, D. S. Ellsworth, J. M. Vose, J. C. Volin, C. Gresham, and W. D. Bowman. 1998. Relationships of leaf dark respiration to leaf nitrogen, specific leaf area and leaf life-span: a test across biomes and functional groups. *Oecologia* 114:471-482.
- Rock, L., B. H. Ellert, and B. Mayer. 2011. Tracing sources of soil nitrate using the dual isotopic composition of nitrate in 2 M KCl-extracts. *Soil Biology and Biochemistry* 43:2397-2405.
- Schimel, J. P. and J. Bennett. 2004. Nitrogen mineralization: Challenges of a changing paradigm. *Ecology* 85:591-602.
- Schlesinger, W. H. and A. M. Pilmanis. 1998. Plant-soil Interactions in Deserts. *Biogeochemistry* 42:169-187.
- Shamir, I. and Y. Steinberger. 2007. Vertical Distribution and Activity of Soil Microbial Population in a Sandy Desert Ecosystem. *Microbial Ecology* 53:340-347.

- Sigman, D. M., K. L. Casciotti, M. Andreani, C. Barford, M. Galanter, and J. K. Bohlke. 2001. A bacterial method for the nitrogen isotopic analysis of nitrate in seawater and freshwater. *Analytical Chemistry* 73:4145-4153.
- Stevens, C. J., N. B. Dise, J. O. Mountford, and D. J. Gowing. 2004. Impact of nitrogen deposition on the species richness of grasslands. *Science* 303:1876-1879.
- Throop, H. L. and M. T. Lerdau. 2004. Effects of Nitrogen Deposition on Insect Herbivory: Implications for Community and Ecosystem Processes. *Ecosystems* 7:109-133.
- Vallano, D. M. and J. P. Sparks. 2008. Quantifying foliar uptake of gaseous nitrogen dioxide using enriched foliar delta N-15 values. *New Phytologist* 177:946-955.
- Venable, D. L., C. E. Pake, and A. C. Caprio. 1993. Diversity and Coexistence of Sonoran Desert Winter Annuals. *Plant species biology* 8:207-216.
- Vitoria, L., N. Otero, A. Soler, and A. Canals. 2004. Fertilizer characterization: Isotopic data (N, S, O, C, and Sr). *Environmental Science & Technology* 38:3254-3262.
- Vitousek, P. M. 1994. Beyond Global Warming: Ecology and Global Change. *Ecology* 75:1861-1876.
- Vitousek, P. M., J. D. Aber, R. W. Howarth, G. E. Likens, P. A. Matson, D. W. Schindler, W. H. Schlesinger, and D. G. Tilman. 1997. Human alteration of the global nitrogen cycle: Sources and consequences. *Ecological Applications* 7:737-750.
- Wankel, S. D., C. Kendall, C. A. Francis, and A. Paytan. 2006. Nitrogen sources and cycling in the San Francisco Bay Estuary: A nitrate dual isotopic composition approach. *Limnology and Oceanography* 51:1654-1664.
- WRCC (Western Regional Climate Center). 2012. Palm Springs, CA (046635), Monthly Climate Summary. 3/1/1906 to 6/04/2012. Website: <http://www.wrcc.dri.edu>
- Yahdjian, L., L. Gherardi, and O. E. Sala. 2011. Nitrogen limitation in arid-subhumid ecosystems: A meta-analysis of fertilization studies. *Journal of Arid Environments* 75:675-680.

Figures

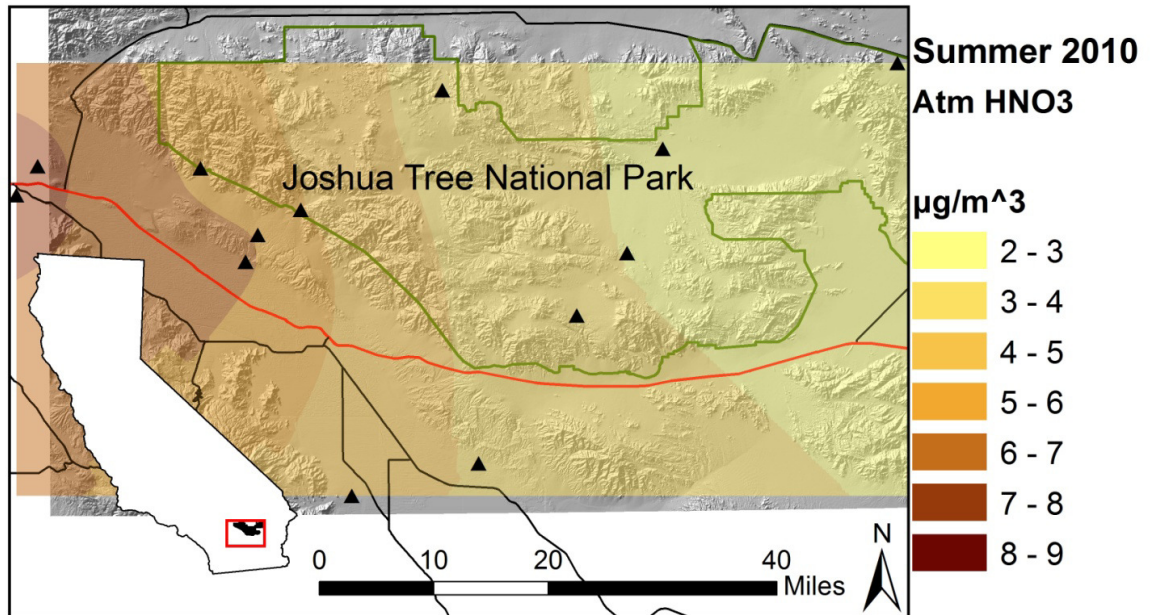


Figure 4.1. Location of field sites in the Sonoran Desert relative to Joshua Tree National Park with the gradient of ambient HNO₃ in the background.

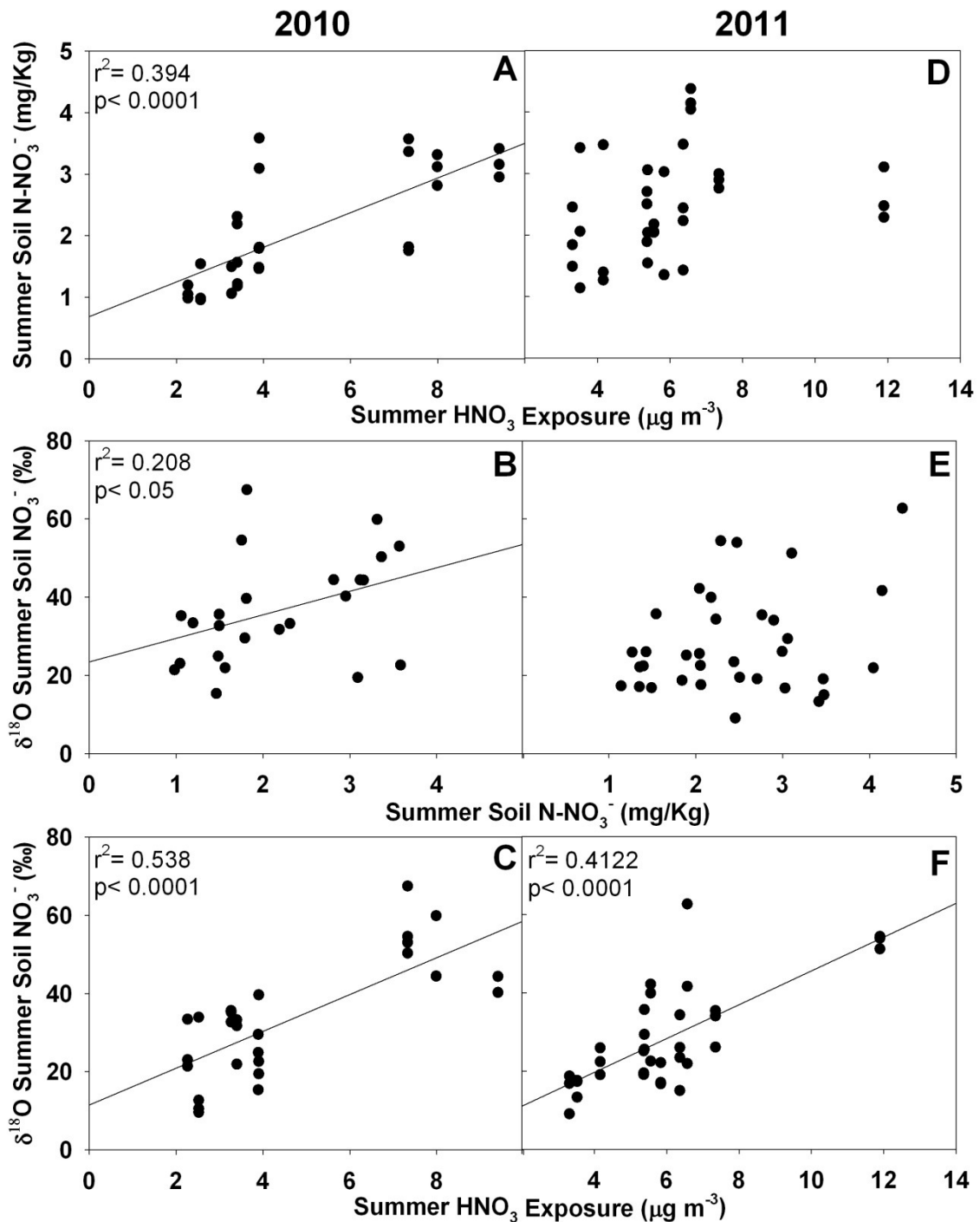


Figure 4.2. Extractable soil nitrate increased during summer sampling in 2010 (A), with a concurrent increase in soil NO₃⁻ δ¹⁸O (B) indicating that the increase was related to anthropogenic inputs. 2011 samples did not display the same patterns due to a precipitation event 2 weeks prior to sampling (D,E). At both sites, soil δ¹⁸O was positively correlated with the amount of ambient atmospheric HNO₃ found at the site during the summer.

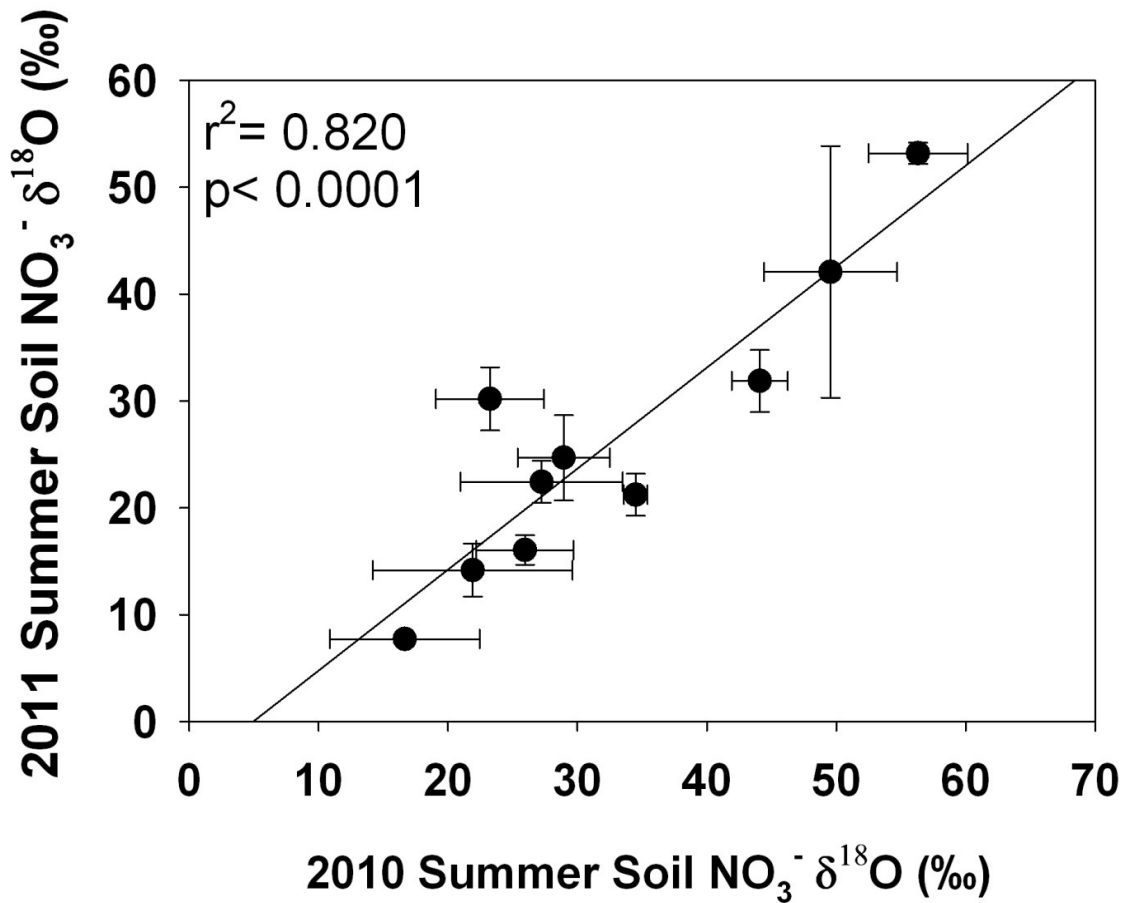


Figure 4.3. Relationship between mean soil extractable NO₃⁻ δ¹⁸O between 2010 and 2011. The slope of the interaction was 0.9451 suggesting a consistent, relative input of anthropogenic N. The intercept of -4.67 indicates that there was a higher percentage of anthropogenic N present in 2010 than 2011 samples. Error bars represent standard error of the mean and r² is based upon mean values from each point.

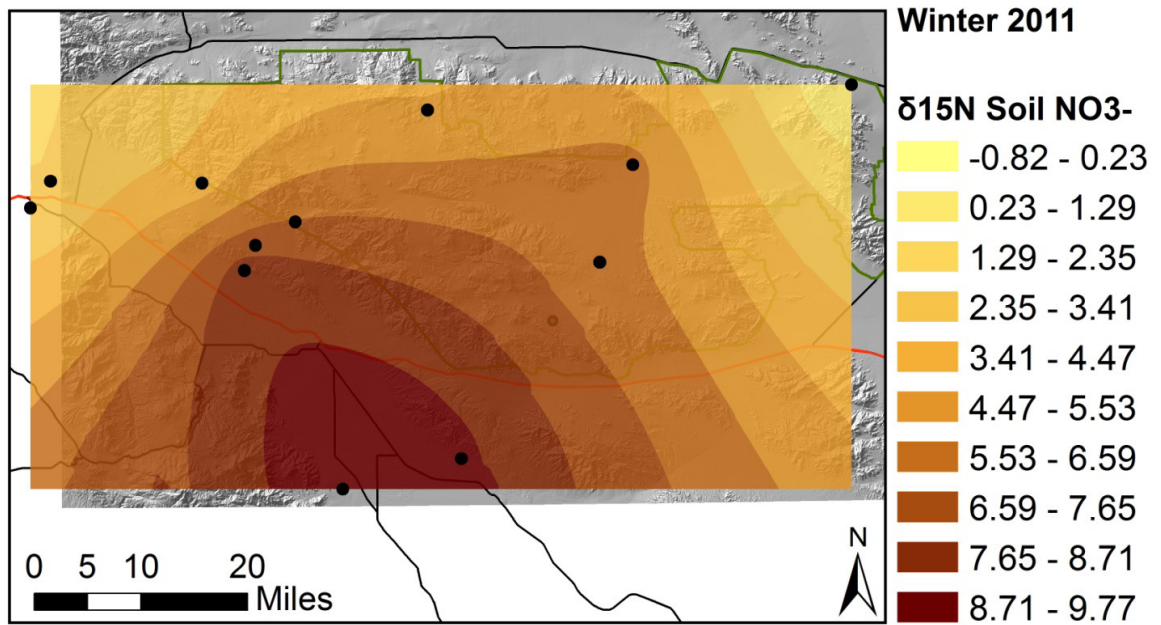


Figure 4.4. Winter soil NO₃⁻ δ¹⁵N increases around agricultural areas near the southern edge of the study area. This is consistent with atmospheric values found in Chapter 2.

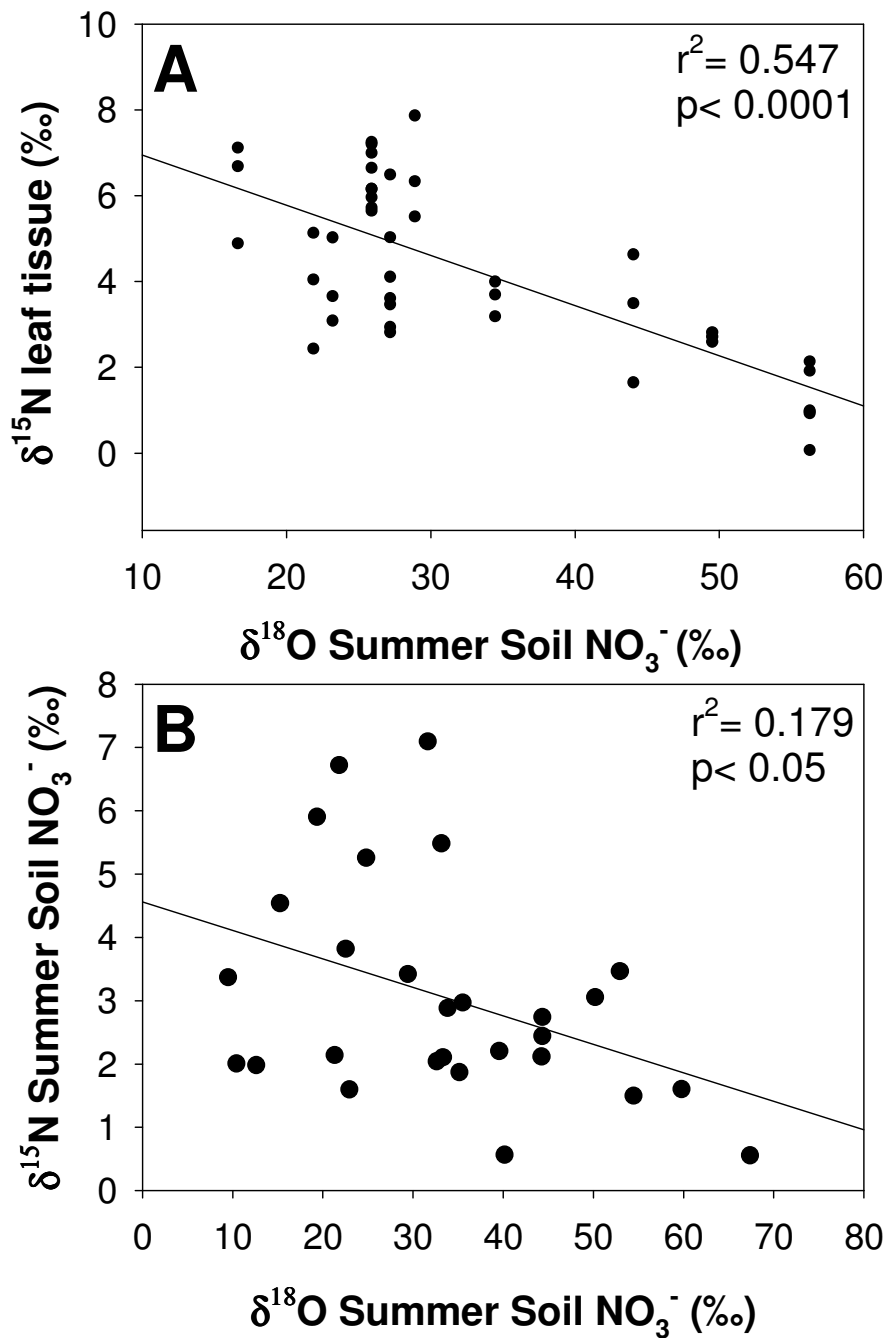


Figure 4.5. (A) *L. tridentata* leaf tissue $\delta^{15}\text{N}$ decreases with increasing levels of anthropogenic nitrogen in the soil. (B) The upper and lower levels of leaf $\delta^{15}\text{N}$ are within the same range as is measured in soil N NO_3^- extracts.

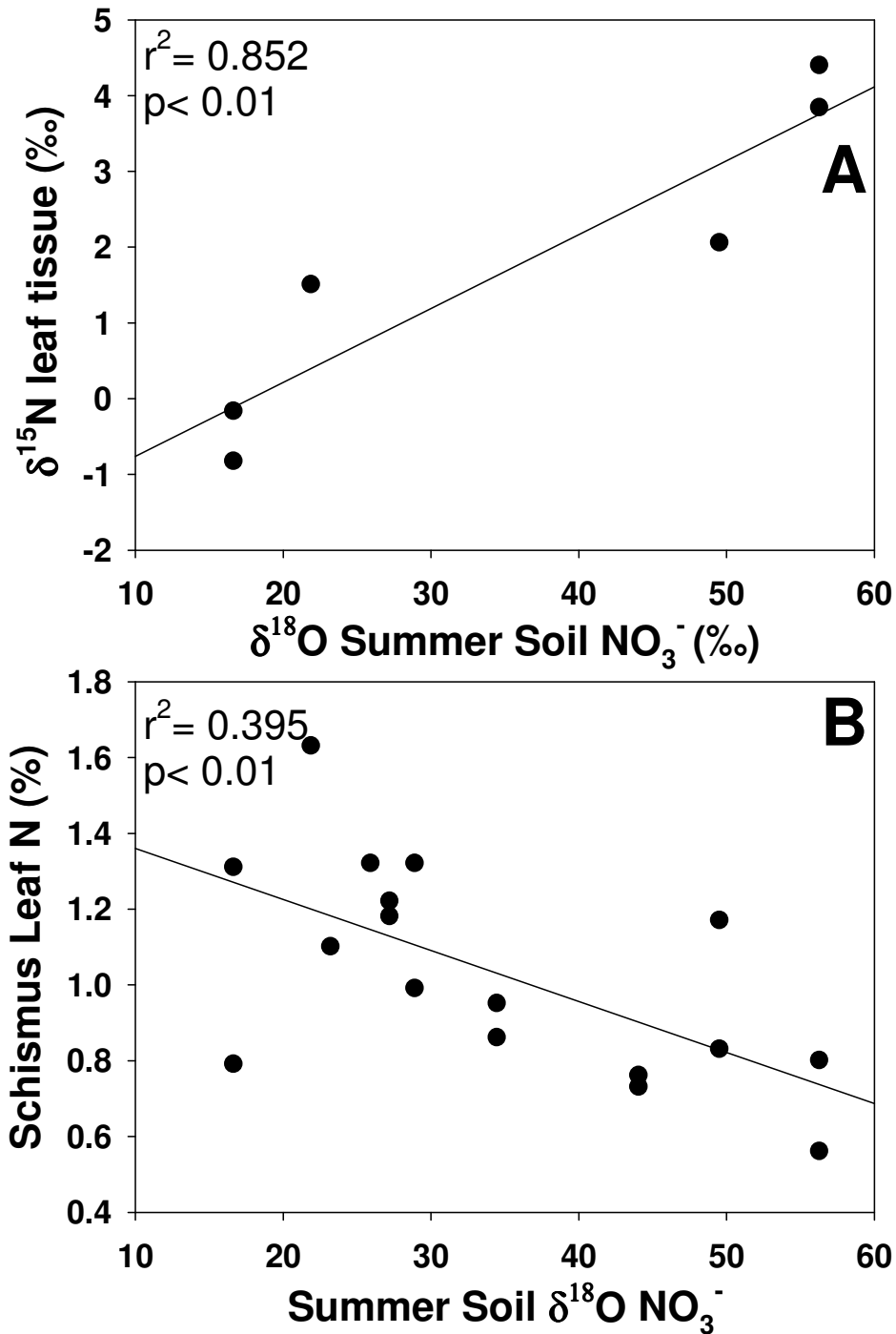


Figure 4.6. (A) *Schismus* leaf tissue $\delta^{15}\text{N}$ increases as summer 2010 soil NO_3^- $\delta^{18}\text{O}$ increases across sampling sites. The change in $\delta^{15}\text{N}$ in leaf tissue is opposite of that in soil samples. Larger soil NO_3^- $\delta^{18}\text{O}$ represents a larger input of anthropogenic N. (B) Spring *Schismus* leaf N% decreases with increasing atmospheric N inputs.

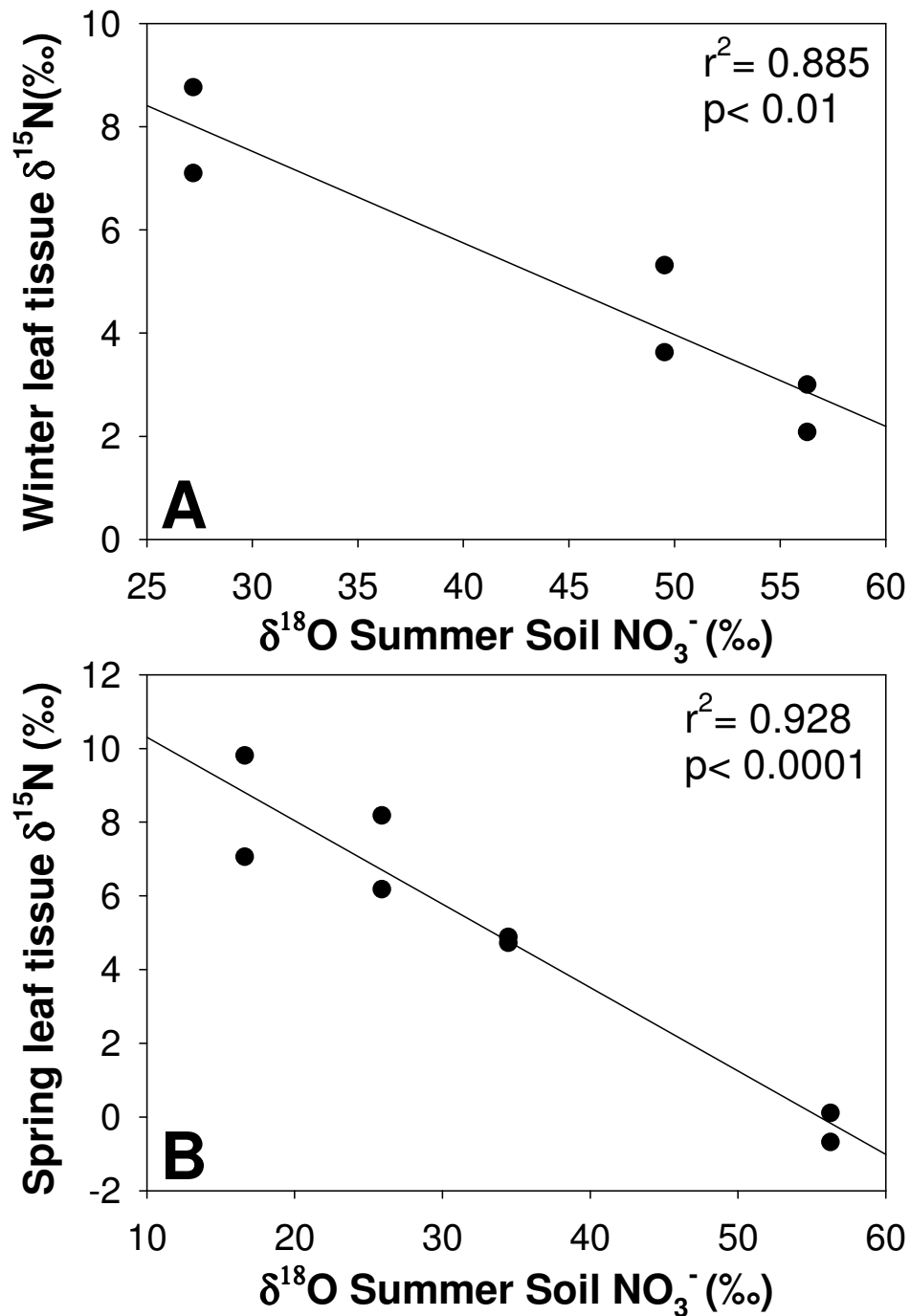


Figure 4.7. Early winter (A) and late spring (B) *C. fremontii* leaf tissue $\delta^{15}\text{N}$ decrease with increasing summer 2010 soil NO_3^- $\delta^{18}\text{O}$ across sampling sites. Larger soil NO_3^- $\delta^{18}\text{O}$ represents a larger input of anthropogenic N. The decrease in leaf $\delta^{15}\text{N}$ is consistent with soil $\delta^{15}\text{N}$ changes with increased HNO_3 inputs.

Conclusion

The research presented in this dissertation was based on the measurements of stable isotopes of nitrogen (N) and oxygen (O) in atmospheric, soil, and plant samples across a nitrogen deposition gradient in the Sonoran desert (Allen et al. 2009). The studies addressed questions regarding methods of collection and analysis of HNO_3 $\delta^{15}\text{N}$ and $\delta^{18}\text{O}$ from atmospheric and soil samples, as well as understanding how different sources of anthropogenic N mix in the region. The isotopic signature of the atmospheric samples identified multiple sources of HNO_3 contributing to local air quality. These sources were able to be traced into the soil in high deposition areas, and produced a measureable effect on plant nitrogen content.

The first chapter developed a method to improve the accuracy of NO_3^- $\delta^{15}\text{N}$ and $\delta^{18}\text{O}$ in low concentration KCl extracts by asking: *Does background NO_3^- contamination in KCl contribute to the final isotopic signature of sample NO_3^- , and is this value consistent in different brands of KCl reagents?* I confirmed the presence of background NO_3^- in reagent grade crystalline KCl. The amount of NO_3^- present in KCl was different among brands and grades and the contaminated NO_3^- $\delta^{15}\text{N}$ and $\delta^{18}\text{O}$ was unique to each brand. By determining that NO_3^- occurs in a consistent concentration within a single batch of KCl, I was able to develop a method to calibrate for its presence and increase the accuracy of the KCl extract measurements.

The second chapter addressed the question: *Do standard passive atmospheric HNO₃ samplers accurately measure isotopes of N and O in both field and controlled conditions?* The HNO₃ collected on filters exposed in the continuously stirred tank reactor was used to confirm that HNO₃ maintains an unbiased measurement of the isotopic signature of both N and O within 0.5‰ accuracy under controlled conditions. The weekly filters exposed in the field were subjected to multiple rain events bringing in air masses from many directions. The resulting mixing that took place across all samples suggested that, while there was variation on individual filters at one site, all the HNO₃ collected on the filters stemmed from two sources. The variation recorded was probably due to a combination of abiotic soil emissions from the wetting of dry desert soil (McCalley and Sparks 2009), the movement of different air masses impacting the sites, and the wetting of filters due to high winds during the rain events. This suggests that the ambient air samplers are best used under stable atmospheric conditions, due to their apparent susceptibility to contamination under intense weather events.

After determining that the passive samplers accurately collected HNO₃ $\delta^{15}\text{N}$ and $\delta^{18}\text{O}$, in Chapter 3 I asked: *Are atmospheric HNO₃ $\delta^{15}\text{N}$ and $\delta^{18}\text{O}$ consistent over a nitrogen deposition gradient between years and seasons?* The data showed that there was not a relationship between HNO₃ $\delta^{15}\text{N}$ or $\delta^{18}\text{O}$ between summer and winter samples. The HNO₃ $\delta^{15}\text{N}$ and $\delta^{18}\text{O}$ values recorded in this study were consistent with previously collected values of vehicle emissions and soil emissions (Michalski et al. 2004, Rock and Ellen 2007, Elliott et al. 2009). The most enriched HNO₃ $\delta^{18}\text{O}$ was higher in

winter than summer exposure periods, which was consistent with previous research (Hastings et al. 2003, Hastings et al. 2004). Summer HNO_3 $\delta^{15}\text{N}$ and $\delta^{18}\text{O}$ did not maintain a consistent pattern between 2010 and 2011. This was influenced by precipitation events and a change in the direction of air mass movement across the sites. Even with the variability among years and seasons, there was a consistent relationship where HNO_3 $\delta^{15}\text{N}$ and $\delta^{18}\text{O}$ from sites within the Coachella Valley mixed distinctly relative to sites within Joshua Tree National Park (JOTR). This suggests that the Little San Bernardino Mountains acts as a barrier to the movement of pollution coming from the Los Angeles air basin and that much of the N impacting JOTR comes from within the park.

The final chapter examined the isotopic signature of soil and plant material across the N deposition gradient and asked the question: *Can soil and plant material be used as environmental indicators of anthropogenic nitrogen inputs?* The summer soil samples collected before a precipitation event were the most effective indicator of deposition to the region, as N concentration increased across the gradient similar to measurements in other arid areas (Padgett et al. 1999). The concomitant increase in soil NO_3^- $\delta^{18}\text{O}$ at these sites suggests that the increase in soil N is directly related to anthropogenic inputs. Interestingly, the soil NO_3^- $\delta^{18}\text{O}$ retained its relationship with the deposition gradient even after a precipitation event that caused soil NO_3^- concentration to fluctuate across the gradient. Across the sampling sites, *Larrea tridentata* was the only plant species common to all the sites. Its leaf $\delta^{15}\text{N}$ decreased linearly with

increasing anthropogenic N inputs, even though there was no consistent change in leaf N. This was consistent with previous *L. tridentata* fertilization studies (Barker et al. 2006), and suggests that the plants in high deposition zones have access to different pools of nitrogen that they take up preferentially.

In conclusion, this dissertation determined that stable isotopes of N and O are a powerful tool to identify sources of N inputs to the Sonoran Desert and where they accumulate in the ecosystem. The mixing that takes place across the region in the summer isolates two separate anthropogenic sources of N on the eastern and western sides of the Little San Bernardino Mountains, each mixing with emissions from the agricultural region around the Salton Sea. The soil analysis techniques should be applicable in any arid region impacted by N dry deposition inputs to identify the percentage of anthropogenic nitrogen available. These techniques will allow researchers to use soil samples from a local region and create a spatial model of deposition.

References

- Allen, E. B., L. E. Rao, R. J. Steers, A. Bytnerowicz, and M. E. Fenn. 2009. Impacts of atmospheric nitrogen deposition on vegetation and soils in Joshua Tree National Park. Pages 78-100 in R. H. Webb, L. F. Fenstermaker, J. S. Heaton, D. L. Hughson, E. V. McDonald, and D. M. Miller, editors. *The Mojave Desert: Ecosystem Processes and Sustainability*. University of Nevada Press, Las Vegas.
- Barker, D. H., C. Vanier, E. Naumburg, T. N. Charlet, K. M. Nielsen, B. A. Newingham, and S. D. Smith. 2006. Enhanced monsoon precipitation and nitrogen deposition affect leaf traits and photosynthesis differently in spring and summer in the desert shrub *Larrea tridentata*. *New Phytologist* 169:799-808.
- Elliott, E. M., C. Kendall, E. B. Boyer, D. A. Burns, G. Lear, H. E. Golden, K. Harlin, A. Bytnerowicz, T. J. Butler, and R. Glatz. 2009. Dual nitrate isotopes in actively and passively collected dry deposition: Utility for partitioning NO_x sources, understanding reaction pathways, and comparison with isotopes in wet nitrate deposition. *Journal of Geophysical Research: Biogeosciences*.
- Hastings, M. G., D. M. Sigman, and F. Lipschultz. 2003. Isotopic evidence for source changes of nitrate in rain at Bermuda. *J. Geophys. Res.* 108:4790.
- Hastings, M. G., E. J. Steig, and D. M. Sigman. 2004. Seasonal variations in N and O isotopes of nitrate in snow at Summit, Greenland: Implications for the study of nitrate in snow and ice cores. *J. Geophys. Res.* 109:D20306.
- McCalley, C. K. and J. P. Sparks. 2009. Abiotic Gas Formation Drives Nitrogen Loss from a Desert Ecosystem. *Science* 326:837-840.
- Michalski, G., T. Meixner, M. Fenn, L. Hernandez, A. Sirulnik, E. Allen, and M. Thiemens. 2004. Tracing atmospheric nitrate deposition in a complex semiarid ecosystem using Delta(17)O. *Environmental Science & Technology* 38:2175-2181.
- Padgett, P. E., E. B. Allen, A. Bytnerowicz, and R. A. Minich. 1999. Changes in soil inorganic nitrogen as related to atmospheric nitrogenous pollutants in southern California. *Atmospheric Environment* 33:769-781.

Rock, L. and B. H. Ellen. 2007. Nitrogen-15 and oxygen-18 natural abundance of potassium chloride extractable soil nitrate using the denitrifier method. *Soil Science Society of America Journal* 71:355-361.